



UNIVERSIDAD CARLOS III DE MADRID

**Departamento de Mecánica de Medios Continuos y
Teoría de Estructuras**

Grado en Ingeniería Tecnologías Industriales

Trabajo Fin de Grado

Main Landing Gear Design for Piper Arrow IV

Alumno:

Patricia Camarero Ruiz

Tutor:

Marcos Rodríguez Millán

Julio 2014

Abstract

The main topic of this mechanical engineering design project is to redesign the landing gear of the Piper Arrow IV- PA-28RT-201 Aircraft. The new designed needed to take into account a 66% decrease in aircraft weight respect to the original Piper Arrow. With the decrease weight of the aircraft, the landing gear components must be individually redesigned to accommodate the stress and forces applied. When considering the redesign of each component some of the factors focused on were high strength, safety factor, durability and finally overall cost by reducing the overall weight of the landing gear.

One major key in the redesign of the landing gear components was the use of SolidWorks, as stress analysis along with high-cycle fatigue analysis was easily simulated with this program. This software also gave us the ability to change and compare material strength and cost for further simulation without the need of prototyping or testing.

Once this was done, I was then able to determine the best alternative in redesigning my landing gear. I decided that the price of the material was an important factor, so I avoided high valued materials and I also wanted to reduce the weight of the landing gear in order to increase the payload. These two important factors were really the backbone of my decisions. I also had to make sure that all of the possible changes that I was going to make met with the Federal Aviation Regulations (FAR).

This report documents the iterative process and summarizes the challenges in designing a landing gear.

Table of Contents

ABSTRACT	3
TABLE OF CONTENTS	4
LIST OF FIGURES	7
LIST OF TABLES	9
LIST OF GRAPHS.....	9
1. INTRODUCTION	10
1.1 Goals and requirements.....	10
1.2 Proposed solution	11
1.2.1.Problem statement.....	11
1.2.2. Design procedures	11
1.2.3. Design constraints	12
1.2.4. Proposed solutions.....	12
2. DESIGN OF MAIN COMPONENTS.....	14
2.1 Tire, Rim and Shaft.....	14
2.1.1 Specific Tire Requirements.....	15
2.1.2 Tire Trade Study.....	18
2.1.3 Material Selection for Rim.....	19
2.1.4 FEA Study of Rim during hard landing	21
2.1.5 FEA Study of Rim during braking.....	24
2.1.6 Shaft analytical design	27
2.1.7 Trade study on shaft material	29
2.1.8 Finite element solid and beam analysis of shaft.....	33
2.1.9 Bearing selection.....	36
2.1.10 Summary of tire, rim and shaft design	37
<u>COMPONENT TECHNICAL DRAWINGS.....</u>	<u>38</u>

2.2 Brake.....	40
2.2.1 Specific brake requirements	41
2.2.2 Design, thermal modeling and material selection	41
2.3 Oleo-Pneumatic Strut.....	47
2.3.1 Specific oleo-pneumatic requirements.....	48
2.3.2 Design and modeling of Oleo-Pneumatic strut.....	48
2.3.3 Analysis and design of strut Shaft.....	56
2.3.3.1 MATERIAL SELECTION	56
2.3.3.2 ANALYTICAL CALCULATIONS USING BUCKLING ANALYSIS.....	56
2.3.3.3 FEA MODEL FOR BUCKLING OF THE STRUT SHAFT	63
2.3.3.4 SUMMARY OF STRUT SHAFT DESIGN.....	66
2.3.4 Analysis and design of strut body	67
2.3.4.1 ANALYTICAL CALCULATIONS FOR MAXIMUM STRESSES	67
2.3.4.2 FEA STRESS STUDY	71
2.3.4.3 FEA FATIGUE STUDY.....	74
2.3.4.4 SUMMARY OF STRUT BODY DESIGN	75
2.3.5 Strut motion study.....	76
2.4 Torque Link.....	79
2.4.1 Specific torque link requirements	80
2.4.2 Material selection.....	81
2.4.3 Fatigue analysis	83
2.4.4 Fatigue analysis calculations.....	84
2.4.5 Finite element analysis.....	85
2.4.6 Summary of torque link design.....	91
2.5 Fork	93
2.5.1 Specific fork requirements.....	94
2.5.2 Material selection.....	95
2.5.3 FEA fork analysis.....	99
2.5.4 Summary of fork design	108
3. LANDING GEAR ASSEMBLY AND INTEGRATION	109
3.1 Final landing gear design.....	110
3.2 Landing gear exploded view and Bill of materials	111

4. CONCLUSION

113

4.1 Goal and requirements re-evaluation.

113

5. REFERENCES

116

List of Figures

FIGURE 1 GRAPHICAL DETERMINATION OF CG

FIGURE 2 PRICE VERSUS DENSITY FOR CASTABLE ALUMINUM ALLOYS

FIGURE 3 DENSITY VERSUS ELASTIC LIMIT OF CASTABLE ALUMINUM ALLOYS

FIGURE 4 SOLID MESH OF THE RIM, LOADING CONDITIONS AND BOUNDARY CONDITIONS

FIGURE 5 VON MISES STRESSES (PSI) EXPERIENCED BY RIM DURING HARD LANDING

FIGURE 6 ERROR PLOT OF VON MISES STRESSES EXPERIENCED BY RIM DURING HARD LANDING

FIGURE 7 VON MISES STRESSES (PSI) EXPERIENCED BY RIM DUE TO BRAKING

FIGURE 8 ERROR PLOT OF VON MISES STRESSES EXPERIENCED BY RIM DURING BRAKING

FIGURE 9 LOAD FACTOR FOR FATIGUE ANALYSIS OF RIM DURING HARD LANDING

FIGURE 10 SHAFT MODEL

FIGURE 11 SHAFT MATERIAL SELECTION

FIGURE 12 SOLID MESHING OF SHAFT FOR FEA

FIGURE 13 VON MISES STRESSES EXPERIENCED BY SHAFT DURING HARD LANDING

FIGURE 14 SHAFT MODELED AS A BEAM FOR FEA ANALYSIS

FIGURE 15 FEA MODEL OF VON MISES STRESSES EXPERIENCED BY SHAFT DURING HARD LANDING
(REFINED MESH)

FIGURE 16 ERROR PLOT FOR SHAFT FEA ANALYSIS

FIGURE 17 BEARING DIMENSIONS

FIGURE 18 RIM TECHNICAL DRAWING

FIGURE 19 WHEEL SHAFT TECHNICAL DRAWING

FIGURE 20 ESTIMATED BRAKE ENERGY VERSUS BRAKE ASSEMBLY WEIGHT

FIGURE 21 ESTIMATED NUMBER OF STOPS VERSUS KINETIC ENERGY PER POUND [3]

FIGURE 22 HEAT SINK VOLUME VERSUS BRAKE ASSEMBLY WEIGHT [3]

FIGURE 23 TIRE RIM DIAMETER VERSUS HEAT SINK DIAMETER [3]

FIGURE 24 EFFICIENCY-TO-WEIGHT RATIOS FOR VARIOUS SHOCK ABSORBERS [5]

FIGURE 25 SHAFT MODEL

FIGURE 26 FEA MESH MODEL AND BUCKLING DEFLECTION (IN)

FIGURE 27 FINAL MESH FOR STATIC ANALYSIS OF STRUT

FIGURE 28 FATIGUE ANALYSIS OF STRUT

FIGURE 29 SHAFT SECTIONS

FIGURE 30 FINAL ITERATION OF MESH USED FOR THE STRUT BODY STRUCTURAL SIMULATIONS

FIGURE 31 WORST CASE LANDING FEA STRESSES AND ERROR PLOT

FIGURE 32 HARD LANDING FEA STRESSES AND ERROR PLOT

FIGURE 33 FE FATIGUE STUDY RESULTS FOR WORST CASE LANDING – EXPECTED LIFE AND LOAD FACTOR

FIGURE 34 FE FATIGUE STUDY RESULT FOR HARD LANDING – EXPECTED LIFE AND LOAD FACTOR

FIGURE 35 DENSITY VERSUS ELASTIC LIMIT OF ALL POTENTIAL METALS

FIGURE 36 DENSITY VERSUS ELASTIC LIMIT OF POTENTIAL LOW ALLOY STEELS

FIGURE 37 STATIC ANALYSIS OF FORK

FIGURE 38 ERROR PLOT OF FEA ANALYSIS FOR FORK

FIGURE 39 FATIGUE ANALYSIS OF FORK

FIGURE 40 LOAD FACTOR FOR FORK

FIGURE 41 3D MODEL OF TORQUE LINK

FIGURE 42 FORK MESHING

FIGURE 43 FORK STRESSES DURING WORST CASE LANDING

FIGURE 44 ERROR PLOT OF FORK STRESSES DURING WORST CASE LANDING

FIGURE 45 LOAD FACTOR FEA ANALYSIS OF FORK

FIGURE 46 FORK STRESSES DURING HARD LANDING

FIGURE 47 ERROR PLOT OF FORK STRESSES DURING HARD LANDING

FIGURE 48 LOAD FACTOR PLOT FOR THE HARD CASE LANDING (4233LBF) OF THE FORK

FIGURE 49 TOTAL LIFETIME ESTIMATION PLOT FOR THE HARD CASE LANDING (4233 LBF) OF THE FORK

FIGURE 50 FORK TECHNICAL DRAWING

FIGURE 51 FINAL LANDING GEAR ASSEMBLY

FIGURE 52 LANDING GEAR EXPLODED VIEW

FIGURE 53 GANT CHART

List of Tables

TABLE 1 SUMMARY OF LOADING REQUIREMENTS

TABLE 2 TYPE III TIRES – ENGINEERING DATA

TABLE 3 TIRE REQUIREMENTS AND SPECIFICATIONS

TABLE 4 MATERIAL PROPERTIES AND COST FOR VARIOUS STEELS

TABLE 5 PROPERTIES OF AISI 5160

TABLE 6 SUMMARY OF SELECTED COMPONENT PARAMETERS AND DIMENSIONS

TABLE 7 HEAT SINK MATERIALS COMPARISON [1]

TABLE 8 CYCLES FOR VARIOUS LANDING CONDITIONS

TABLE 9 PARAMETERS FOR STRUT SHAFT CALCULATIONS

TABLE 10 SUMMARY STRUT SHAFT DESIGN

TABLE 11 STRUT BODY DESIGN SUMMARY

TABLE 12 SUMMARY OF MATERIAL SELECTION FOR TORQUE LINK

TABLE 13 SUMMARY OF TORQUE LINK REQUIREMENTS

TABLE 14 SUMMARY OF FORK DESIGN

TABLE 15 REQUIREMENTS FOR FORK

TABLE 16 SUMMARY OF FORK DESIGN

TABLE 17 BILL OF MATERIALS FOR ONE MAIN LANDING GEAR

List of Graphs

GRAPH 1 SHAFT COST FACTOR AND WEIGHT FOR DIFFERENT STEEL FAMILIES

GRAPH 2 MOTION STUDY OF STRUT DISPLACEMENT DURING LANDING

GRAPH 3 MOTION STUDY OF STRUT VELOCITY DURING LANDING

GRAPH 4 MOTION STUDY OF STRUT ACCELERATION DURING LANDING

Section 1: Introduction

1. Introduction

1.1 Goals and requirements

The goal of this project is to design a landing gear for a small plane that is 66% lighter than the Piper Arrow IV. The landing configurations that were analysed during my redesign stage were: worse case landing (level landing- nose wheel clear), level landing with inclined reactions and hard landings (approach speed higher than 10 ft/s).

The landing gear of an aircraft has several functions: it keeps the aircraft stable on the ground, during loading, unloading and taxing and absorbs the landing shocks. The main landing gear must also satisfy its function not to produce drag (retractability) as well as other specifications (overall size, maintenance, servicing, number of landings, etc.). The critical functions are that it opens safely before landing and safely lock into position.

The design is constrained by having to optimize material selection for weight and cost and applicable standards. Limitations in the design include the knowledge of the designer. Though an ideal design would be an optimization of weight reduction, low cost and would minimize maintenance requirements; the primary goal in designing this landing gear is to minimize its total weight.

There are several FAR standards that will be respected at each step in the design process, namely *Part 25 – Airworthiness standards: transport category airplanes*. Subpart D contains landing gear requirements, which includes general requirements as well as requirements on the retracting mechanism, wheels, tires, brakes/braking system and shock absorption tests.

The retracting mechanism must be designed for flight condition loading when the gear is extended up to 67% of cruise speed. Also, there must be an emergency means for extending the landing gear. The main landing gear wheels must be designed for maximum weight. Similarly, the tires must be designed for loads corresponding to the most critical combination of airplane weight. The braking system must be capable of bringing the airplane to rest in less than two times the regular landing distance, in the event of a failure of an element in the brake system.

1.2 Proposed solution

1.2.1. Problem statement

The main landing gear of Piper Arrow 28-201 R is to be re-designed in order to reduce its weight. Furthermore, the new technologies made it possible to design an aircraft that weighs less with an improved performance. In this report, a few technological advancements related to landing gear, such as materials, configuration, kinematics, etc. will be studied in order to assess how to implement these new and improved technologies into the original design, taking all the original design criteria into consideration.

1.2.2. Design procedures

In order to solve a design problem, there are nine steps that must be followed:

1. Recognizing the need
2. Defining the problem
3. Planning the project
4. Gathering information
5. Conceptualizing alternative approaches
6. Evaluating the alternatives
7. Selecting the best alternative
8. Communicating the design
9. Implementing the preferred design

At the beginning of a design process, the original design must be analyzed and inspected in order to determine what are the most important parts and features and which parts could be replaced or redesigned to achieve a newer, better and more efficient design. For the Piper Arrow landing gear, the analysis was carried out on an individual part-by-part basis. A force analysis was performed for each part in order to determine the minimum dimension each part must have so as to avoid failures during the operation. The next step in designing the aircraft would be to select from a wide range of possible designs, dimensions and materials. This will take place by eliminating the heavier and/or weaker alternatives available. Once the elimination has occurred, the designer must choose some parameters that are deemed to be more necessary and essential than others.

Finally, the designer will choose the best design and materials for the landing gear of this specific aircraft.

1.2.3. Design constraints

During the design process, a set of constraints has been respected for every proposed solution. In addition to that, analyses have been made in order to check if the proposed solutions comply with these constraints. The design constraints taken into consideration include: Federal Aviation Regulations (FAR), performance (ground and flight), margins of safety, reliability, and cost.

It is noted that these constraints are inter-connected and they sometimes even contradict each other. However, one of the designer's responsibilities is to find a solution that respects all the constraints as much as possible. In special cases, if a constraint was not to be met, the results of this noncompliance must be studied to make sure the design is safe and can be implemented into the aircraft's system.

1.2.4. Proposed solutions

The main purpose of this design is to reduce the mass of the main landing gear. As discussed in the design process, a few solutions are proposed in the conceptual phase, then refined during the preliminary phase and finally implemented in the detailed phase. Here are the changes to the original design that have been proposed:

- Brake Material
- Rim Material
- Tire Replacement
- Fork Design
- Torque Link design
- Shaft and strut design
- Re-designing oversized parts

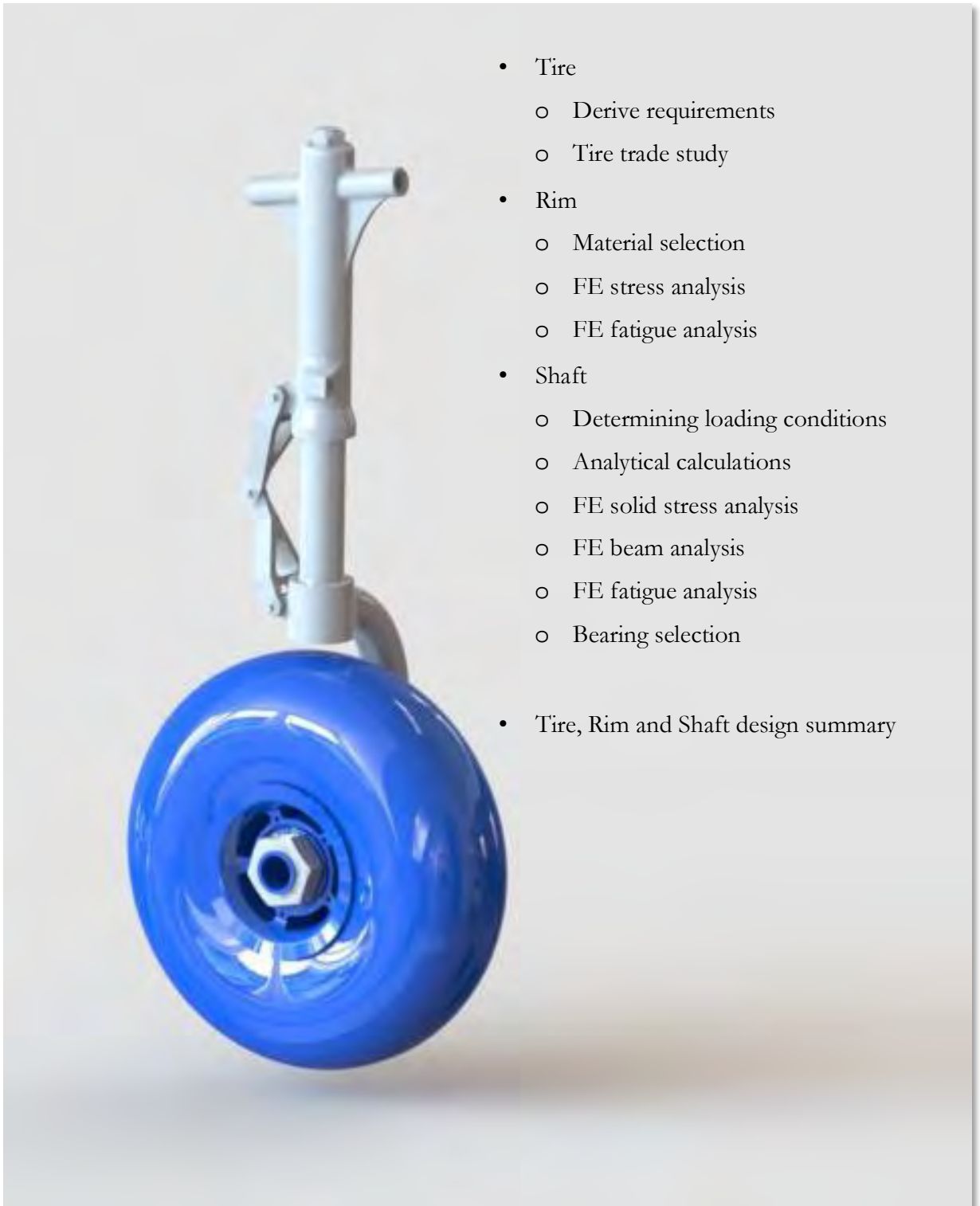
Each one of these proposed solutions has been studied and is discussed further in this report. According to the results, the new design of this aircraft's landing gear will use the solutions that prove to be the most efficient and effective.

Section 2: Design of main components.



2. Design of main components.

2.1 Tire, Rim and Shaft



2.1.1 Specific Tire Requirements

1. FAR requirements

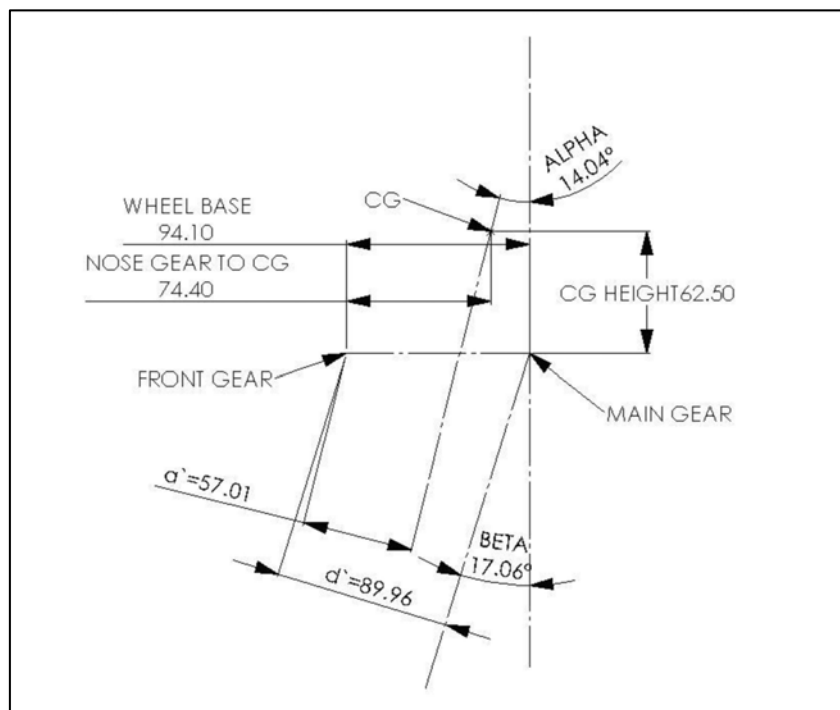
- FAR 25.729 Section 731 – Wheels:
 - Each main wheel must be approved.
 - Designing with maximum weight and critical center of gravity, the maximum static load rating of each wheel may not be less than the corresponding static ground reaction.
 - Means must be provided of preventing overpressure burst.
- FAR 25.733 – Tires:
 - When a landing gear axle is fitted with a single wheel and tire assembly, the wheel must be fitted with a suitable tire of proper fit with a speed rating approved by the Administrator that must account for maximum loading

2. Model-specific requirements

- The tire, rim and shaft must be able to support the corresponding fraction of the weight of the aircraft. The weight of the aircraft is taken as 1914lbs (66% of the original weight of 2950lbs). An assumed factor of safety of 1.5 will be used.

Calculate expected static load on each wheel using the modified weight, the CG position and the wheel base values.

FIGURE 1 GRAPHICAL DETERMINATION OF CG



$$\sum M_{about\ nose\ datum} = 0$$

$$2F_{main\ LG} = FS \frac{(W)(74.4)}{(94.1)} = 1.5 \frac{(1914\ lbs)(74.4\ in)}{(94.4\ in)}$$

$$F_{main\ LG\ after\ SF} = 1200\ lbs$$

After applying the Factor of Safety, the required static load that the tire should support is 1200 lbs.

- The tire, rim and shaft must be capable of operating at a maximum landing velocity of the airplane. Calculations can be found below:

$$Ground\ roll = \frac{V_{app}^2}{2 \cdot (deceleration\ of\ airplane\ on\ track)}$$

Where the ground roll is 645 ft. as per the specifications of the plane manual and the deceleration of the airplane on the track is assumed as $0.3 \cdot g$:

$$g = 32.2 \frac{ft}{s^2} = 9.81 \frac{m}{s^2} \quad mph\ (miles\ per\ hour) = 1.46667 \frac{ft}{s}$$

$$V_{app} = \sqrt{Ground\ roll \cdot 2 \cdot 0.3 \cdot g} = \sqrt{645\ ft \cdot 2 \cdot 0.3 \cdot 32.2 \frac{ft}{s^2}} = 111.634 \frac{ft}{s}$$

$$V_{app} = \frac{111.634}{1.46667} = 76\ mph$$

$$V'_{app} = FS \cdot V_{app} = 1.5 \cdot 76 = 114\ mph$$

The tire must support a maximum landing velocity of 114 mph.

- The tire, rim and shaft must be capable of bringing the plane to a stop over the ground roll. Calculations can be found below:

$$F_{brake} = A_{gr} \cdot \frac{W}{g} = 0.7 \cdot g \cdot \frac{1914}{g} = 1340\ lbs$$

Where the average ground roll deceleration is $A_{gr} = 0.7 \cdot g$ as the worst-case scenario. Note that the FS is not applied because 0.7 is the theoretical maximum deceleration that tires can provide without slip.

So, the maximum braking force that each tire should provide is 1340 lbs (assuming that the plane is capable of coming to a stop with one functional brake only.)

- The tire, rim and shaft must be capable of supporting the worst-case scenario standard landing conditions. Calculations can be seen below:

Assumptions:

- $n = 3.5$
- L = the ratio of the assumed wing lift to the airplane weight, but no more than 0.667. Assume worst case scenario - 0.667
- $W = 1914$ lbs, the weight of the aircraft
- $K = 0.25$

Loading of both main landing gears for level landing, nose wheel clear:

$$V_R = (n - L) \cdot W = (3.5 - 0.667) \cdot 1914 = 5422 \text{ lbs}$$

$$D_R = K \cdot n \cdot W = 0.25 \cdot 3.5 \cdot 1914 = 1675 \text{ lbs}$$

Therefore, the worst-case level landing reaction forces that the tire, rim and shaft must support are:

$$F_{vertical} = \frac{V_R}{2} = \frac{5422}{2} = 2711 \text{ lbs}$$

$$F_{horizontal} = \frac{D_R}{2} = \frac{1675}{2} = 838 \text{ lbs}$$

$$F_{resultant} = \sqrt{V_R^2 + D_R^2} = 2880 \text{ lbs}$$

- The tire, rim and shaft must be capable of surviving a hard landing. Hard landing is defined as a landing with a sink speed of 10ft/s or more

TABLE 1 SUMMARY OF LOADING REQUIREMENTS

Requirement type	Requirement statement	Requirement target value
FAR	Use of Factor of Safety (FS)	1.5
Model-specific	Support static weight of aircraft	1200 lbs
Model-specific	Support maximum landing velocity	114 mph
Model-specific	Maximum braking force	1340 lbs
Model-specific	Level landing, nose gear clear, max vertical force	2711 lbs
Model-specific	Level landing, nose gear clear, max horizontal force	838 lbs
Model-specific	Level landing, nose gear clear, max resultant force	2880 lbs
Model-specific	Worst case landing	4233 lbs

2.1.2 Tire Trade Study

The weight of the plane has been reduced by 33%, which is not a significant enough change to require the use of a different type of tires. For this reason, Type III tires will be chosen, same as the original design:

TABLE 2 TYPE III TIRES – ENGINEERING DATA

TIRE DATA

*Table IV Type III Tires — Engineering Data

Size	Construction Ply Rating TT or TL	Service Rating					Inflated Dimensions (in.)										Wheel (in.)					
		Speed (mph)	Load (lbs)	Infl. (psi)	Max Braking (lbs)	Bot. Load (lbs)	Tread Design	Weight (lbs)	Outside Dia	Section Width	Shoulder Dia	Width	Loaded Rad (in.)	Flat Tire Rad (in.)	Aspect Ratio	1 = Width Between Flanges 2 = Ledge Diameter 3 = Flange Height 4 = Min Ledge Width						
									Max	Min	Max	Max				Size	1	2	3	4		
3.50-8	4 TT	40	770	45	1,120	2,100	Rib	2.8	12.80	12.40	3.70	3.45	5.3	4.4	923	3.50-8	2.45	6.000	.563			
3.50-6	6 TT	40	1,200	70	1,740	3,200	Rib	2.8	12.80	12.40	3.70	3.45	5.3	4.5	923	3.50-6	2.45	6.000	.563			
5.00-4	4 TT	120	700	25	1,020	1,900	Rib	3.8	13.25	12.70	9.05	4.75	11.60	4.80	915	5.00-4	3.50	4.000	.750	.800		
5.00-4	6 TT	120	1,200	55	1,740	3,240	Rib	3.9	13.25	12.70	9.05	4.75	11.60	4.80	915	5.00-4	3.50	4.000	.750	.800		
5.00-5	4 TT	120	800	31	1,160	2,200	Rib	4.8	14.20	13.65	4.95	4.65	12.55	4.20	929	5.00-5	3.50	5.000	.750	.800		
5.00-5	6 TT	120	1,260	50	1,830	3,400	Rib	4.7	14.20	13.65	4.95	4.65	12.55	4.20	929	5.00-5	3.50	5.000	.750	.800		
5.00-5	8 TT	120	1,285	50	1,865	3,300	Rib	4.8	14.20	13.65	4.95	4.65	12.55	4.20	929	5.00-5	3.50	5.000	.750	.800		
6.00-6	4 TT	120	1,150	29	1,670	3,100	Rib	7.7	17.50	16.80	6.30	5.90	15.45	5.35	913	6.00-6	5.00	6.000	.750	.800		
6.00-6	6 TT	120	1,730	42	2,340	4,700	Rib	7.7	17.50	16.80	6.30	5.90	15.45	5.35	913	6.00-6	5.00	6.000	.750	.850		
6.00-6	8 TT	120	2,350	55	3,410	6,300	Rib	7.3	17.50	16.80	6.30	5.90	15.45	5.35	913	6.00-6	5.00	6.000	.750	.900		
6.50-8	4 TT	120	1,500	30	2,180	4,000	Rib	11.7	19.85	19.15	6.90	6.50	17.70	5.85	858	6.50-8	3.25	8.000	.812	.800		
6.50-8	6 TT	120	2,300	51	3,340	6,200	Rib	12.0	19.85	19.15	6.90	6.50	17.70	5.85	858	6.50-8	3.25	8.000	.812	.850		
6.50-8	8 TT	120	3,150	75	4,570	8,500	Rib	12.4	19.85	19.15	6.90	6.50	17.70	5.85	858	6.50-8	3.25	8.000	.812	.900		
6.50-10	6 TT	120	2,770	60	4,020	7,500	Rib	13.0	22.10	21.35	8.45	8.20	19.90	5.65	911	6.50-10	4.75	10.000	.812	.850		
6.50-10	8 TT	120	3,750	80	5,440	10,100	Rib	14.9	22.10	21.35	8.45	8.20	19.90	5.65	908	6.50-10	4.75	10.000	.812	.850		
6.50-10	10 TT	120	4,750	100	6,890	12,800	Rib	14.2	22.10	21.35	8.45	8.20	19.90	5.65	911	7.0				1,100		
7.00-6	4 TT	120	1,250	23	1,810	3,400	Rib	10.8	18.75	18.00	7.00	6.60	16.45	5.95	7.3	4.8	909	7.00-6	5.00	6.000	.750	.800
7.00-6	6 TT	120	1,900	38	2,760	5,100	Rib	10.6	18.75	18.00	7.00	6.60	16.45	5.95	7.3	4.6	909	7.00-6	5.00	6.000	.750	.850
7.00-6	8 TT	120	2,550	54	3,700	6,900	Rib	10.4	18.75	18.00	7.00	6.60	16.45	5.95	7.3	4.7	909	7.00-6	5.00	6.000	.750	.900
7.00-8	4 TT	120	1,600	30	2,320	4,300	Raw	9.6	20.85	20.10	7.30	6.85	18.55	6.20	8.3	5.6	881	7.00-8	5.50	8.000	.812	.800
7.00-8	6 TT	120	2,400	48	3,480	6,500	Raw	9.7	20.85	20.10	7.30	6.85	18.55	6.20	8.3	5.7	881	7.00-8	5.50	8.000	.812	.850
7.00-8	14 TL	139K	5,800	110	8,410	15,700	Rib	18.7	20.85	20.10	7.30	6.85	18.55	6.20	8.3	6.2	881	7.00-8	5.50	8.000	.812	1,300
7.50-10	TL	120	3,000	46	4,350	8,100	Rib	13.8	24.15	23.30	7.65	7.20	21.60	6.50	9.7	6.7	924	7.50-10	5.50	10.000	.812	.900
8.00-4	4 TT	120	1,100	24	1,600	3,000	Rib	8.3	18.00	17.15	8.30	7.80	15.50	7.05	6.7	3.5	843	8.00-4	5.50	4.000	.690	
8.00-6	4 TT	120	1,350	23	1,960	3,600	Rib	9.7	19.50	18.75	7.95	7.50	17.05	6.75	7.5	4.6	849	8.00-6	5.00	6.000	.750	.800
8.00-6	6 TT	120	2,050	35	2,970	5,300	Rib	10.7	19.50	18.75	7.95	7.50	17.05	6.75	7.5	4.7	849	8.00-6	5.00	6.000	.750	.850
8.50-6	4 TT	120	1,600	20	2,320	4,300	Rib	12.5	22.10	21.15	8.85	8.30	19.20	7.50	8.4	4.7	911	8.50-6	6.00	6.000	.875	.900
8.50-6	6 TT	120	2,275	30	3,300	6,100	Rib	12.4	22.10	21.15	8.85	8.30	19.20	7.50	8.4	4.8	911	8.50-6	6.00	6.000	.875	.900
8.50-10	8 TT	120	4,400	55	6,380	11,800	Rib	22.6	25.65	24.70	8.70	8.20	22.40	7.40	10.2	6.8	897	8.50-10	6.25	10.000	.812	1,150
8.50-10	10 TL	120	5,900	70	7,980	14,800	Rib	31.1	25.65	24.70	8.70	8.20	22.80	7.40	10.2	7.0	897	8.50-10	6.25	10.000	.812	1,350

NOTE: Sizes shown in this table were limited to a static load of 6,000 lbs. For larger capacities see manufacturers catalogs. Inflation pressure is unloaded.

Comparing the requirements to the available standard tires in the above table, 5.00-5 Ply Rating 6 tire was selected for the main landing gear. The lightest tire that meets the requirements is 5.00-4 Ply 6, however a rim diameter of 5 in was chosen because of the size of available bearings. The following table shows a comparison between the selected tire specifications and the requirements:

TABLE 3 TIRE REQUIREMENTS AND SPECIFICATIONS

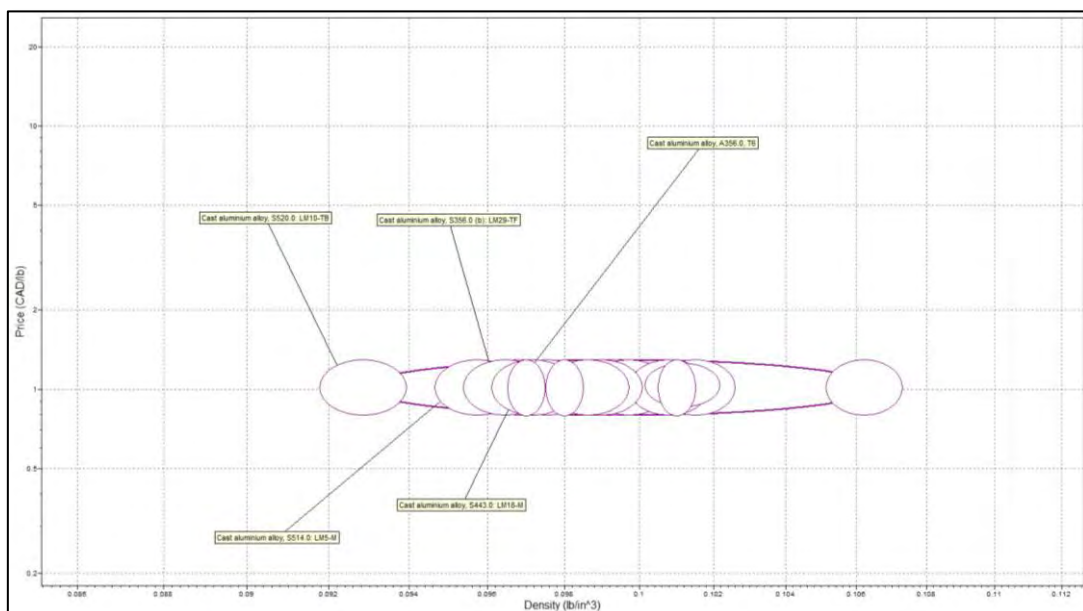
Specification type	5.00-5 Ply Rating 6	Calculated requirements
Maximum speed (mph)	120	114
Static load (lbs)	1260	1200
Maximum braking (lbs)	1830	1340
Bottom load (lbs) (worst case landing)	3400	2880

2.1.3 Material Selection for Rim

1. Rim material requirements

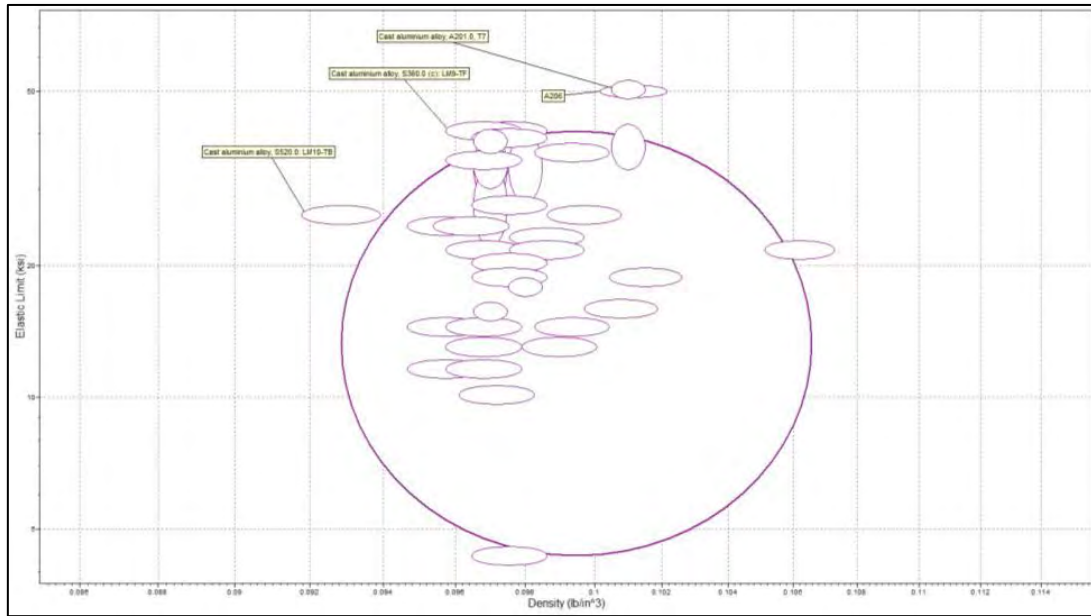
- Rims will be exposed to water, salt and other corrosive environments therefore they will be manufactured from aluminum for its corrosion resistance and light weight.
- Component needs to be easy to manufacture, but it will have an intricate shape, therefore it will be casted. Furthermore, it is important for the rims to retain their shape and casted parts are generally harder than forged ones. Any yield in the rim will have a significant effect on the balance of the tire, which is very dangerous during landing.
- List of corrosion related criteria used in CES 2005 for the aluminum selection:
 - Very good resistance to fresh water
 - Very good resistance to organic solvents
 - Good resistance to sea water
 - Very good resistance to strong acid
 - Very good resistance to UV
 - Average resistance to wear
 - Very good resistance to weak acid
 - Good resistance to weak alkalis
- Material price and density were chosen as the selection parameters. The following plot from CES 2005 illustrates the relationship between the two for all the castable aluminum alloys that meet the above requirements:

FIGURE 2 PRICE VERSUS DENSITY FOR CASTABLE ALUMINUM ALLOYS



- The price is almost the same, therefore new criteria must be chosen. A second plot is made of density versus elastic limit to select the strongest and lightest material among the potential castable aluminum alloys:

FIGURE 3 DENSITY VERSUS ELASTIC LIMIT OF CASTABLE ALUMINUM ALLOYS



2. Reasons for selecting Aluminum A356.0-T6 and key material properties

- Key mechanical properties of selected material (taken from CES 2005 database):
 - a) $S_{ut} = 24.95$ ksi
 - b) $S_y = 22.05$ ksi
 - c) Density = 0.09749 lb/in³
 - This material does not have the best density to elastic limit ration however, its mechanical properties are sufficient for the application and it is made further attractive by its wide availability and frequent use in aerospace (Source: CES 2005)
- Using 356.0-T6, a finite element model is set up with the following.

2.1.4 FEA Study of Rim during hard landing

1. Determine loading conditions:

- Tire pressure of 50 psi (from selected tire specifications).
- Bearing load of 4233 lbs (load experienced during a hard landing).
- Centrifugal force due to an angular velocity of 298 rad/s, which is the angular velocity of the tire when the plane is moving with 120 mph (the maximum tire speed).

2. Determine boundary conditions:

- Bearings are assumed to be fixed.

3. Meshing

- The complicated component geometry does not allow for a uniformly dense mesh, but since the component has many rounded and/or circular features, a curvature based mesh was used where the mesher automatically increases the density of the elements based on the radius of curvature.
- The size of the mesh was refined until the error plot started giving reasonable deviations (in the order of 20-30%, for more details please refer to discussion following the FE analysis). The following image shows the final meshing of the rim and the arrow representation of the loads and boundary conditions:

FIGURE 4 SOLID MESH OF THE RIM, LOADING CONDITIONS AND BOUNDARY CONDITIONS

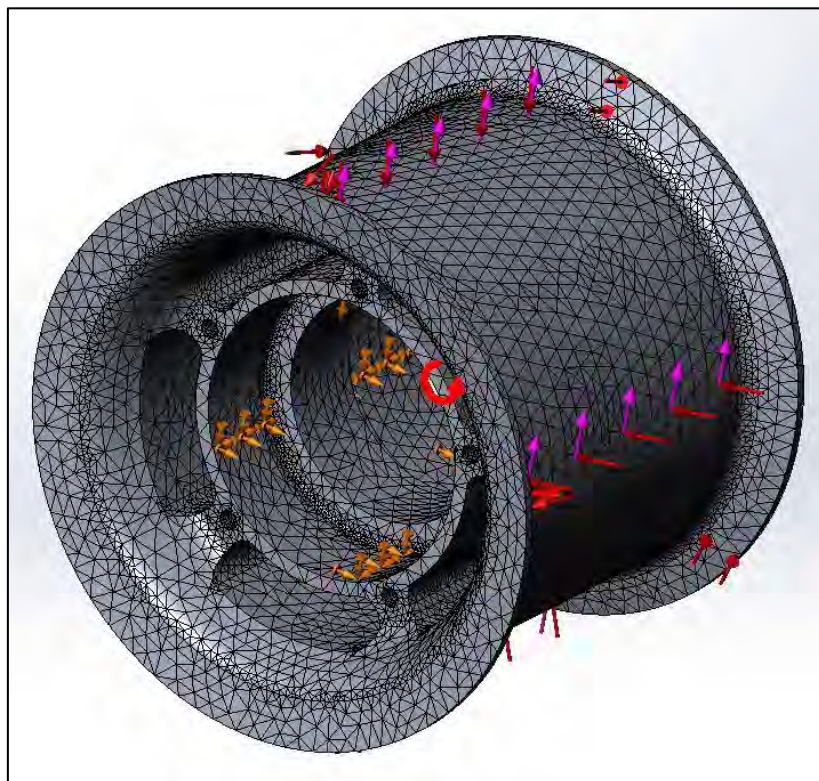


FIGURE 5 VON MISES STRESSES (PSI) EXPERIENCED BY RIM DURING HARD LANDING

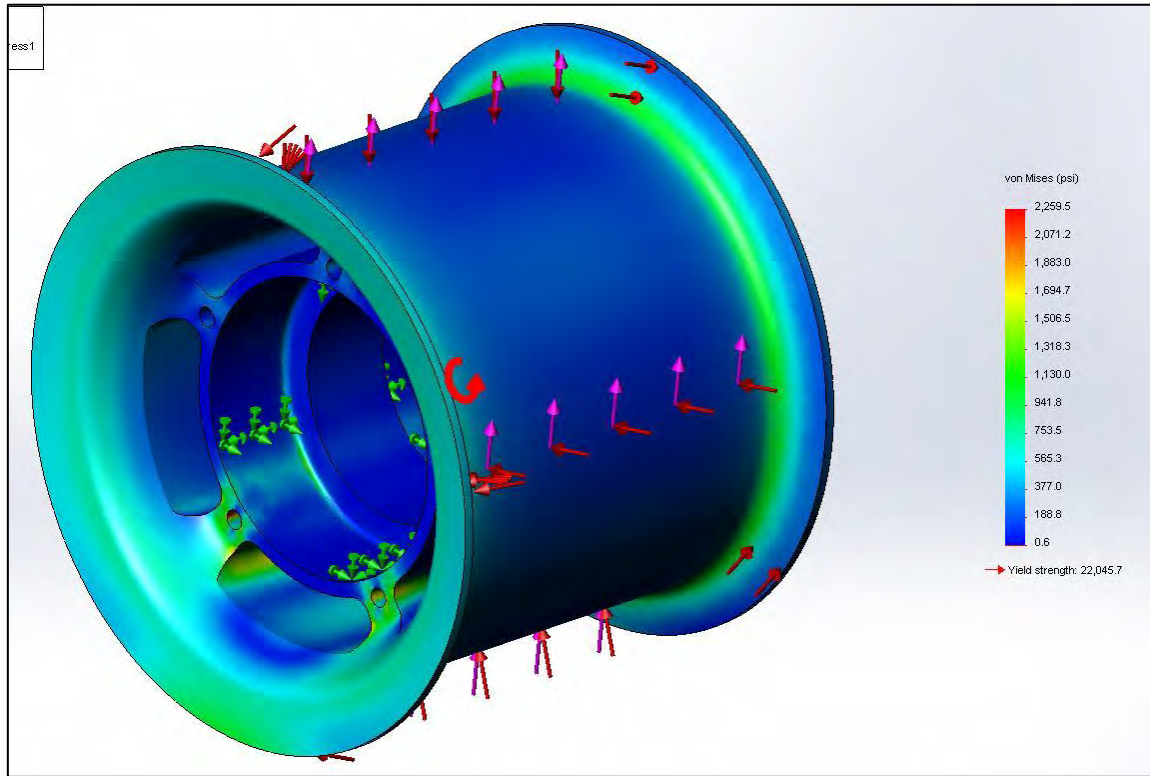
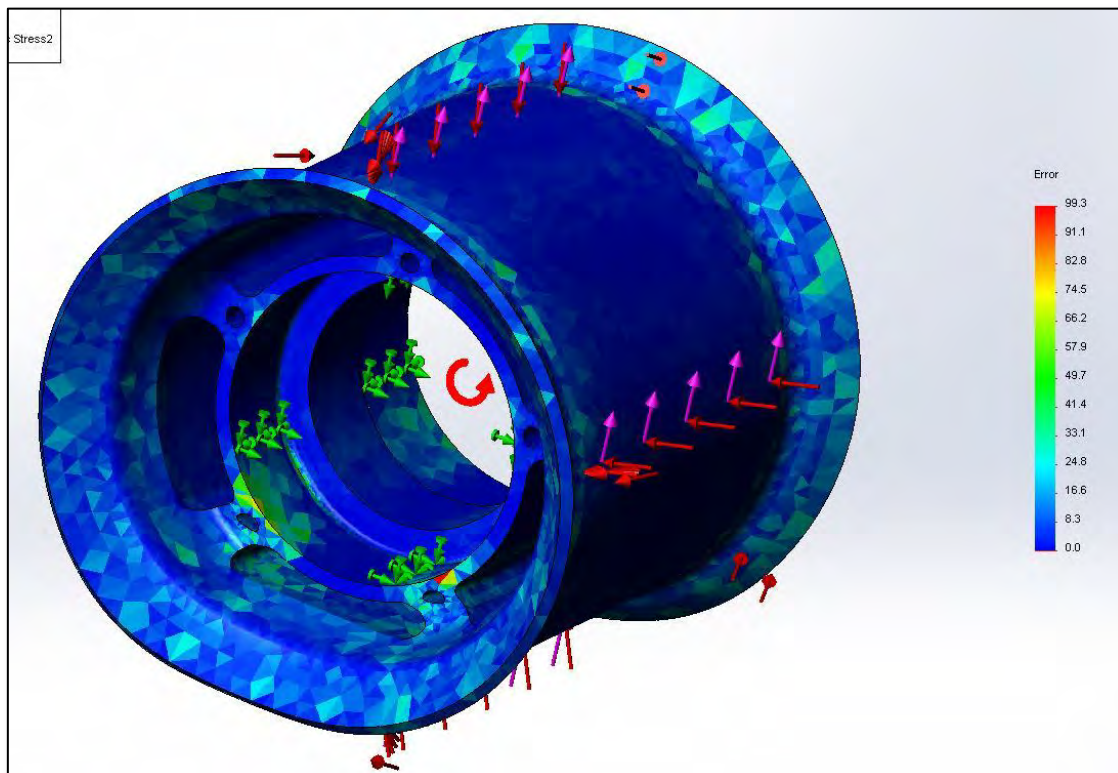


FIGURE 6 ERROR PLOT OF VON MISES STRESSES EXPERIENCED BY RIM DURING HARD LANDING



4. Discussion of FEA model for hard landing

- The error plot reveals a deviation of up to 100% in certain spots. It can be seen that upon close observation, these deviations occur near the boundary conditions and the stress concentrations in those spots are in fact wrong, so they can be ignored. The cause for this error around the boundary conditions arises from the way the part is fixed. The surface in contact with the bearing is assumed to be perfectly fixed therefore, any stress that travels through the material will eventually reach the last fixed node which cannot transmit the stress anywhere due to the boundary condition and thus – the stress concentration goes to infinity at those spots. We do know however, that in reality the stress will be transmitted further through the components (like the bearings which are not in the given model) and there will not be a stress concentration at those particular spots of the FEA model. For this reason these spots can be ignored in the analysis.
- The deviation around features, which are known to experience concentrated stresses (like the spokes), is mostly blue (~20-30%). Running the simulation with different mesh sizes shows that values are converging around a maximum von Mises stress of ~2000psi. Further mesh refinement requires too much resources, however this precision is sufficient as the yield stress of Al 356.9 T6 is ~22 ksi. Thus the factor of safety at this stage is around 10.

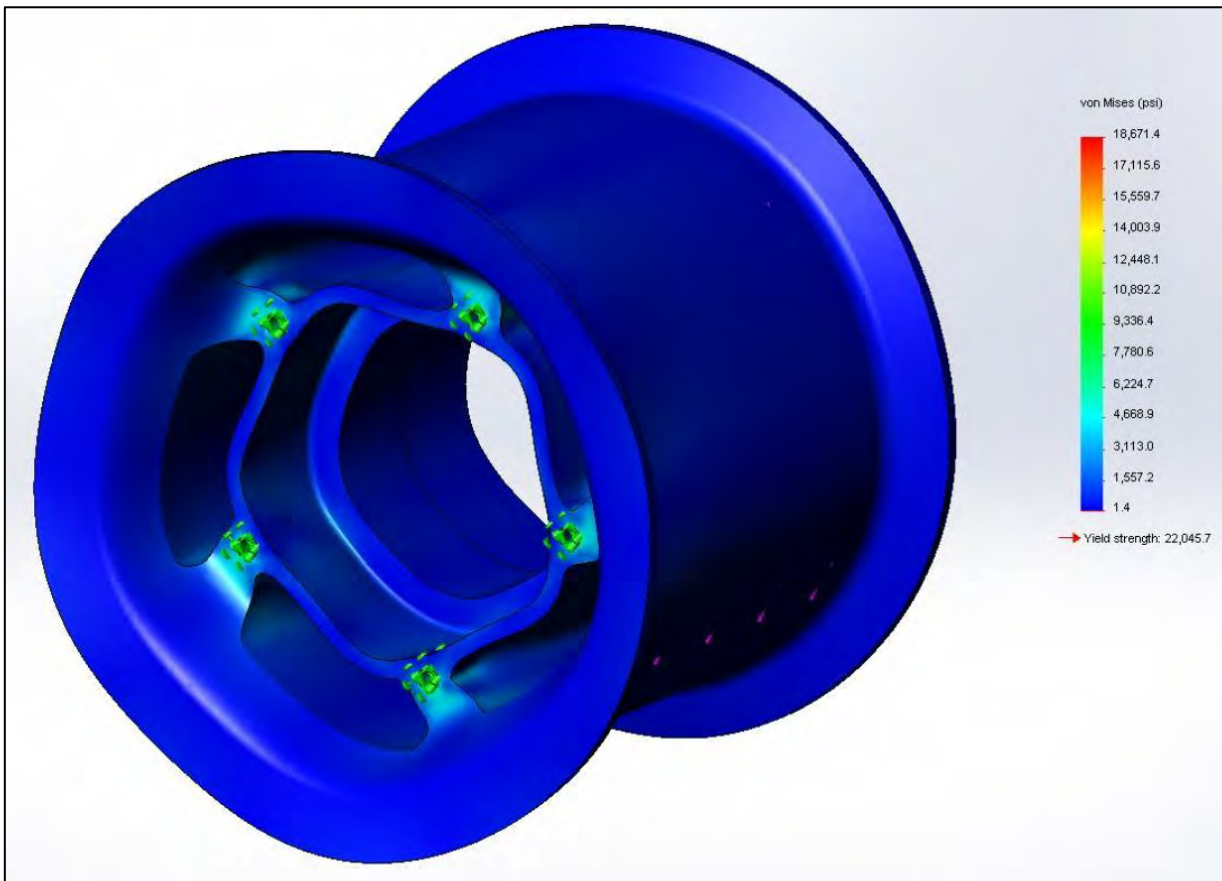
2.1.5 FEA Study of Rim during braking

During braking, the rim will experience an additional torque due to the friction in the brake. A separate simulation is made to illustrate this phenomenon.

1. Determine loading and boundary conditions:

- As calculated in the section for model specific requirements for the tire, rim and shaft components, a force of 1340lbs is required to bring the plane to a stop over the ground roll (645ft). Assuming the plane is brought to a stop by the main landing gears only, each gear will be required to provide a braking force of 670lbs.
- Therefore the torque experience by the rim due to braking is $7.1\text{in (the radius of the tire)} \times 670\text{lbs} = 4757\text{lbs-in}$.
- The same mesh is used as the previous simulation.
- The screw holes where the brake disc is mounted are assumed stationary.
- The torque is applied on the external surface of the rim, which is in contact with the tire.

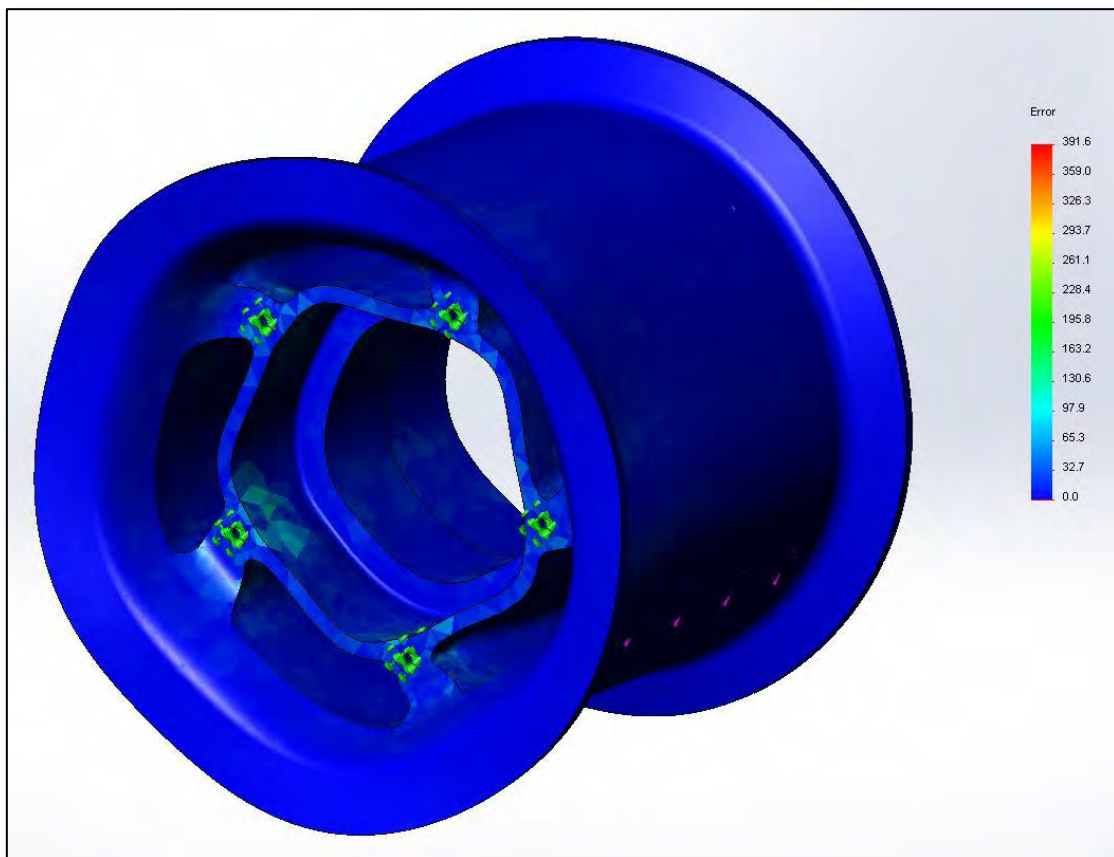
FIGURE 7 VON MISES STRESSES (PSI) EXPERIENCED BY RIM DUE TO BRAKING



2. Stress study discussion

- The maximum stress of 18.7 ksi is due to a false singularity inside the screw thread resulting from the way the boundary conditions are defined (for detailed explanations, please refer to the discussion of the error plot on the model of the rim for hard landing). Using the probing tool in Solid Works to measure stresses in specific nodes, the stress of interest is determined to be between 6 and 8 ksi in the spokes of the wheel taking under consideration the % deviation from the error plot below:

FIGURE 8 ERROR PLOT OF VON MISES STRESSES EXPERIENCED BY RIM DURING BRAKING



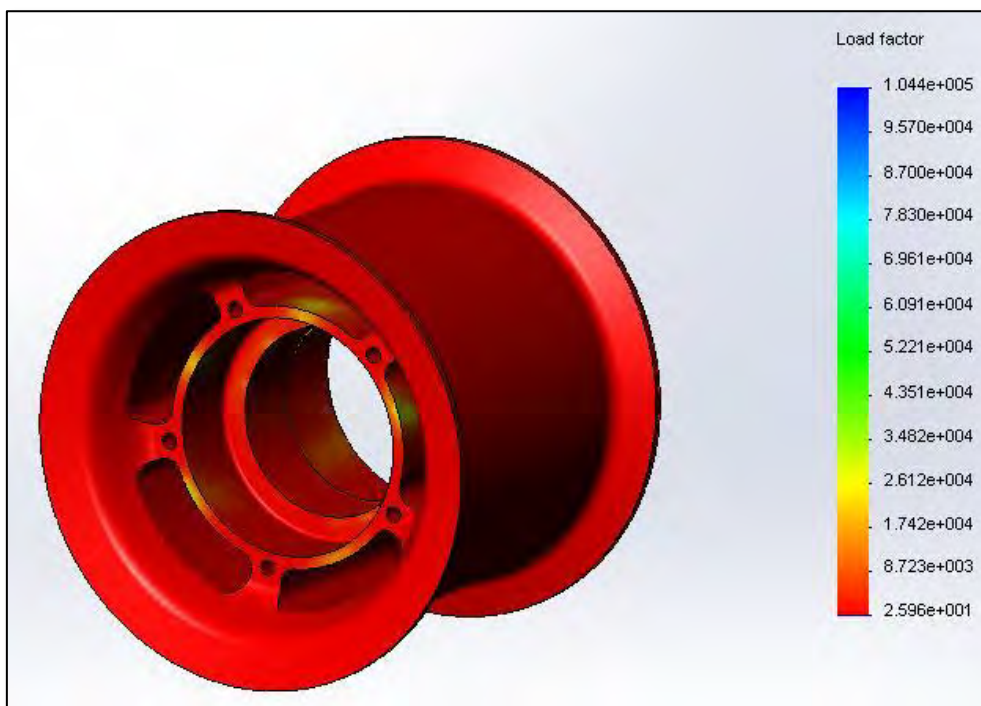
3. Error plot discussion

- Combining the two stresses in the spokes gives $\sim 10\text{ksi}$ which still gives a safety factor of around 2 (S_y for A356.0 T6 is 22ksi).
- Further refining of the FEA model could include boundary conditions for the surface in contact with the bearings and the surface in contact with the brake disc. Applying these conditions may give a more accurate result of the situation, however the current approach is more conservative and still yields sufficient strength.
- Mass optimizations were performed by thinning the spokes until obtaining a reasonable safety factor. The current thickness of each spoke is $\sim 0.44\text{in}$ at the thinnest point.
- Another way of saving material will be to find smaller bearings. A more detailed discussion can be found at the end of this section, in procurement and integration.

4. Fatigue study during braking

- Running fatigue analysis using the above specified conditions the life of the component is estimated to exceed 10^6 cycles. The load factor plot shows we need to increase the current load by a factor of 25.96 to have the material fail in $\sim 10^6$ cycles.

FIGURE 9 LOAD FACTOR FOR FATIGUE ANALYSIS OF RIM DURING HARD LANDING

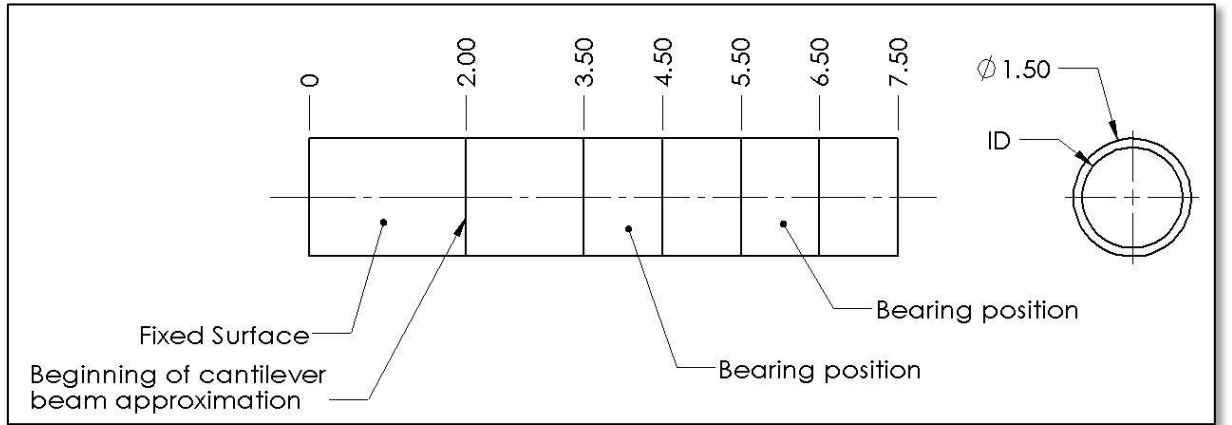


2.1.6 Shaft analytical design

1. Determining loading conditions of simplified shaft model

- Following the selection of the rim (based on the tire selection criteria) and leaving 3.5 inches to secure the shaft to the fork and to fix the brake, the following diagram of the shaft was constructed. The dimension which will be optimized is the inside diameter (ID) to minimize the weight of the shaft:

FIGURE 10 SHAFT MODEL



2. Derive deflection equations of shaft based on diagram. Note, because the shaft is treated as a cantilever beam, all the dimensions start from the 2 in. point:

$$Q(x) = -w(x - 1.5)^0 + w(x - 2.5)^0 - w(x - 3.5)^0 + w(x - 4.5)^0$$

$$V(x) = -w(x - 1.5)^1 + w(x - 2.5)^1 - w(x - 3.5)^1 + w(x - 4.5)^1$$

$$M(x) = -w(x - 1.5)^2 + w(x - 2.5)^2 - w(x - 3.5)^2 + w(x - 4.5)^2$$

Where: $w = \frac{\text{weight}}{2}$

$$M_{max} \text{ occurs at } x = 1 \rightarrow M_{max} = \frac{w}{4} \cdot 12 = 3 \cdot w$$

- Calculating the stress:

$$\sigma_{max} = \frac{M_{max}D}{2I} = \frac{3 \cdot W \cdot D \cdot 64}{2\pi(D_o^4 - D_i^4)} = \frac{96 \cdot W \cdot D}{\pi(D_o^4 - D_i^4)}$$

$$\sigma_a = \sigma_m = \frac{\sigma_{max}}{2} = \frac{48WD}{\pi(D_o^4 - D_i^4)} \text{ (Equation 1)}$$

- Calculating the fatigue concentration factors [1]:

$$C_{\text{load}}=1 \text{ (for bending load)}$$

$$C_{\text{temp}}=1 \text{ (room temperature)}$$

$$C_{\text{reliab}}=0.753 \text{ (99.9\% reliability)}$$

$$C_{\text{surface}}=2.7 \cdot (S_{\text{ut}})^{-0.265} \text{ (machined surface)}$$

$$C_{\text{size}}=0.869 \text{ Deq}^{-0.097}$$

$$A_{95}=0.010462 \quad d_o^2=0.032$$

$$\text{Deq}=(A_{95}/0.0766)^{1/2}$$

$$S_e'=0.5 \cdot S_{\text{ut}}$$

$$S_e=C_{\text{load}} C_{\text{temp}} C_{\text{reliab}} C_{\text{surface}} C_{\text{size}} S_e' \text{ (Equation 2)}$$

- Safety factor calculation for CASE III loading ($\sigma_m/\sigma_a=\text{const}$)(assume $N=1.5$)

$$N = \frac{S_e \cdot S_{\text{ut}}}{\sigma_a S_{\text{ut}} + \sigma_m S_e}$$

$$\sigma_a = \frac{S_e \cdot S_{\text{ut}}}{N(S_{\text{ut}} + S_e)} \text{ (Equation 3)}$$

- Combining Equation 2 and Equation 3:

$$\frac{48WD}{\pi(D_o^4 - D_i^4)} = \frac{S_e \cdot S_{\text{ut}}}{N(S_{\text{ut}} + S_e)}$$

$$D_i^4 = D_o^4 - \frac{48 \cdot W \cdot D \cdot N \cdot (S_{\text{ut}} + S_e)}{\pi \cdot S_e \cdot S_{\text{ut}}}$$

- The derived above equation describes the size of the internal shaft diameter as a function of the external diameter and safety factor for repeated fluctuating stresses. The loading is assumed to vary from the maximum loading during landing to zero. S_e is the corrected endurance strength and S_{ut} is the ultimate tensile strength of the material.

2.1.7 Trade study on shaft material

1. High level material selection:

- Aluminum alloys will not be used for the shaft because aluminum will always fail eventually due to fatigue. Furthermore, preliminary calculations reveal that the maximum expected stress in the shaft is 38.3 ksi for hard landings, which is too close to the yield stress of most Al alloys. Lastly, the maximum tensile stress is too low for the specific application.
- Titanium, magnesium and nickel alloys are too expensive or too weak for the application.
- Steel is the most appropriate material for the specific application

2. The following table shows preliminary calculations for potential steel families, their expected mass and material cost (note the material cost was used as a factor for comparison assuming that the cheaper material is also cheaper to manufacture/machine):

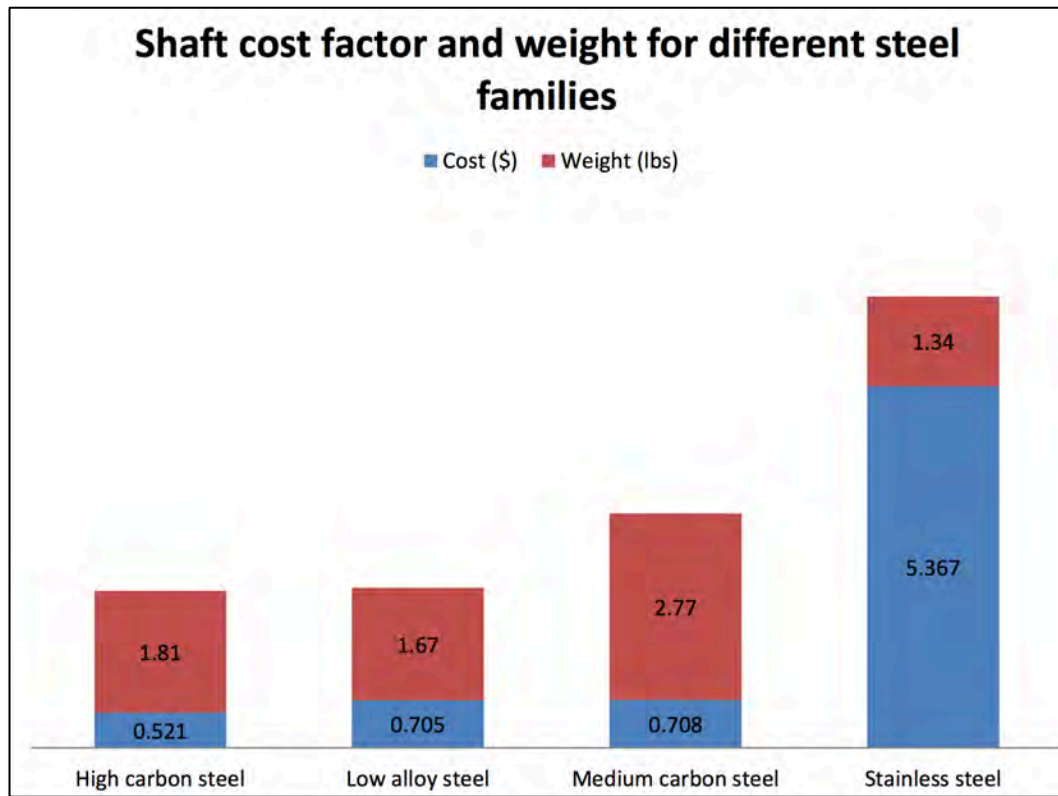
TABLE 4 MATERIAL PROPERTIES AND COST FOR VARIOUS STEELS

Material	High carbon steel	Low alloy steel	Low carbon steel	Medium carbon steel	Stainless steel
S_{ut} (ksi)	237.9	255.3	84.12	174	324.9
S_y (ksi)	167.5	217.6	57.29	130.5	145
S_e (ksi)	47.39		22.07	37.66	59.59
W hard landing (lbs)	4233	4233	4233	4233	4233
W worst landing (lbs)	2880	2880	2880	2880	2880
ID, hard landing (in)	1.08	1.12	FAIL	0.78	1.21
ID, worst landing (in)	1.26	1.28	FAIL	1.17	1.33
σ_{max} , hard landing (ksi)	52.69	55.67	FAIL!	41.28	67.14
σ_{max} , worst landing (ksi)	52.69	55.67	FAIL	41.28	67.14
S_y/σ_{max} , hard landing	3.18	3.91	FAIL	3.16	2.16
S_y/σ_{max} , worst landing	3.18	3.91	FAIL	3.16	2.16
Density (lb/in ³)	0.29	0.29	0.29	0.29	0.29
Mass (ID hard landing) (lbs)	1.81	1.67	#NUM!	2.77	1.34
Mass (ID worst landing) (lbs)	1.09	1.02	#NUM!	1.49	0.85
Cost (\$/kg)	0.4762	0.6878	0.4762	0.4762	6.349
Cost (\$)	0.521	0.705	#NUM!	0.708	5.367
Does the material satisfy the requirements?	YES	YES	NO	YES	YES

3. Values were taken from CES material selection software 2005

4. The following table shows the shaft cost factor (the material cost) and the weight for different steel families:

GRAPH 1 SHAFT COST FACTOR AND WEIGHT FOR DIFFERENT STEEL FAMILIES



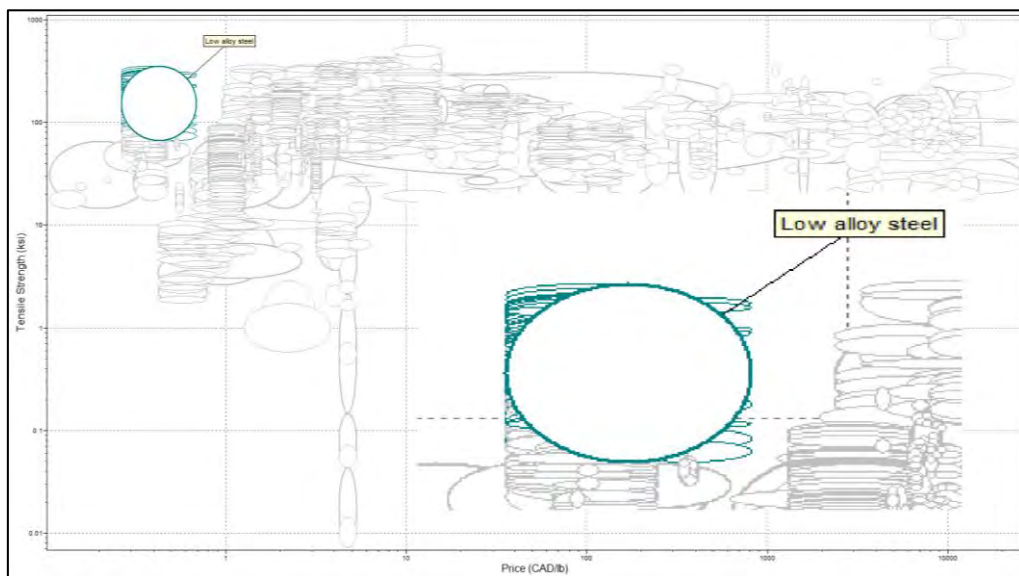
5. Low alloy steel seems like the most appropriate choice. Stainless steel has good corrosion resistance but it is very expensive and not strong enough (thus the high weight). Low alloy steel is not the cheapest solution but the difference in price is justified by the lower weight. Furthermore, high carbon steels will tend to be harder and thus more expensive to machine and more brittle. Therefore, low alloy carbon steel will be used for the shaft

6. Browsing through the materials in CES 2005, the following criteria were selected to choose a steel from the low alloy steel family:

- a. Material should be available in shapes like tubes or rods
- b. Material should have:
 - i. High resistance to flammability
 - ii. Good resistance to fresh water
 - iii. Good resistance to organic solvents
 - iv. Average resistance to sea water
 - v. Average resistance to strong alkalis
 - vi. Good resistance to UV
 - vii. Very good resistance to wear
 - viii. Average resistance to weak acid
 - ix. Good resistance to weak alkalis

Applying the above conditions to low alloy steels gives the following region of materials:

FIGURE 11 SHAFT MATERIAL SELECTION



Out of the low alloy steels the strongest and cheapest material available is AISI 5160 tempered@205C, oil quenched. Therefore, this will be the shaft material. The table below shows the calculations for the shaft using AISI 5160:

TABLE 5 PROPERTIES OF AISI 5160

Material	AISI 5160
S_{ut} (ksi)	354.6
S_y (ksi)	286.4
S_e (ksi)	63.55
W hard landing (lbs)	4233
W worst landing (lbs)	2880
ID, hard landing (in)	1.24
ID, worst landing (in)	1.34
$\sigma_{max,hard\ landing}$ (ksi)	71.86
$\sigma_{max,worst\ landing}$ (ksi)	71.86
$S_y/\sigma_{max,hard\ landing}$	3.99
$S_y/\sigma_{max,worst\ landing}$	3.99
Density (lb/in ³)	0.2854
Mass (ID hard landing) (lbs)	1.20
Mass (ID worst landing) (lbs)	0.76
Cost (\$/kg)	0.4762
Cost (\$)	0.36

2.1.8 Finite element solid and beam analysis of shaft

1. Finite element model of the shaft using Solid Works (a custom material AISI 5160 was defined using properties from CES 2005)
 - a. Model the shaft as a solid model, 5.5in long cantilever beam and bearing load of 4233lbs (hard landing) over the position of the bearings. The bearing load has a sinusoidal distribution; the green arrows indicate which surface is fixed (in this case, the cross-sectional surface)
 - b. For preliminary calculations, a course solid mesh was defined as illustrated below:

FIGURE 12 SOLID MESHING OF SHAFT FOR FEA

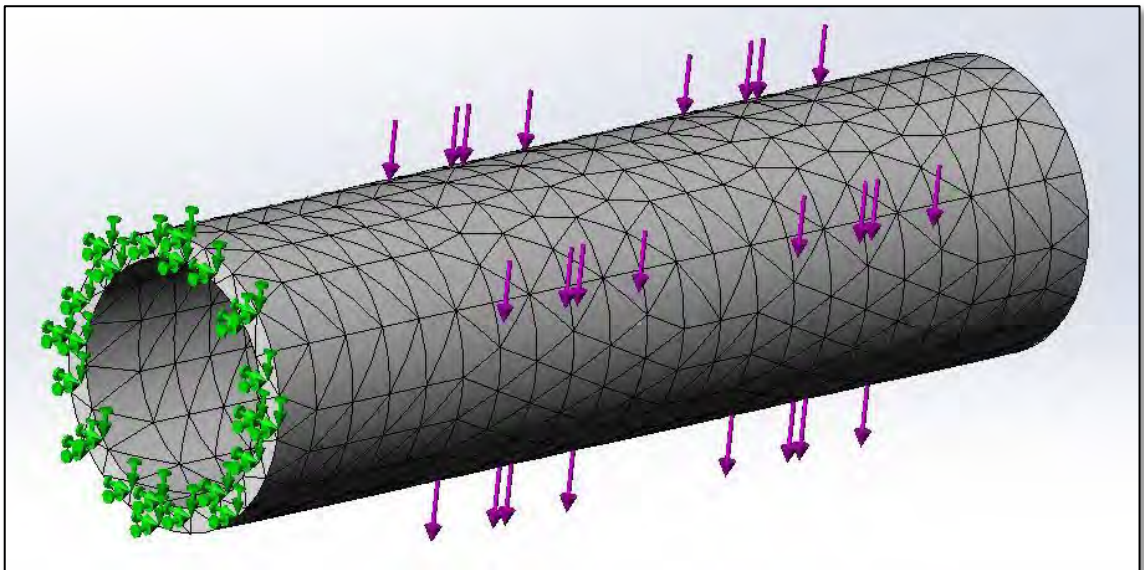
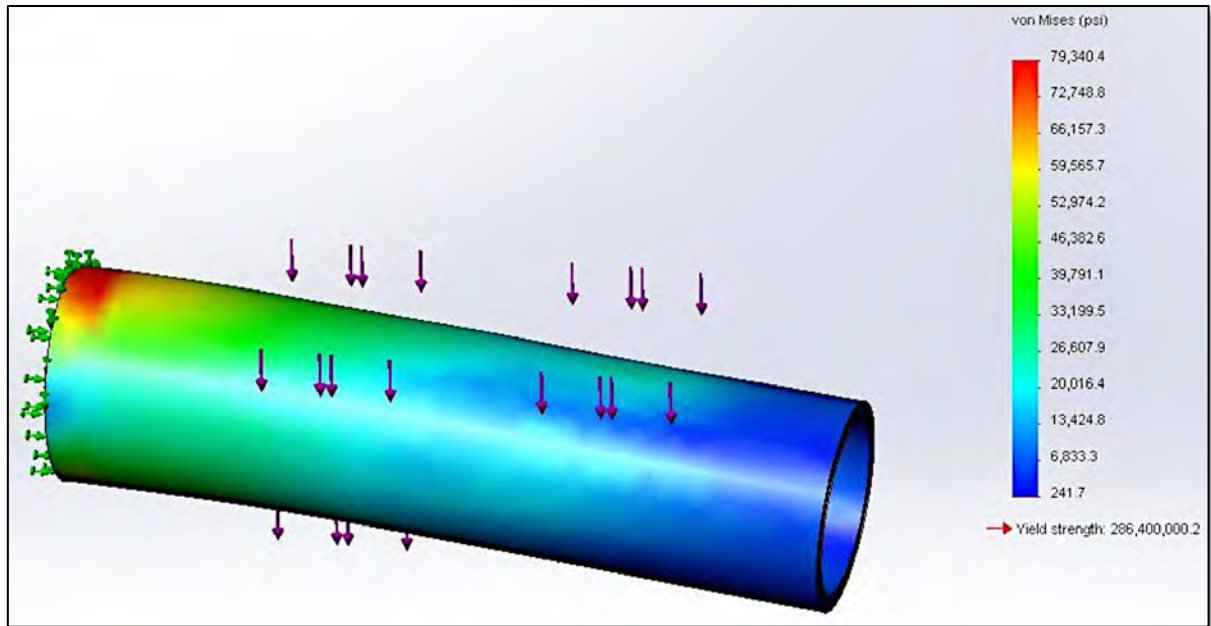
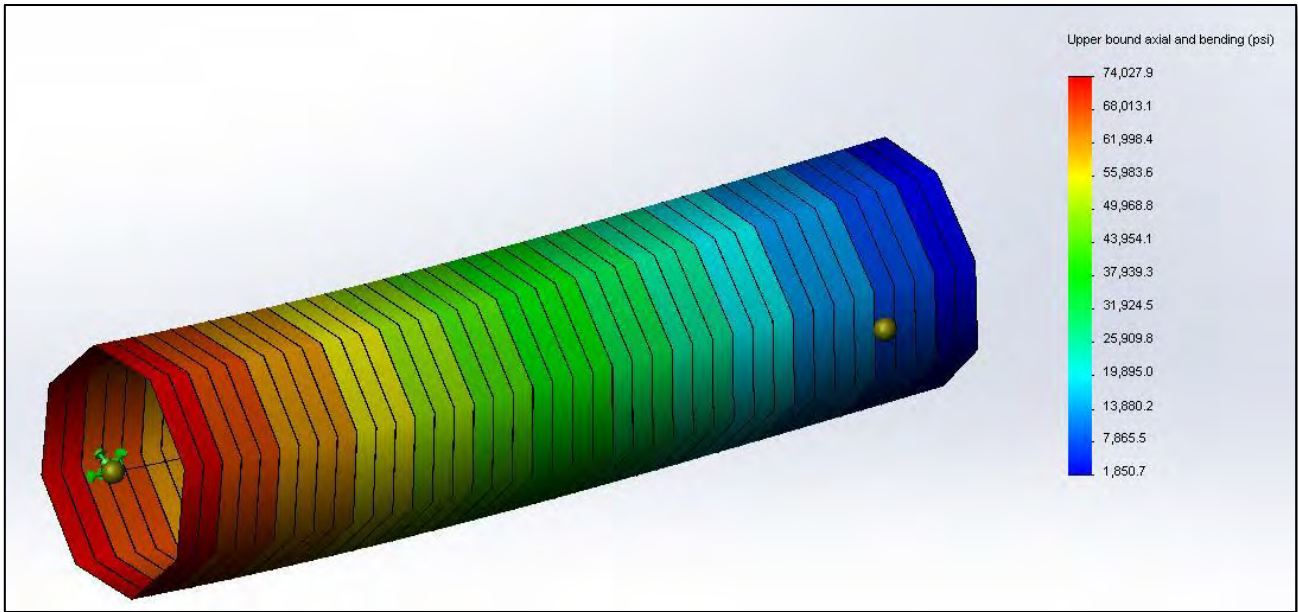


FIGURE 13 VON MISES STRESSES EXPERIENCED BY SHAFT DURING HARD LANDING



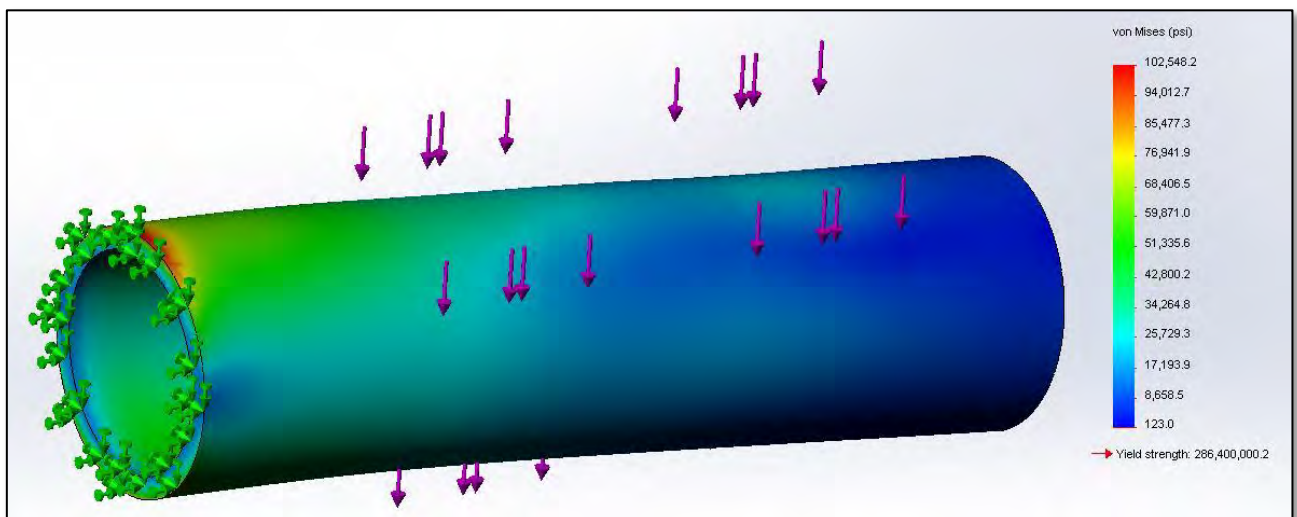
2. Ignoring the stress concentration due to the constraint conditions (for more information please refer to the discussion of the rim FEA model for hard landing above) the approximate maximum stress is between 72 and 80 ksi. In order to further refine the simulation, the shaft is then modeled as a beam in a second study. Note that for simplicity the load is modeled as an equivalent load of 2309 lbs applied at the end of the cantilever. This load will result in the same moment about the base of the cantilever, which is the area of interest for this study. In this case the stresses will be accurate, but not the final displacement:

FIGURE 14 SHAFT MODELED AS A BEAM FOR FEA ANALYSIS



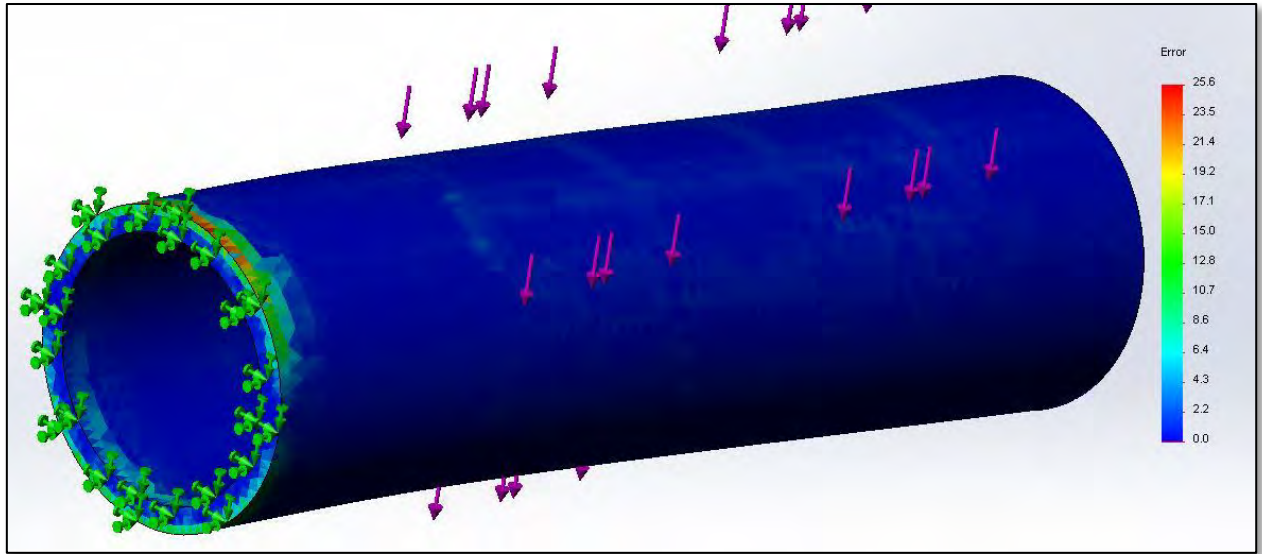
3. This time the results are much more accurate. Modeling the shaft as a 40 element cantilever beam gives a maximum stress of 74 ksi which is very close to the theoretical calculation of 71.86 ksi. The mesh in the solid FEA model is now refined to match the maximum expected stresses

FIGURE 15 FEA MODEL OF VON MISES STRESSES EXPERIENCED BY SHAFT DURING HARD LANDING (REFINED MESH)



4. The values near the fixed surface are suspiciously high (102 ksi). This is due to the location of a false stress concentration arising from the way the fixture is defined. This can be observed better in the error plot below:

FIGURE 16 ERROR PLOT FOR SHAFT FEA ANALYSIS

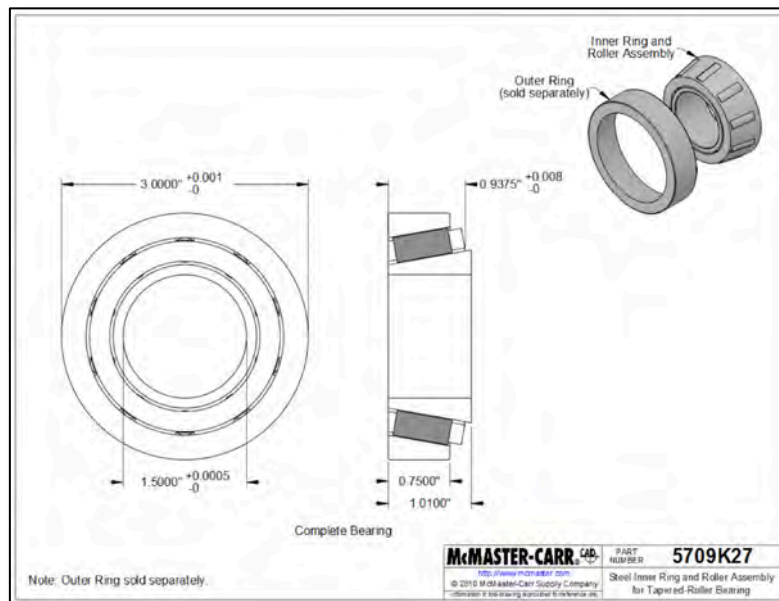


5. The error is listed in percent so taking 25.6% off 102.55 ksi gives 76.3 ksi. The model can now be used for further FEA analysis

2.1.9 Bearing selection

A bearing was selected from McMaster Carr's inventory with the following characteristics: radial load capacity of 4690lbs and thrust load capacity of 2430lbs. This was the only tapered bearing that could carry the expected loads during hard landing. It may be possible to find smaller tapered bearings, which will allow for some weight reduction by removing material from the rim:

FIGURE 17 BEARING DIMENSIONS



2.1.10 Summary of tire, rim and shaft design

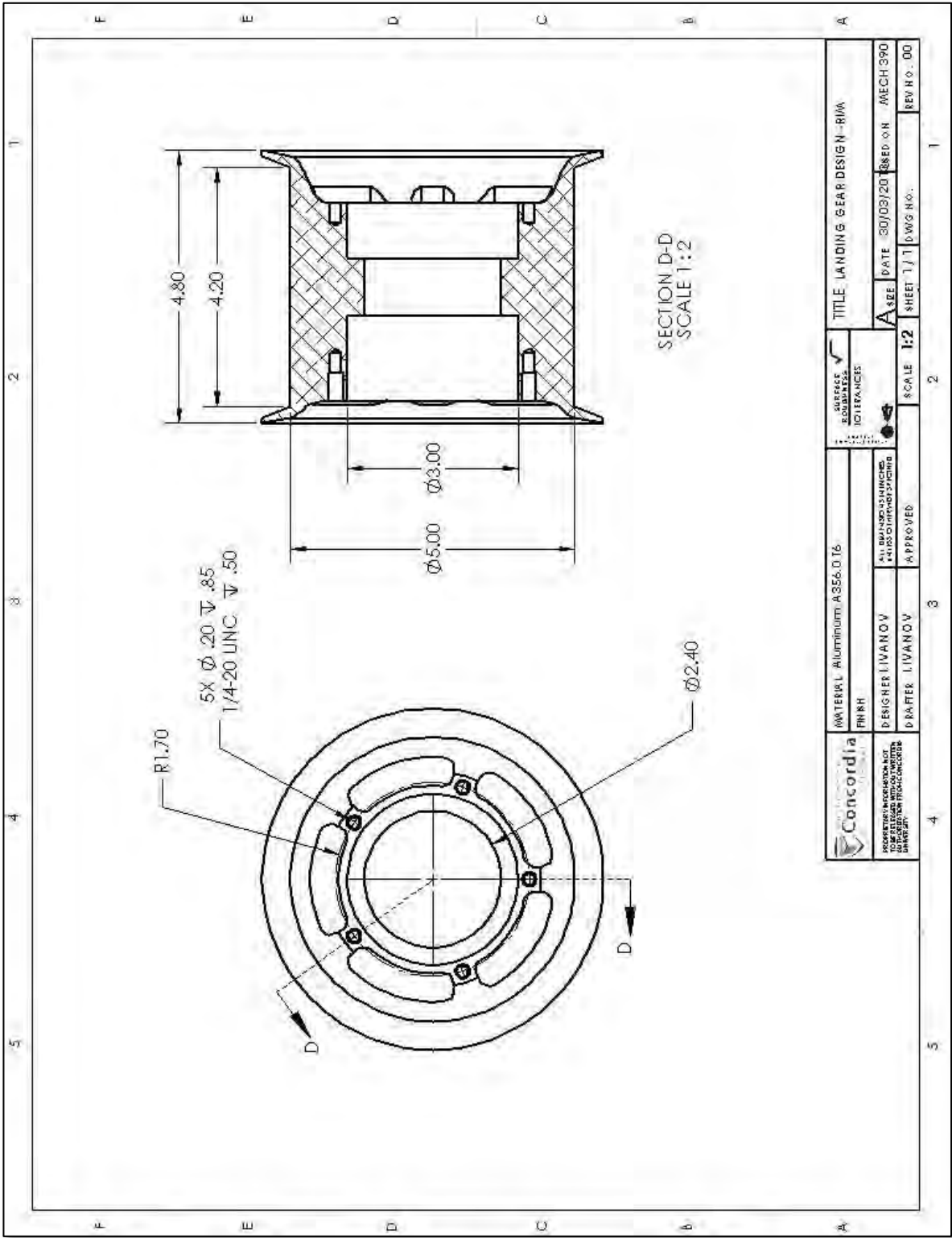
TABLE 6 SUMMARY OF SELECTED COMPONENT PARAMETERS AND DIMENSIONS

Component	Parameter/Dimension	Value	Source
Tire	Tire type	5.00-5 Ply Rating 6	Type III Tires – Engineering Data and landing requirements – section 3.1.1 and 3.1.2
	Speed (mph)	120	
	Load (lbs)	1260	
	Inflation (psi)	50	
	Max Braking (lbs)	1830	
	Bottom Load (lbs)	3400	
	Thread design	Rib	
	Weight (lbs)	4.7	
	Outside Diameter (in)	14.2-13.65	
	Section width (in)	4.95-4.65	
	Shoulder diameter (in)	12.55	
	Shoulder width (in)	4.2	
	Loaded radius (in)	5.7	
	Flat tire radius (in)	4.2	
	Aspect ratio	0.929	
	Safety Factor	1.5	
Rim	Material	Aluminum A356.0-T6	Material selection trade study
	Outside diameter (in)	5	Tire specs
	Bearing diameter (in)	3	Bearing specs
	Safety Factor	2	FEA model
	Weight (lbs)	3.55	SolidWorks model
	Expected life (cycles)	>10 ⁶	FEA model
	Width (in)	4.8	Tire specs plus shoulder for tire
Bearing	P/N	5709K27	McMaster-Carr inventory
	Bearing number	2788	
	Shaft diameter (in)	1.5	
	Outside diameter (in)	3	
	Roller assembly width (in)	15/16	
	Inner ring width (in)	1 1/64	
	Dynamic load capacity, radial (lbs)	4690	
	Dynamic load capacity, thrust (lbs)	2430	
	Price (\$/unit)	30.64	
	Weight (lbs)	1.2	Assuming made from 4340 steel
Shaft	Material	AISI 5160	Material selection trade study
	Outside diameter (in)	1.5	Bearing specs/design decision
	Inside diameter (in)	1.2	Analytical fatigue calculations
	Weight (lbs)	1.36	SolidWorks model
	Safety Factor	1.5	Analytical fatigue calculations
	Length (in)	7.5	Design decision/room for brake
	Expected life	Infinite	Fatigue analysis (analytical and FE)

COMPONENT TECHNICAL DRAWINGS

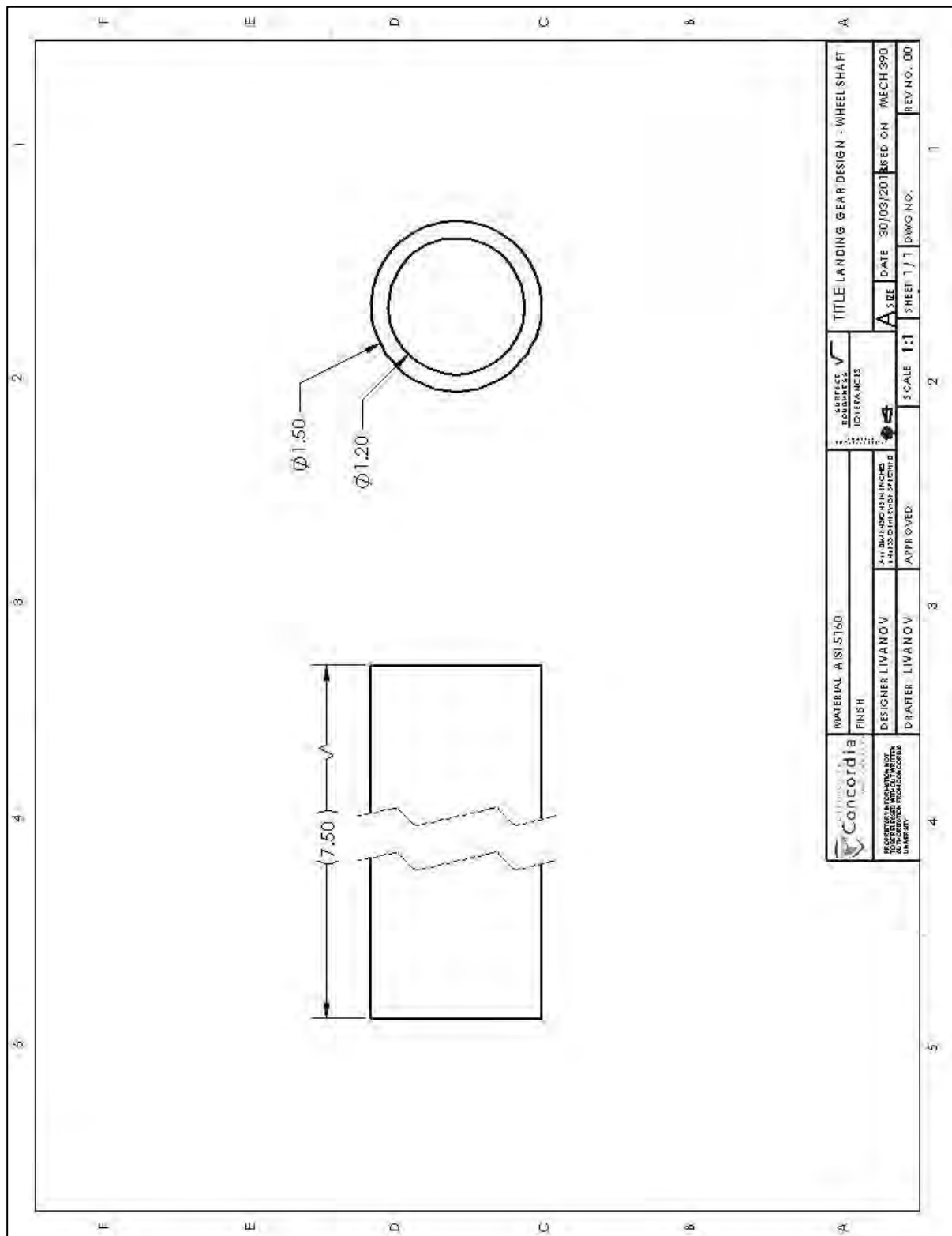
a. Rim

FIGURE 18 RIM TECHNICAL DRAWING



b. Shaft

FIGURE 19 WHEEL SHAFT TECHNICAL DRAWING



2.2 Brake



- Derive requirements
- Design, thermal modeling and material selection
 - Heat sink material
 - Heat generation
 - Kinetic energy capacity
 - Brake sizing
- Procurement, integration and design summary

2.2.1 Specific brake requirements

1. FAR requirements

- FAR 25.729 Section 735— Brake and braking systems:
 - Must be designed such that it could bring the aircraft to zero speed without any reverse thrust
 - The Braking system must be able to bring the airplane to rest with a braked roll stopping distance less than twice the landing distance
 - Fluid lost from the hydraulic system failure near or in the brakes should not be enough to start a fire
 - An airplane must have a parking brake to prevent rolling on dry and level paved runway and must be able to override the braking system

2. Model-specific requirements

- The tire, rim and shaft must be able to support the corresponding fraction of the weight of the aircraft. The weight of the aircraft is taken as 1914lbs (66% of the original weight of 2950lbs)

2.2.2 Design, thermal modeling and material selection

Heat sink material

There are two common materials used as heat sink materials: steel and carbon. Of the two, carbon is best in a number of mechanical properties: carbon is more than four times less dense than steel, but has more than double the specific heat capability, more than four times the thermal conductivity, more than five times less of a thermal expansion coefficient, more than twenty-five times the thermal shock resistance and has a temperature limit that almost doubles that of steel [1].

Furthermore, carbon brakes have a longer service, low maintenance requirements and was estimated to permit up to five to six times more landings compared to steel [1]. In terms of drawbacks, carbon requires more volume to absorb the same amount of energy, experiences oxidation and has a higher initial cost [1]

TABLE 7 HEAT SINK MATERIALS COMPARISON [1]

Property	Steel	Carbon	Desired
Density, lb/in ³	0.283	0.061	High
Specific heat at 500°F, Btu/lb•°F	0.13	0.31	High
Thermal conductivity at 500°F, Btu/h•ft ² •°F	24.0	100.0	High
Thermal expansion at 500°F, 1.0E-6 in•°F/in	8.4	1.5	Low
Thermal shock resistance index, ×10 ⁵	5.5	141.0	High
Temperature limit, °F	2,100	4,000	High

Heat generation

The following is a conservative estimate of the amount of heat generated when landing, where m is the mass of the plane at touchdown:

$$KE = \frac{1}{2}mv_{stall}^2$$

The stall speed will be the deciding factor in the heat generated, since the mass of the airplane is harder to control [2].

Kinetic energy capacity

As per FAR 25.733, the kinetic energy absorption must be determined for the three following conditions:

1. Design landing stop
2. Maximum kinetic energy accelerate stop (rejected takeoff)
3. Most severe landing stop (maximum landing weight)

The brake heat sink, among other assemblies such as the wheel-tire assembly, must be able to absorb no less than the level of kinetic energy produced at the most critical combination of airplane landing weight and speed.

Brake sizing

Brake sizing is designed neglecting the contribution of thrust reverse. A conservative estimate of the kinetic energy at landing can be expressed in a simply energy balance [4] :

$$k \frac{1}{2} M v^2 = m c_v \cdot \Delta T$$

k = fraction of energy converted to brake heat (often approximated to 0.8)

M = aircraft mass (maximum landing mass)

v = landing velocity (maximum landing velocity) m = total heat sink mass

c_v = heat sink specific heat (0.310 Btu/lb°F for carbon at 500°F)

ΔT = temperature increment during braking (difference between the allowable disc material temperature and the highest possible initial temperature)

The maximum temperature is considered the main criteria in dimensioning the braking system. The kinetic energy absorption requirements for each main wheel-brake assembly may be derived from the following formula, assuming equal braking distribution [1]:

The following calculations provide guidelines for the approximate size of the brakes:

KE = kinetic energy

DSA = disk swept area

BT = brake torque

WT = wheel torque

r_b = brake radius

r_r = rolling radius

k = lining friction coefficient

Lining coefficient is a measure of total energy absorbed per square inch of lining:

$$\text{Lining loading} = \frac{KE}{DSA} \left[\frac{ft \cdot lb}{in^2} \right]$$

Heat sink loading is a measure of the total amount of

$$\text{Heat sink loading} = \frac{KE}{\text{disk and lining carrier sement weight}} \left[\frac{ft \cdot lb}{lb} \right]$$

Friction unit force is a measure of the shearing force on the friction material

$$\text{Friction unit force} = \frac{T}{r \cdot DSA} \left[\frac{lb \cdot in}{in^3} \right]$$

Actuation pressure is the pressure required to develop the require calculated torque

$$\text{Actuation pressure} = \frac{BT}{k \cdot r \cdot \frac{\text{number of surfaces}}{A_{\text{piston}}}} \cdot \frac{\text{pressure to overcome retractor springs}}{A_{\text{piston}}}$$

Calculated wheel torque is the torque required to stop the aircraft

$$WT = IE \cdot r_r \cdot \frac{\text{deceleration}}{g}$$

Under the assumed landing conditions, the amount of torque inflicted upon the rotor per landing can be calculated. Under these conditions, there is a corresponding brake energy. From Figure 20, a brake assembly weight can be determined based on that energy and the type of landing condition (rejected take off, maximum landing condition, normal landing condition).

FIGURE 20 ESTIMATED BRAKE ENERGY VERSUS BRAKE ASSEMBLY WEIGHT [3]

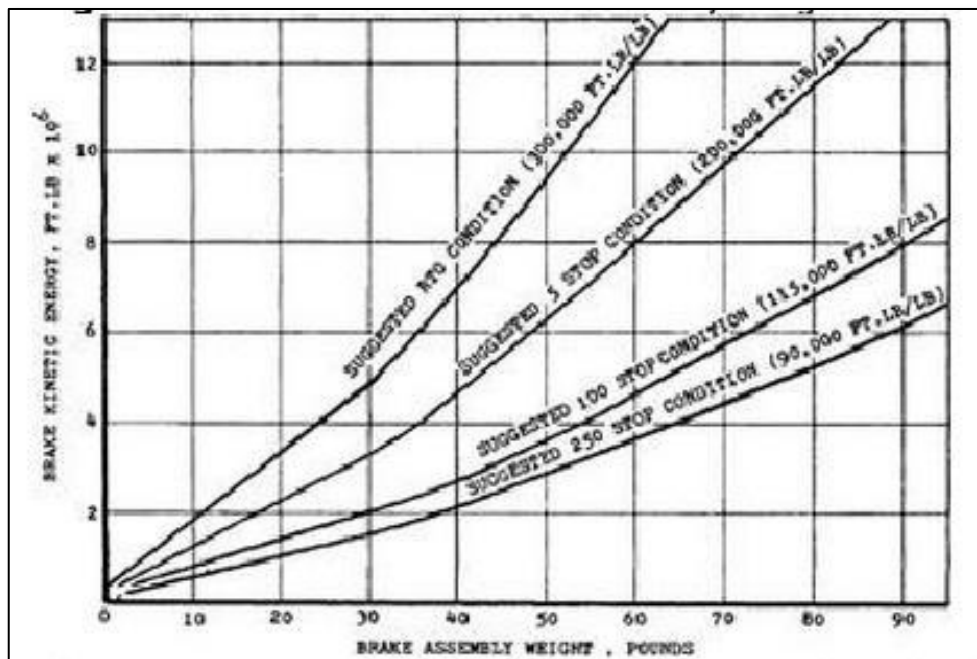
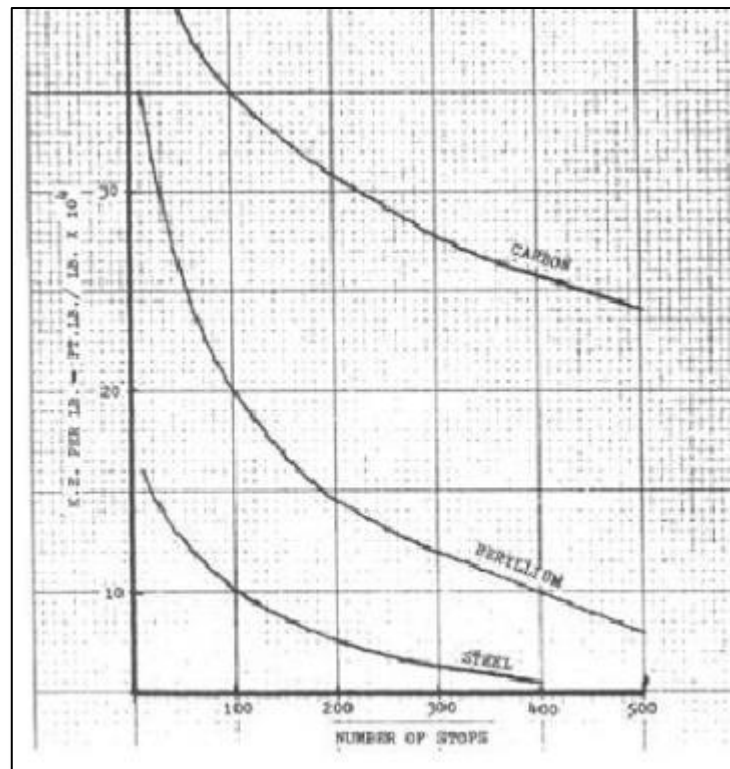


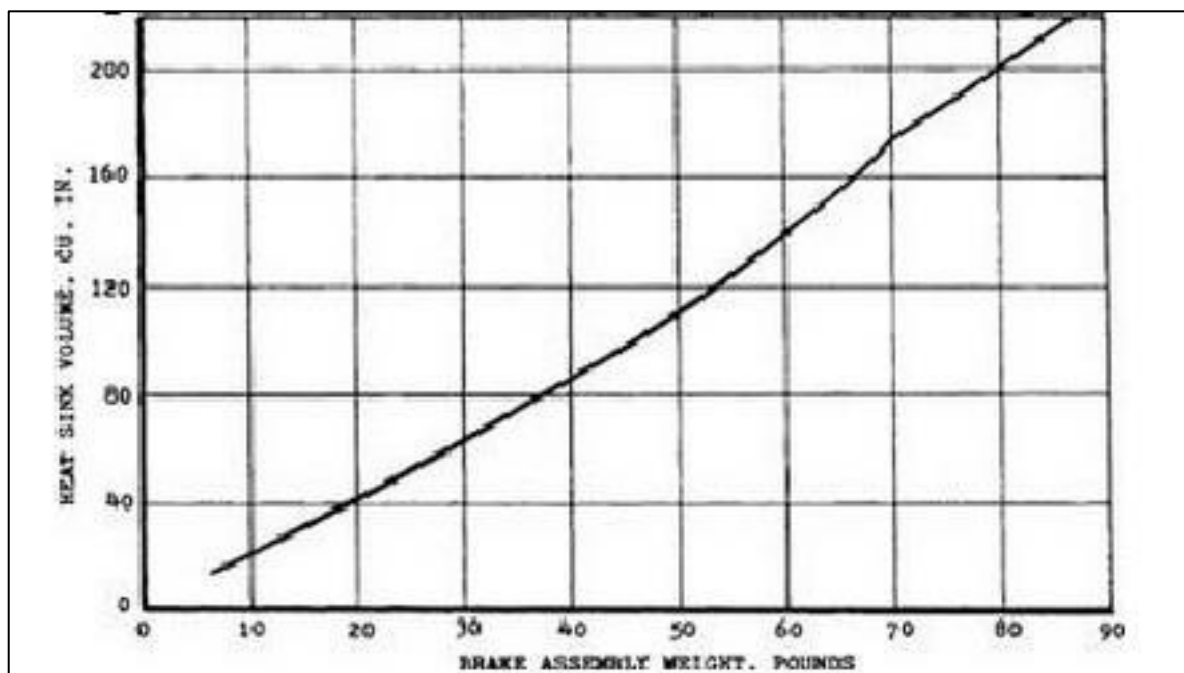
Figure 21 can be used to extrapolate data for a carbon brake.

FIGURE 21 ESTIMATED NUMBER OF STOPS VERSUS KINETIC ENERGY PER POUND [3]



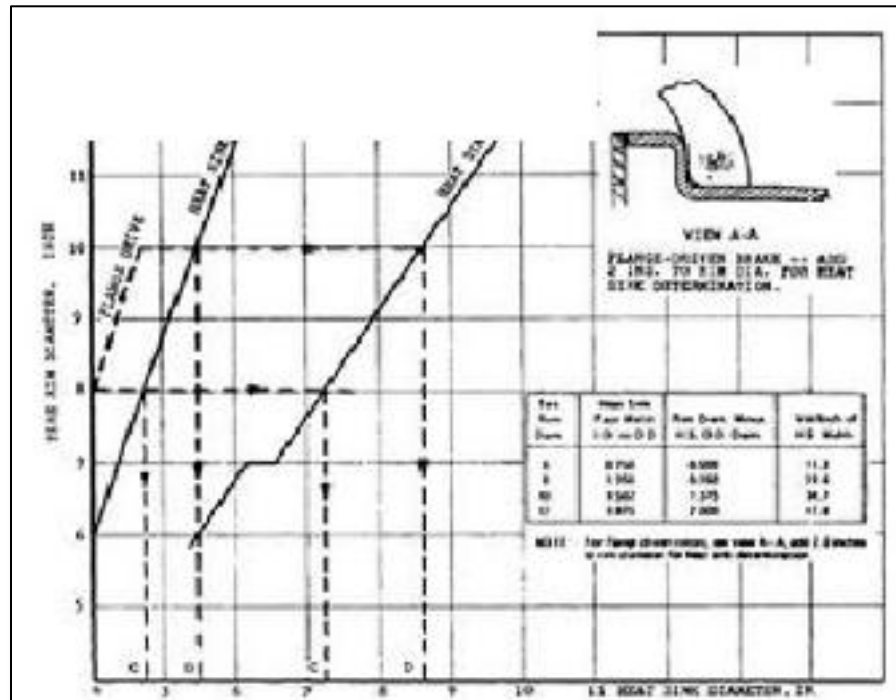
Once the brake assembly weight is determined, the heat sink volume can be found from Figure 22:

FIGURE 22 HEAT SINK VOLUME VERSUS BRAKE ASSEMBLY WEIGHT [3]



Next, the heat sink dimensions (inside and outside diameters) can be found from the heat sink volume, from Figure 23:

FIGURE 23 TIRE RIM DIAMETER VERSUS HEAT SINK DIAMETER [3]



Three-quarters of an inch can be added to these dimensions for safety.

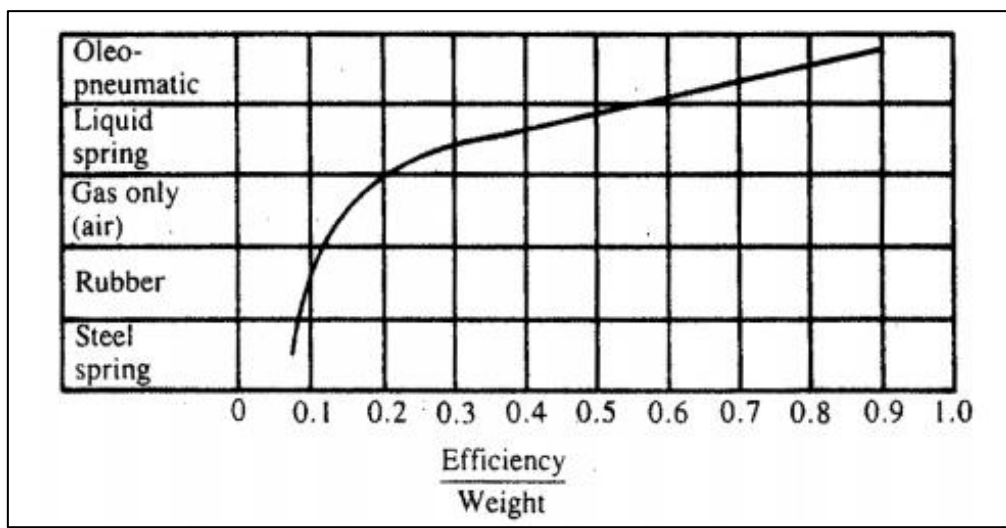
2.3 Oleo-Pneumatic Strut



2.3.1 Specific oleo-pneumatic requirements

The basic considerations that affect the shock absorber are sink speed, load factor, stroke, and shock absorber type. The shock absorber of a landing gear has the function of absorbing and dissipating the impact kinetic energy in order to reduce the accelerations imposed on the airframe to a tolerable level [1]. Of the various types of shock absorbers, an oleo-pneumatic type was chosen since it is the preferred design for commercial transport.

FIGURE 24 EFFICIENCY-TO-WEIGHT RATIOS FOR VARIOUS SHOCK ABSORBERS [5]



2.3.2 Design and modeling of Oleo-Pneumatic strut

Shock absorber stroke calculation based on worse loading:

· Tire efficiency:

$$K_t = 0.45$$

· Shock absorber efficiency:

$$K_s = 0.85 \text{ for oleo pneumatic with orifice control}$$

Oleo-pneumatic (hydraulic) shock absorber is one of the most efficient types.

· Tire deflection:

$$d_t = (\text{loaded radius} - \text{flat tire radius}) \cdot 0.75 = (5.7 \text{ in} - 4.2 \text{ in}) \cdot 0.75 = 1.125 \text{ in} = 0.09375 \text{ ft.}$$

· Airplane weight:

$$W = 0.66 \cdot 2900 = 1914 \text{ lbs}$$

· Area:

$$S = 170 \text{ ft}^2$$

· Shock absorber stroke:

$$d_s = \frac{0.3 \sqrt{\frac{W}{S}} - d_t [(n_z \cdot k_t) - 0.333]}{(n_z \cdot k_s) - 0.333} = \frac{0.3 \sqrt{\frac{1914}{170}} - 0.09375 [(3 \cdot 0.45) - 0.333]}{(3 \cdot 0.85) - 0.333} = 0.4110 \text{ ft} = 4.933 \text{ in}$$

· Total deflection

$$d = d_s + d_t = 4.933 + 1.125 = 6.05 \text{ in}$$

· Level landing load on each wheel in hard landing:

$$E_0 = E_{Tire} + E_{Shock} + E_{Lift} + E_{Static}$$

$$\frac{1}{2} m V_0^2 + W h_0 = k_t P d_t + k_s P_{hard} d_s + r m g d + W h$$

$$m = \frac{W}{g} = \frac{1914 \text{ lbs}}{32.2 \text{ ft/s}^2} = 59.44 \text{ slug}$$

· Vertical (sink) speed specified by FAR 23.473 (d):

$$v_0 = 4.4 \left(\frac{W}{S} \right)^{\frac{1}{4}} = 4.4 \left(\frac{1914 \text{ lbs}}{170 \text{ ft}^2} \right)^{\frac{1}{4}} = 8.0598 \frac{\text{ft}}{\text{s}} \rightarrow 10 \frac{\text{ft}}{\text{s}} (\text{for safety})$$

$$r = \frac{L}{w} = \frac{2}{3} (\text{Max. according to FAR 23.473 (e)})$$

$$h_0 - h \simeq d \quad \text{if: } h = 30 \text{ in} = 2.5 \text{ ft.} \rightarrow h = 23.95 \text{ in} = 1.995 \text{ ft.}$$

$$P_{hard} = \frac{\frac{1}{2} m V_0^2 + W h_0 - r m g d - W h}{k_t d_t + k_s d_s}$$

$$P_{hard} = \frac{\frac{1}{2} 59.44 \text{ slug} (10 \text{ ft/s})^2 + (1914 \text{ lbs}) (2.5 \text{ ft}) - \frac{2}{3} 59.44 \text{ slug} \cdot 32.2 \text{ ft/s}^2 \cdot 0.505 \text{ ft} - 1914 \text{ lbs} \cdot 1.995 \text{ ft}}{0.45 \cdot 0.09375 + 0.85 \cdot 0.4410 \text{ ft}}$$

$$P_{hard} = 8412.484 \text{ lbs for both tires or } 4206 \text{ lbs for one tire}$$

Bore area of shock absorber:

· Max. Static load:

$$\text{Max. static load} = w \frac{74.4 \text{ in } 1}{94.1 \text{ in } 2} = 1914 \text{ lbs} \frac{74.4 \text{ in } 1}{94.1 \text{ in } 2} = 756.65 \text{ lbs}$$

· Bore Area

$$\text{Bore area} = \text{Piston area} = \frac{\text{Max Static load}}{1500 \text{ psi}} = \frac{756.65 \text{ lbs}}{1500 \text{ psi}} = 0.504 \text{ in}^2$$

Oleo-Pneumatic Shock Strut Sizing

Compression ratio assumptions:

Static to extend: 2.1/1

Compressed to static: 1.9/1

$$\begin{aligned} \text{Load extended} &= \text{max. static load} \cdot \text{static to extend ratio} = 756.6 \text{ lbs} \cdot \frac{1}{2.1} = 360.31 \text{ lbs} \\ \text{static load} &= \text{max. static load} = 756.6 \text{ lbs} \end{aligned}$$

$$\text{Load compressed} = \text{max. static load} \cdot \frac{\text{compressed to static ratio}}{\text{static ratio}} = 756.6 \text{ lbs} \cdot 1.9 = 1437.64 \text{ lbs}$$

· Air pressure at full extension:

$$P_1 = 1500 \text{ psi} \cdot \frac{1}{2.1} = 714.29 \text{ psi}$$

· Air volume at full extension:

$$V_1 = \text{bore area} \cdot d_s = 0.504 \text{ in}^2 \cdot 4.933 \text{ in} = 2.488 \text{ in}^3$$

· Air pressure at static position:

$$P_2 = 1500 \text{ psi}$$

· Air volume at static extension:

$$V_2 = \frac{P_1 V_1}{P_2} = \frac{714.29 \text{ psi} \cdot 2.488 \text{ in}^3}{1500 \text{ psi}} = 1.185 \text{ in}^3$$

· Air pressure at compressed position:

$$P_3 = 1500 \text{ psi} \cdot 1.9 = 2850 \text{ psi}$$

· Air volume at compressed position displacement:

$$V_3 = 0.1 \cdot V_1 = 0.1 \cdot 2.488 \text{ in}^3 = 0.2488 \text{ in}^3$$

“To accommodate excess energy produced in a heavy or semi-crash landing, shock absorbers are designed such that the piston is not fully bottomed even at the compressed position, i.e., $V_3 \neq 0$. [1]”

$$\begin{aligned} \text{Stroke}_{\text{Extension to static}} &= \frac{V_1 - V_2}{A_{\text{bore}}} = \frac{2.488 \text{ in}^3 - 1.185 \text{ in}^3}{0.504 \text{ in}^2} = 2.548 \text{ in} \\ \text{Stroke}_{\text{Static to Compression}} &= \frac{V_2 - V_3}{A_{\text{bore}}} = \frac{1.185 \text{ in}^3 - 0.2488 \text{ in}^3}{0.504 \text{ in}^2} = 1.858 \text{ in} \end{aligned}$$

$$\text{Stroke}_{\text{Total}} = \text{Stroke}_{\text{Extension to static}} + \text{Stroke}_{\text{Static to Compression}} = 2.548 \text{ in} + 1.858 \text{ in}$$

$$\text{Stroke}_{\text{Total}} = 4.44 \text{ in} \rightarrow 5.44 \text{ in (at least one extre inch for safety)}$$

Internal cylinder length

$$L_{Piston} = s + 2.75D = 7.7 \text{ in}$$

$$\text{Where: } D = \sqrt{\frac{4 \cdot A_{piston}}{\pi}} = \sqrt{\frac{4(0.504) \text{ in}^2}{\pi}} = 0.801 \text{ in}$$

Thickness of hollow strut

$$l_1 = 12 \text{ in (actual measurement)}$$

$$l_2 = 5.5 \text{ in}$$

$$F_y = 2711.181 \text{ lbs}$$

$$F_x = 837.375 \text{ lbs}$$

$$I = \frac{\pi(D_1^4 - D_2^4)}{64} \quad A = \frac{\pi(D_1^2 - D_2^2)}{4}$$

$$\sigma_y = \frac{Mc}{I} + \frac{F}{A} = \frac{F_x(l_1 + l_2) \cdot \left(\frac{D_1}{2}\right)}{\frac{\pi(D_1^4 - D_2^4)}{64}} + \frac{-F_y}{\frac{\pi(D_1^2 - D_2^2)}{4}} = \frac{32F_x(l_1 + l_2) \cdot D_1}{\pi(D_1^4 - D_2^4)} - \frac{4F_y}{\pi(D_1^2 - D_2^2)}$$

(F_y negative because in compression)

$$N_f = \frac{s_y}{\sigma_y} \text{ (For buckling using fixed – free condition)}$$

$$s_r = \frac{l_{eff}}{k}$$

$$l_{eff} = 2l \text{ for fixed – free}$$

$$l_{eff} = 35 \text{ in}$$

$$k = \sqrt{\frac{I}{A}} = \sqrt{\frac{\frac{\pi(D_1^4 - D_2^4)}{64}}{\frac{\pi(D_1^2 - D_2^2)}{4}}} = \sqrt{\frac{(D_1^4 - D_2^4)}{16(D_1^2 - D_2^2)}}$$

$$s_r = \frac{2l}{\sqrt{\frac{(D_1^4 - D_2^4)}{16(D_1^2 - D_2^2)}}} = 8l \sqrt{\frac{(D_1^2 - D_2^2)}{(D_1^4 - D_2^4)}}$$

$$P_{cr} = \sigma_{cr} = \frac{\pi^2 E}{S_r^2} = \frac{\pi^2 E}{\left(8l \sqrt{\frac{(D_1^2 - D_2^2)}{(D_1^4 - D_2^4)}}\right)^2} = \frac{\pi^2 E (D_1^4 - D_2^4)}{64l^2 (D_1^2 - D_2^2)}$$

$$N = \frac{\sigma_{cr}}{\sigma_{axial}}$$

$$\sigma_{axial} = \frac{F_y}{A} = \frac{F_y}{\frac{\pi(D_1^2 - D_2^2)}{4}}$$

$$\sigma_{axial} \cdot N = \sigma_{cr}$$

$$\frac{4F_y}{\pi(D_1^2 - D_2^2)} \cdot N = \frac{\pi^2 E (D_1^4 - D_2^4)}{64l^2 (D_1^2 - D_2^2)}$$

For 4340 steel, E = 30000 kpsi. Assuming D₁=1.5in and N=1.5:

$$\frac{4 \cdot 2711 \text{ lbs}}{\pi(1.5^2 - D_2^2)} \cdot 1.5 = \frac{\pi^2 300000000 (1.5^4 - D_2^4)}{64l^2 (1.5^2 - D_2^2)}$$

$$D_2 = 1.38 \text{ in}$$

$$2t = D_2 - D_1 = 1.38 - 1.5 \quad \rightarrow \quad t = 0.06 \text{ in}$$

Second iteration with D₁ = 1.6 in: D₂ = 1.51 in and t = 0.045 in, which is worse.

Third iteration with D₁ = 1.4 in: D₂ = 1.25 in and t = 0.075 in, which is also bad.

Using distortion energy theory:

$$N_f = \frac{s_y}{\sigma_y} = \frac{s_y}{\frac{32F_x(l_1 + l_2) \cdot D_1}{\pi(D_1^4 - D_2^4)} - \frac{4F_y}{\pi(D_1^2 - D_2^2)}}$$

Assuming N_f = 1.5, D₁ = 1.6 in

$$1.5 = \frac{68500 \text{ psi}}{\frac{32 \cdot 837 \text{ lbs}(17.5) \cdot 1.5}{\pi(1.5^4 - D_2^4)} - \frac{4 \cdot 2711 \text{ lbs}}{\pi(1.5^2 - D_2^2)}}$$

$$D_2 = 0.78 \text{ in}$$

$$2t = D_2 - D_1 = 0.78 - 1.5 \quad \rightarrow \quad t = 0.36 \text{ in}$$

Second iteration with D₁ = 1.7 in: D₂ = 1.33 in and t= 0.19, which is worse

Third iteration with D₁ = 1.8 in: D₂ = 1.43 in and t=0.085, which is worse

Design against high cycle fatigue (calculation of thickness):

For 4340 steel:

$$S_{ut} = 250 \text{ kpsi}, \quad S_y = 230 \text{ kpsi}$$

$$\sigma_{max} = \sigma_y \quad \sigma_{min} = 0$$

$$\sigma_a = \sigma_m = \frac{\sigma_y}{2} = \sigma = \frac{16F_x(l_1 + l_2) \cdot D_1}{\pi(D_1^4 - D_2^4)} - \frac{2F_y}{\pi(D_1^2 - D_2^2)}$$

$$C_{load} = 1 \text{ (bending)}$$

$$C_{temp} = 1 \text{ (Room temp.)}$$

$$C_{reliab.} = 0.753 \text{ (} R = 99.9 \% \text{ reliability)}$$

$$C_{surface} = 1.34S_{ut}^{-0.097} = 0.838 \text{ (machined surface)} \quad S_{ut} = 250 \text{ kpsi}$$

$$C_{size} = 0.869 \text{ deq}^{-0.097} = 0.9202$$

$$A_{95} = 0.010462 \quad d_o^2 = 0.032$$

$$\text{deq} = \left(\frac{A_{95}}{0.0766} \right)^{1/2} = 0.65$$

$$S_e' = 0.5S_{ut} = 125 \text{ kpsi}$$

$$S_e = C_{load}C_{temp}C_{reliab.}C_{surface}C_{size}S_e' = 72.58 \text{ kpsi}$$

$$N_f = \frac{S_{ut}S_e}{\sigma_a S_{ut} + \sigma_m S_e} = 1.5 \text{ (assuming)}$$

$$\sigma = \frac{S_{ut}S_e}{N_f(S_{ut} + S_e)} = \frac{16F_x(l_1 + l_2) \cdot D_1}{\pi(D_1^4 - D_2^4)} - \frac{2F_y}{\pi(D_1^2 - D_2^2)}$$

$$D_2 = 1.37 \text{ in}$$

$$2t = D_2 - D_1 = 1.37 - 1.5 \quad \rightarrow \quad t = 0.1 \text{ in}$$

Second iteration: if $D_1 = 1.8$, $d_{eq} = 0.66522$, $C_{size} = 0.904$, $S_e = 71308.5 \text{ psi}$, $\sigma = 36988.58$ and $D_2 = 1.64 \text{ in}$, meaning that $t = 0.08 \text{ in}$, which is worse.

Design for 20 year life of aircraft:

Assuming 35% of landings are worst landing, 15% are level landing with inclined reaction and 50% of them are hard landing based on FAR:

TABLE 8 CYCLES FOR VARIOUS LANDING CONDITIONS

Component forces for different landings	Cycles
Worst landing: $F_y = 2711.181 \text{ lbs}$ and $F_x = 837.375 \text{ lbs}$	2555 cycles = n_1
Level landing with inclined reaction: $F_y = 1718 \text{ lbs}$ and $F_x = 531 \text{ lbs}$	1095 cycles = n_2
Hard landing: $F_y = 4206 \text{ lbs}$ and $F_x = 1000 \text{ lbs}$ (assumed x-component)	3650 cycles = n_3

$$\frac{n_1}{N_1} + \frac{n_2}{N_2} + \frac{n_3}{N_3} = \frac{\text{Total landings}}{\text{lifetime}} = \frac{7300}{10^6} = 0.0073 \text{ (cannot exceed)}$$

Worst landing:

$F_y = 2711.181 \text{ lbs}$ and $F_x = 837.375 \text{ lbs}$, $D_1 = 1.5 \text{ in}$ and $D_2 = 1.38 \text{ in}$

$$\sigma_{max, wl} = \frac{Mc}{2I} - \frac{F}{2A} = \frac{16F_x(l_1 + l_2) \cdot D_1}{\pi(D_1^4 - D_2^4)} - \frac{2F_y}{\pi(D_1^2 - D_2^2)} = 37.0 \text{ kpsi}$$

Approximating the S-N curve:

$$S(N) = aN^b$$

Where:

$$b = -\frac{\log \frac{S_m}{S_e}}{3} = -\frac{\log \frac{0.9 \cdot 250}{72.57}}{3} = -0.164$$

So:

$$a = 10^{\log S_m - 3b} = 698.53$$

$$S(N) = aN^b = 698.53 \cdot N^{-0.164}$$

Therefore:

$$\sigma_{max,wl} = 698.53 \cdot N^{-0.164}$$

$$37.0 = 698.53 \cdot N^{-0.164}$$

$$N_{1,Worst\ landing} = 6.0 \times 10^7$$

Level landing:

$$F_y = 1718\ lbs\ and\ F_x = 531\ lbs,\ D_1 = 1.5\ in\ and\ D_2 = 1.22\ in$$

$$\sigma_{max,ll} = \frac{Mc}{2I} - \frac{F}{2A} = \frac{16F_x(l_1 + l_2) \cdot D_1}{\pi(D_1^4 - D_2^4)} - \frac{2F_y}{\pi(D_1^2 - D_2^2)} = 23.5\ kpsi$$

Therefore:

$$\sigma_{max,ll} = 698.53 \cdot N^{-0.164}$$

$$23.5 = 698.53 \cdot N^{-0.164}$$

$$N_{2,Level\ landing} = 9.6 \times 10^8$$

Hard landing:

$$F_y = 4206\ lbs\ and\ F_x = 1000\ lbs,\ D_1 = 1.5\ in\ and\ D_2 = 1.22\ in$$

$$\sigma_{max,hl} = \frac{Mc}{2I} - \frac{F}{2A} = \frac{16F_x(l_1 + l_2) \cdot D_1}{\pi(D_1^4 - D_2^4)} - \frac{2F_y}{\pi(D_1^2 - D_2^2)} = 43.4\ kpsi$$

Therefore:

$$\sigma_{max,hl} = 698.53 \cdot N^{-0.164}$$

$$43.4 = 698.53 \cdot N^{-0.164}$$

$$N_{3,Hard\ landing} = 2.3 \times 10^7$$

Calculating the consumed life:

$$\frac{n_1}{N_1} + \frac{n_2}{N_2} + \frac{n_3}{N_3} = \frac{2555}{6.0 \times 10^7} + \frac{1095}{9.6 \times 10^8} + \frac{3650}{2.3 \times 10^7} = 0.00020 < 0.0073$$

Therefore, the estimated thickness of about 0.1 in is valid.

Drop test equations

Vertical kinetic energy: $KE = 0.5W \left(\frac{v_o^2}{g} \right)$ and $KE = WH$

$$WH = 0.5W \left(\frac{v_o^2}{g} \right)$$

$$H = \frac{v_o^2}{2g} = \frac{(10 \frac{ft}{s})^2}{2(32.2 \frac{ft}{s^2})} = 1.55 \text{ ft is the equivalent drop test height}$$

2.3.3 Analysis and design of strut Shaft**2.3.3.1 MATERIAL SELECTION**

AISI 5160 has already been selected for another shaft in the structure so it will be used again. Although the loadings are not the same, the properties that make it suitable for the wheel shaft (like high yield stress for example or high modulus of elasticity) also make it suitable for the strut shaft application

2.3.3.2 ANALYTICAL CALCULATIONS USING BUCKLING ANALYSIS

1. Define loading conditions from previous calculations
 - Vertical load 4233 lbf applied at the wheel shaft (aligned with the center of the strut column)
 - Horizontal load ~ 1500 lbf (assumed) applied at the wheel shaft (aligned with the center of the strut column). Note that due to the attachment through the fork, this force will generate torsion as well as bending
2. Model approximations and assumptions
 - The part inserted in the strut body will be supported laterally by the surrounding structure so it will not buckle. The section of interest is the protruding one during full extension of the strut
 - The section of interest will be modeled as a 6 in long column where one end is fixed and loads are applied at the other
 - The stroke of the strut is 5in and the shaft housing in the fork is 2in. For the purpose of simplifying the calculations, the center of the housing is taken as the loading point, thus the model has a length of 6 in

- These simplifications will be used only for the hand calculations to give an idea of the order of expected loading. The FEA model will aim for a more accurate representation of the loading
- This time the safety factor of 1.5 will not be taken under consideration because the AISI standards that dictate the equations include a safety factor of 1.67

3. Formula derivation

- Allowable stress for centered axial loading of a steel column (considering a safety factor of 1.67 as per AISC specifications) [6]

i. For: $\frac{L_e}{r} < 4.71 \sqrt{\frac{E}{\sigma_y}}$ *L_e is the effective column length*
 r is the radius of gyration

$$\sigma_{all} = \frac{\sigma_{cr}}{1.67} = \frac{(0.658 \frac{\sigma_y}{\sigma_e}) \sigma_y}{1.67}$$

ii. For: $\frac{L_e}{r} > 4.71 \sqrt{\frac{E}{\sigma_y}}$

$$\sigma_{all} = \frac{\sigma_{cr}}{1.67} \frac{0.877 \sigma_y}{1.67}$$

Where $\sigma_y = S_y$ or the yield stress and

$$\sigma_e = \frac{\pi^2 E}{\left(\frac{L_e}{r}\right)^2}$$

The radius of gyration is: $r = \sqrt{\frac{I}{A}}$

- Condition for eccentrically loaded column to withstand stresses [6]

$$\frac{P}{A} + \frac{M_c}{I} \leq \sigma_{all}$$

Where:

P is the resultant axial load on the column **A** is the cross-sectional area of the column

M is the resultant moment from eccentric forces around the tip of the column

c is the distance from the neutral axis (in this case the center axis) to the surface of the column

I is the moment on inertia of the cross-section of the column

Note, for a fixed beam at one end, the effective length is twice the length of the column.

- Find out which equation for allowed stress to use. Assume worst-case scenario for the radius of gyration – a solid shaft. In this condition the expression of the slenderness ratio becomes:

$$\frac{L_e}{r} = \frac{2l}{\sqrt{\frac{OD^2}{16}}} = \frac{2\sqrt{16}L}{OD} = \frac{8 \cdot 6}{1.5} = 32$$

$$4.71 \sqrt{\frac{E}{\sigma_y}} = 4.71 \sqrt{\frac{30.89 \cdot 10^6 psi}{286400 psi}} = 48.915$$

- i. Assuming the strut shaft is solid is a huge overestimate because it is known; the shaft is hollow for a piston with a varying diameter to regulate the damping. Therefore, it is safe to assume that the loadings will take place in the following region:

$$\frac{L_e}{r} < 4.71 \sqrt{\frac{E}{\sigma_y}}$$

$$\sigma_{all} = \frac{\sigma_{cr}}{1.67} = \frac{(0.658 \frac{\sigma_y}{\sigma_e}) \sigma_y}{1.67}$$

4. Derive system of equations that will determine the maximum inside diameter:

- Equation 1: σ_e

$$\sigma_e = \frac{\pi^2 E}{\left(\frac{L_e}{r}\right)^2} = \frac{\pi^2 E \sqrt{\frac{I}{A}}}{4L^2} = \frac{\pi^2 EI}{4L^2 A} = \frac{\pi^2 E \pi(OD^4 - ID^4)}{4L^2 \cdot 64} \cdot \frac{4}{\pi(OD^2 - ID^2)} = \frac{\pi^2 E(OD^4 - ID^4)}{64L^2(OD^2 - ID^2)}$$

- Equation 2: σ_{cr} , σ_e and σ_{all}

$$\sigma_{cr} = (0.658 \frac{\sigma_y}{\sigma_e}) S_y = \left(0.658 \frac{S_y / \frac{\pi^2 E(OD^4 - ID^4)}{64L^2(OD^2 - ID^2)}}{\sigma_e} \right) S_y$$

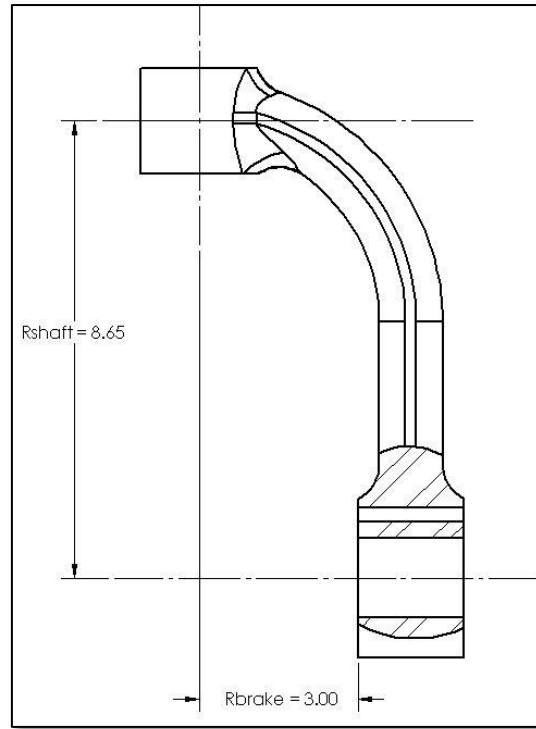
$$\sigma_{all} = \frac{\sigma_{cr}}{1.67} = \frac{1}{1.67} \left(0.658 \frac{S_y / \frac{\pi^2 E(OD^4 - ID^4)}{64L^2(OD^2 - ID^2)}}{\sigma_e} \right) S_y$$

- Equation 3: σ_{max}

$$\sigma_{max} = \frac{P}{A} + \frac{M_c}{I} = \frac{4P}{\pi(OD^2 - ID^2)} + \frac{64M(OD)}{2\pi(OD^4 - ID^4)} = \frac{4P}{\pi(OD^2 - ID^2)} + \frac{32V_x(R_{shaft} + L)OD}{\pi(OD^4 - ID^4)}$$

Where V_x is the horizontal component experienced during hard landing and R_{shaft} is the distance between the center of the wheel shaft and the center of the strut shaft housing on the fork. Measured from the SolidWorks model, $R_{shaft} = 8.65\text{in}$

FIGURE 25 SHAFT MODEL



5. Write a matlab code to solve the following equation for ID (the following equation is derived from equating Eq. 2 and Eq. 3):

$$\frac{S_Y}{1.67} \left(0.658 \frac{S_Y 64 L^2 (OD^2 - ID^2)}{\pi^2 E (OD^4 - ID^4)} \right) = \frac{4P}{\pi (OD^2 - ID^2)} + \frac{32 V_x (R_{shaft} + L) OD}{\pi (OD^4 - ID^4)}$$

TABLE 9 PARAMETERS FOR STRUT SHAFT CALCULATIONS

Parameter	Value	Source
S_Y (psi)	286400	CES 2005 for AISI 5160
E (psi)	30890000	CES 2005 for AISI 5160
Strut shaft OD (in)	1.5	Design decision
L (in)	6	Simplified model of section under buckling
Vertical load P during hard landing (lbf)	4233	Tutorial calculations
Horizon load V_x during hard landing (lbf)	1500	Assumed
R_{shaft} (in)	8.65	SolidWorks model

6. Matlab Sample code:

```

o function StrutShaft_Func = StrutShaftID(x)
o %UNTITLED2 Summary of this function goes here
o % Detailed explanation goes here
o Sy=286400;
o E=30890000;
o OD=1.5;
o L=6;
o P=4233;
o V=1500;
o R=8.65+6;
o StrutShaft_Func = Sy/1.67*(0.658^(Sy*64*L^2*(OD^2-
x^2)/pi^2/E/(OD^4-x^4)))-4*P/pi/(OD^2-x^2)-32*V*R*OD/pi/(OD^4-
x^4);
o End

```

7. Solve for ID using the fsolve function:

```
>> [x,fval]=fsolve(@strutShaftID,1)
```

Equation solved.

fsolve completed because the vector of function values is near zero as measured by the default value of the function tolerance, and the problem appears regular as measured by the gradient.

<Stopping criteria details>

x = 1.2482

fval = -1.4552e-011

- o The result from the calculations shows that the inside diameter must be 1.25in or smaller for the strut shaft to resist buckling

Determine analytically the largest inside diameter such that the strut shaft would not fail due to fatigue for a worst-case landing

1. Loading conditions for worst case landing:

- o Axial load $P=2711\text{lbs}$
- o Horizontal load $V_x=837\text{ lbs}$

2. Calculate stresses (note it is negative because stress is in compression):

$$\sigma_{max} = \frac{P}{A} + \frac{M_c}{I} = \frac{4P}{\pi(OD^2 - ID^2)} + \frac{32V_x(R_{shaft} + L)OD}{\pi(OD^4 - ID^4)}$$

$$\sigma_{min} = 0$$

3. Calculate σ_a and σ_m

$$\sigma_a = \sigma_m = \frac{2P}{\pi(OD^2 - ID^2)} + \frac{16V_x(R_{shaft} + L)OD}{\pi(OD^4 - ID^4)}$$

4. Calculate the corrected value for the fatigue strength:

$$S_e' = 0.5S_{ut} = 0.5 \cdot 854.6 \text{ kpsi} = 177.3 \text{ kpsi}$$

$$C_{load} = 0.7 \text{ (for axial loading)}$$

$$C_{temp} = 1 \text{ (Room temp.)}$$

$$C_{reliab.} = 0.753 \text{ (} R = 99.9 \% \text{ reliability)}$$

$$C_{surface} = 1.34S_{ut}^{-0.085} = 0.814 \text{ (for ground surface)} \quad S_{ut} = 354.6 \text{ kpsi}$$

$$C_{size} = 0.869 \text{ deq}^{-0.097} = 0.835$$

$$S_e = C_{load}C_{temp}C_{reliab.}C_{surface}C_{size}S_e' = 63.52 \text{ kpsi}$$

5. Calculating the inside diameter that will give a safety factor of 1.5

$$N_f = \frac{S_{ut}S_e}{\sigma_a S_{ut} + \sigma_m S_e} = 1.5 \text{ (assume case 3 fluctuating stresses loading)}$$

$$\sigma = \frac{S_{ut}S_e}{N_f(S_{ut} + S_e)} = \frac{354600 \cdot 63520}{1.5(354600 + 63520)} = 35913.44$$

$$\sigma = \sigma_a = \sigma_m = \frac{2P}{\pi(OD^2 - ID^2)} + \frac{16V_x(R_{shaft} + L)OD}{\pi(OD^4 - ID^4)} = 35913.44$$

$$\sigma = \frac{P}{\pi(OD^2 - ID^2)} + \frac{8V_x(R_{shaft} + L)OD}{\pi(OD^4 - ID^4)} = 56413$$

6. Sample matlab code for the above function:

```
function StrutShaft_Fatigue = StrutShaftIDfatigue(x)

Sy=286400;
E=308900000;
OD=1.5;
L=6;
P=2711;
V=837;
R=14.65;

StrutShaft_Fatigue = 56413-P/(OD^2-x^2)-8*V*R*OD/(OD^4-x^4);
end
```

7. Solve equation using matlab:

```
>> [x,fval]=fsolve(@strutShaftIDfatigue,1)
```

Equation solved.

fsolve completed because the vector of function values is near zero as measured by the default value of the function tolerance, and the problem appears regular as measured by the gradient.

```
<stopping
criteria
details> x
= 1.2279
fval = -2.1828e-011
```

8. The solution for the ID of the shaft is smaller than the minimum value to prevent buckling so we adopt the smaller more conservative size of 1.2in inside diameter

Scenario analysis – experienced loading during braking

1. Modified loading during braking:

- Assuming the plane starts braking only after the landing shock has been absorbed, the vertical loading will be 800lbs (as calculated in section 2.1.1 but excluding the safety factor because it will be applied during the calculations that follow).
- The horizontal load will originate from the brake. As calculated in section 2.1.1, the required force per main landing gear (there are two) to bring the airplane to a stop is 670lbs.

2. The modified loads are significantly smaller than the loads for a worst landing; therefore, it is safe to assume that the strut will not fail under buckling nor under fatigue during braking.

2.3.3.3 FEA MODEL FOR BUCKLING OF THE STRUT SHAFT

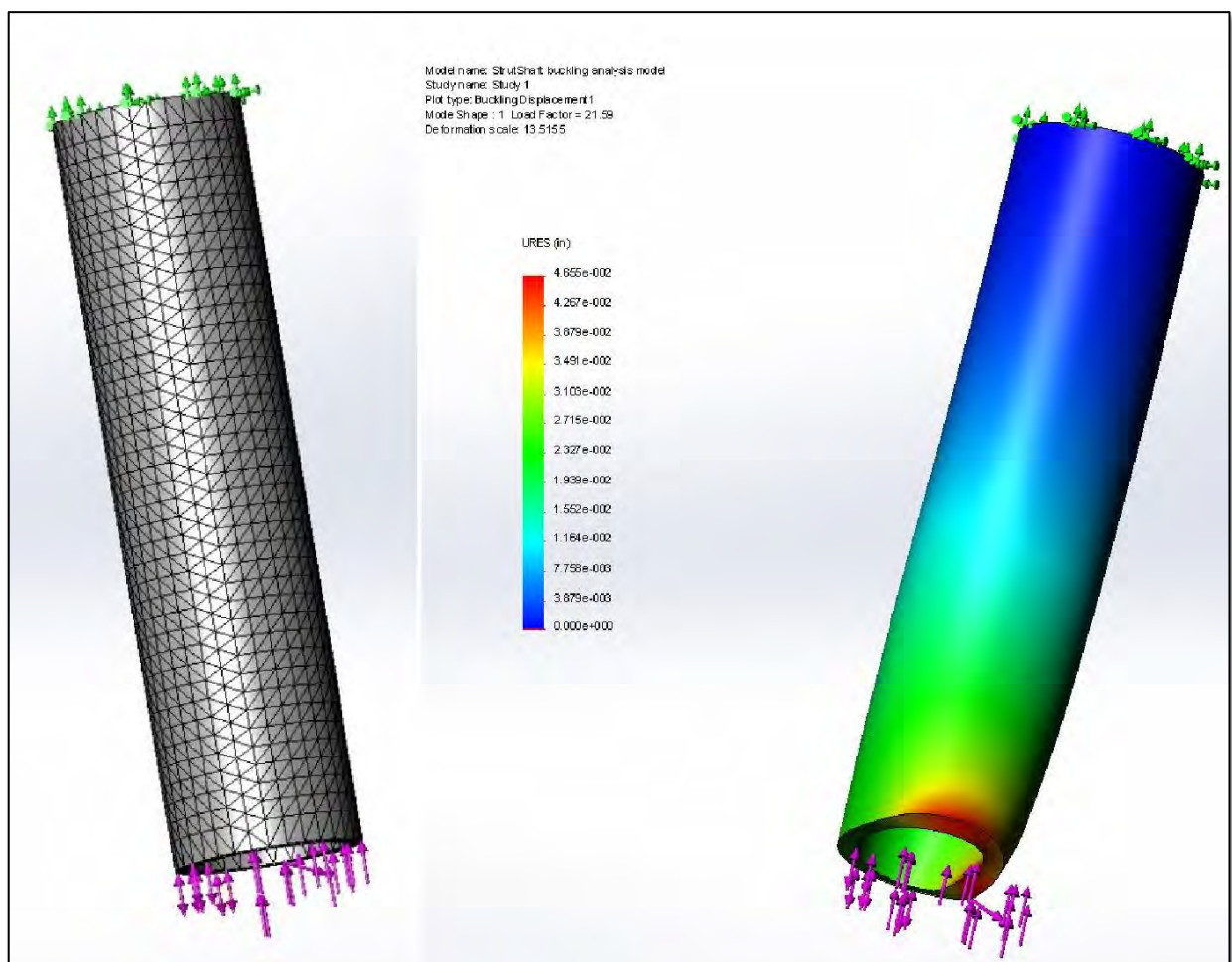
1. Loading conditions:

- Axial load of 4233lbs due to plane weight
- Moment at the tip of the shaft due to tire friction = $8.65\text{in} \times 1500\text{lbs} = 12975\text{in-lbf}$

2. Boundary conditions

- One of the cross-sectional faces is fixed, the loading is applied on the other

FIGURE 26 FEA MESH MODEL AND BUCKLING DEFLECTION (IN)

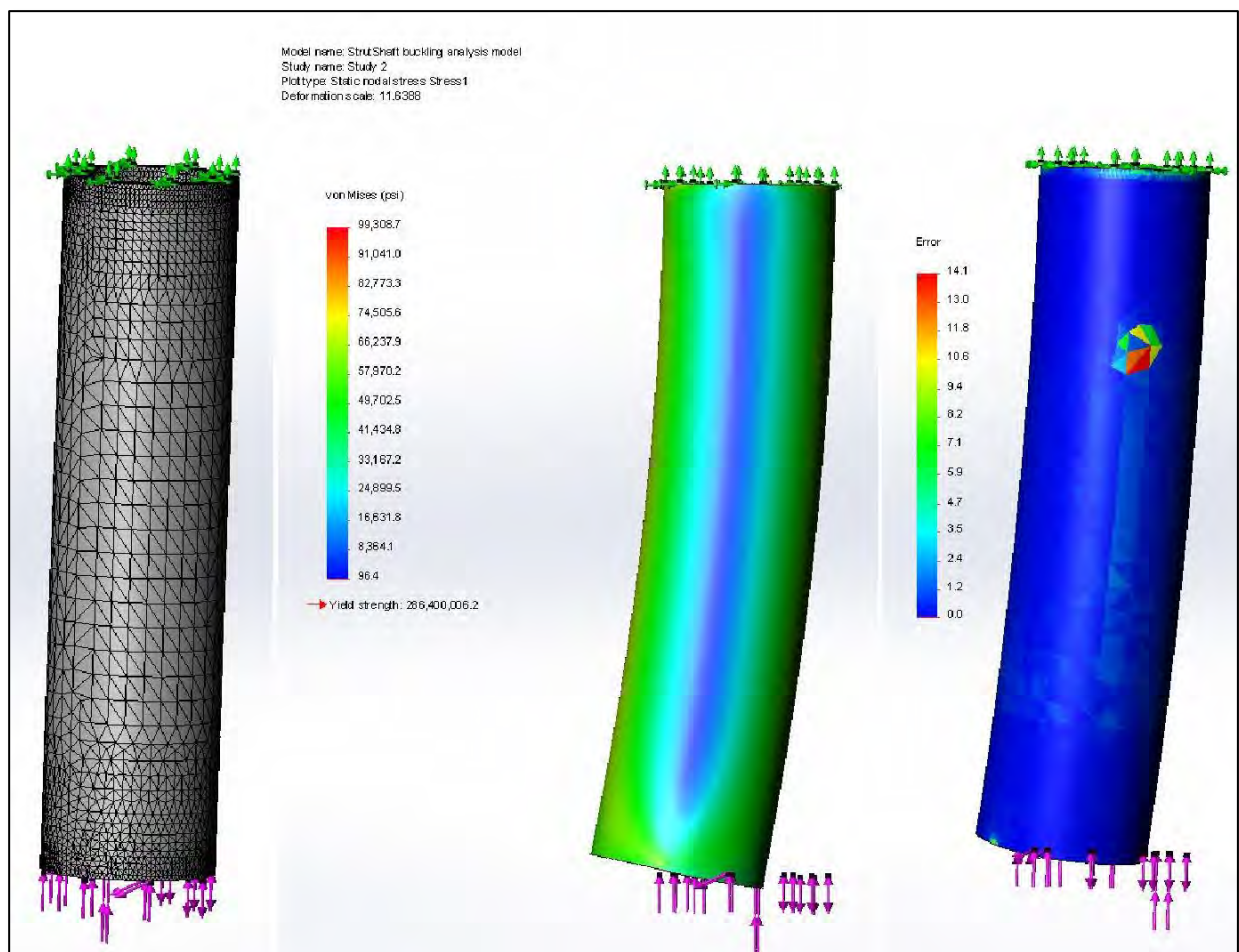


The expected deflection under the specified loads is 0.04655 in, which is insignificant relative to the size of the landing gear. Furthermore the loading factor calculated by SolidWorks is 21.59, which indicates that the current load should be multiplied by a factor of 21.59 in order to have the shaft fail under buckling. Changes to these values are insignificant using a finer mesh. It is safe to conclude that the shaft will not fail due to buckling.

3. FE fatigue analysis of strut shaft

- Set up an FEA model that illustrates the loading on the strut shaft. Use the hard landing loads and the boundary conditions from the buckling analysis. This static model will be later used as the basis for fatigue analysis.
- After running a couple of simulations it became clear that the mesh needs to be significantly finer around the edges of the shaft to minimize the error. The image below illustrates the final mesh used for the static analysis, the stresses and the error plot.

FIGURE 27 FINAL MESH FOR STATIC ANALYSIS OF STRUT



- The FEA model shows that deviations in the critical area are of the order of $\sim 5\%$. The maximum error is in a non-critical element of the structure and its due to a weird non-symmetric mesh at that point – it is safe to ignore it. Therefore, according to the FEA model, the experienced stresses by the shaft will be 100ksi ± 5 ksi.

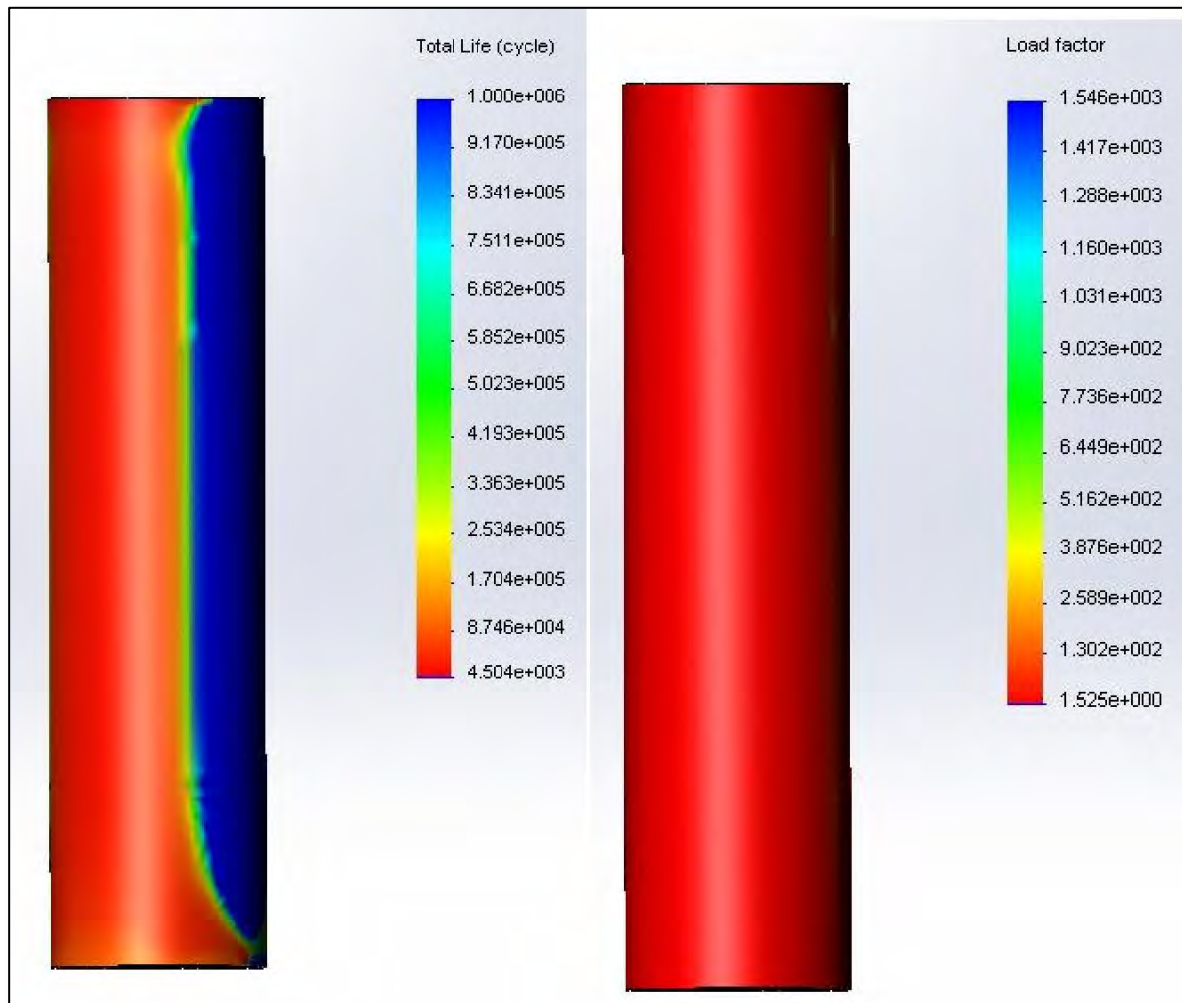
- Validate the model using the hand calculations (apply hard landing loads):

$$\sigma_{max} = \frac{P}{A} + \frac{M_c}{I} = \frac{4P}{\pi(OD^2 - ID^2)} + \frac{32V_x(R_{shaft} + L)OD}{\pi(OD^4 - ID^4)} = \frac{4 \cdot 4233}{\pi(1.5^2 - 1.2^2)} + \frac{32 \cdot 1500 \cdot 14.65 \cdot 1.5}{\pi(1.5^4 - 1.2^4)} = 119 \text{ ksi}$$

- The hand calculation is very close to the FEA model value therefore, the FEA model is accurate enough to use for the fatigue analysis.

4. Perform FE fatigue analysis using the static loading from the above model

FIGURE 28 FATIGUE ANALYSIS OF STRUT



- The expected number of hard landings the part will survive is ~4500 and the lowest loading factor or factor of safety across the part is 1.525.

2.3.3.4 SUMMARY OF STRUT SHAFT DESIGN

TABLE 10 SUMMARY STRUT SHAFT DESIGN

Parameter	Value	Source
Material	AISI 5160	Design decision, point 2.3.3.1 of strut shaft section
Outside diameter (in)	1.5	Design decision
Inside diameter (in)	1.2	Lowest diameter that ensures infinite life for worst case landings and a safety factor of at least 1.5 for buckling failure. Point 2.3.3.2 from the strut shaft section
Expected worst case landings before failure	Infinite	Designed for infinite worst case landing conditions, point 2.3.3.2 from the strut shaft section
Expected hard landings before failure	4500	FEA fatigue analysis, point 2.3.3.3 from strut shaft section
Lowest factor of safety	1.5	Designed for a safety factor of 1.5
Mass (lbs)	1.82	SolidWorks model
Total length (in)	10	Design decision – 2in for the fork, 5in for the stroke and 3 in inside the strut body when shock fully extended

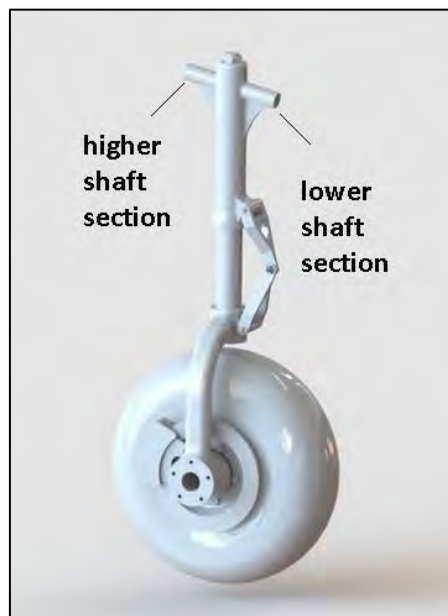
2.3.4 Analysis and design of strut body

2.3.4.1 ANALYTICAL CALCULATIONS FOR MAXIMUM STRESSES

The stress analysis to be performed is based on several assumptions and simplifications. The higher shaft section is assumed to only have a y-component reaction force. The shaft sections will be modeled as hollow cantilever beams. These conservative calculations will show the worst-case stresses at critical points in the shaft based on various loading conditions. The designed shaft sections have ribs and fillets to reduce stress concentration. If the maximum stresses found through analytical calculations based on the following assumptions are far greater than the stresses found through FEA modeling, the assumptions are valid:

- Wheel shaft to lower/back joint - this joint has both an x and y reaction force (R_x and R_y)
 - Vertical distance - 22.58in
 - Horizontal distance - 2.94in
- Wheel shaft to higher/front joint - this joint has only a y reaction force (Q_y)
 - Vertical distance - 23.72in
 - horizontal distance - 2.94in
- Loadings on shaft
 - Worst case landing - $P_y = 2711$ lbf; $P_x = 837$ lb
 - Hard landing - $P_y = 4233$ lb, $P_x = 1500$ lb (assumed)
- Cantilever calculations use the following dimensions:
 - OD = 1in
 - Length ~ 2.18 in
 - Material - SAE 4340 (quench and tempered at 600°C) $S_y = 230$ kpsi

FIGURE 29 SHAFT SECTIONS



· Worst landing:

Force calculations for worst landing:

$$\sum F_x = -837 \text{ lbs} + R_x = 0 \rightarrow R_x = +837 \text{ lbs (pointing towards center)}$$

$$\sum F_y = R_y + Q_y + 2711 \text{ lbs} = 0$$

$$\sum M = +Q_y(5.88 \text{ in}) + 2711 \text{ lbs}(2.94 \text{ in}) - 837 \text{ lbs}(22.58 \text{ in}) = 0$$

$$Q_y = +1858.6939 \text{ lbs (pointing upward)}$$

$$R_y = -1858.6939 \text{ lbs} - 2711 \text{ lbs} = -4569.6939 \text{ lbs (pointing downward)}$$

Bending stress at critical point of lower joint:

$$\sigma_{crit} = \frac{M_c}{I} - \frac{R_x}{A}$$

For hollow cylinder (assumed ID based on FEA model):

$$M = R_y \cdot l = -4569.6939 \text{ lbs} \cdot \sin(79) \cdot 2.18 \text{ in} = 9778.9039 \text{ lbs} \cdot \text{in}$$

$$I = \frac{\pi}{64}(OD^4 - ID^4) = \frac{\pi}{64}(1 \text{ in}^4 - 0.7 \text{ in}^4) = 0.03730 \text{ in}^4$$

$$c = 0.5 OD = 0.5 \cdot 1 \text{ in} = 0.5 \text{ in}$$

$$A = \frac{\pi}{4}(OD^2 - ID^2) = \frac{\pi}{4}(1 \text{ in}^2 - 0.7 \text{ in}^2) = 0.40055 \text{ in}^2$$

$$\sigma_{crit} = \frac{M_c}{I} - \frac{R_x}{A} = \frac{9778.9039 \text{ lbs} \cdot \text{in}}{0.03730 \text{ in}^4} - \frac{873 \text{ lbs} \cdot \cos 79}{0.40055 \text{ in}^2} = 130.6907 \text{ kpsi}$$

Von Mises stress:

$$\sigma_1 = 116.7438 \text{ kpsi}; \quad \sigma_2 = 0; \quad \sigma_3 = 0; \quad \tau = 0;$$

$$\sigma' = \sqrt{\sigma_1^2 + \sigma_2^2 + \sigma_3^2 + 3 \tau^2} = 130.6907 \text{ kpsi for lower shaft section}$$

Safety factor using distortion-energy theory:

$$N = \frac{S_y}{\sigma'} \frac{230 \text{ kpsi}}{130.6907 \text{ kpsi}} = 1.76 \text{ for lower shaft section}$$

Bending stress at critical point of higher shaft section:

$$\sigma_{crit} = \frac{M_c}{I}$$

$$M = Q_y \cdot l = 2711 \text{ lbs} \cdot \sin 79 \cdot 2.18 \text{ in} = 5801.39710 \text{ lb} \cdot \text{in}$$

$$\sigma_{crit} = \frac{M_c}{I} = \frac{5801.39710 \text{ lb} \cdot \text{in} \cdot 0.5 \text{ in}}{0.03730 \text{ in}^4} = 77.7667 \text{ kpsi}$$

Von Mises stress:

$$\sigma_1 = 77.7667 \text{ kpsi}; \quad \sigma_2 = 0; \quad \sigma_3 = 0; \quad \tau = 0;$$

$$\sigma' = \sqrt{\sigma_1^2 + \sigma_2^2 + \sigma_3^2 + 3 \tau^2} = 77.7667 \text{ kpsi for higher shaft section}$$

Safety factor using distortion-energy theory:

$$N = \frac{S_y}{\sigma'} \frac{230 \text{ kpsi}}{77.7667 \text{ kpsi}} = 2.96 \text{ for higher shaft section}$$

· Hard landing static stress analysis:

Force calculations for worst landing:

$$\sum F_x = -1500 \text{ lbs} + R_x = 0 \rightarrow R_x = +1500 \text{ lbs (pointing towards center)}$$

$$\sum F_y = R_y + Q_y + 4233 \text{ lbs} = 0$$

$$\sum M = +Q_y(5.88 \text{ in}) + 4233 \text{ lbs}(2.94 \text{ in}) - 1500 \text{ lbs}(22.58 \text{ in}) = 0$$

$$Q_y = +3643.7041 \text{ lbs (pointing upward)}$$

$$R_y = -3643.7041 \text{ lbs} - 4233 \text{ lbs} = -7876.7041 \text{ lbs (pointing downward)}$$

Bending stress at critical point of lower joint:

$$\sigma_{crit} = \frac{M_c}{I} - \frac{R_x}{A}$$

$$M = R_y \cdot l = -7876.7041 \text{ lbs} \cdot \sin(79) \cdot 2.18 \text{ in} = 16855.7314 \text{ lbs} \cdot \text{in}$$

$$\sigma_{crit} = \frac{M_c}{I} - \frac{R_x}{A} = \frac{16855.7314 \text{ lbs} \cdot \text{in}}{0.03730 \text{ in}^4} - \frac{1500 \text{ lbs} \cdot \cos 79}{0.40055 \text{ in}^2} = 225.2336 \text{ kpsi}$$

Von Mises stress:

$$\sigma_1 = 225.2336 \text{ kpsi}; \quad \sigma_2 = 0; \quad \sigma_3 = 0; \quad \tau = 0;$$

$$\sigma' = \sqrt{\sigma_1^2 + \sigma_2^2 + \sigma_3^2 + 3 \tau^2} = 225.2336 \text{ kpsi for lower shaft section}$$

Safety factor using distortion-energy theory:

$$N = \frac{S_y}{\sigma'} \frac{230 \text{ kpsi}}{225.2336 \text{ kpsi}} = 1.02 \text{ for lower shaft section}$$

This safety factor value is lower than the preferred. But since these calculations are an overestimate, no optimization calculations need to be performed.

Bending stress at critical point of higher shaft section:

$$\sigma_{crit} = \frac{M_c}{I}$$

$$M = Q_y \cdot l = 3643.7041 \text{ lbs} \cdot \sin 79^\circ \cdot 2.18 \text{ in} = 7797.3346 \text{ lb} \cdot \text{in}$$

$$\sigma_{crit} = \frac{M_c}{I} = \frac{7797.3346 \text{ lb} \cdot \text{in} \cdot 0.5 \text{ in}}{0.03730 \text{ in}^4} = 104.5219 \text{ kpsi for higher shaft section}$$

Von Mises stress:

$$\sigma_1 = 104.5219 \text{ kpsi}; \quad \sigma_2 = 0; \quad \sigma_3 = 0; \quad \tau = 0;$$

$$\sigma' = \sqrt{\sigma_1^2 + \sigma_2^2 + \sigma_3^2 + 3\tau^2} = 104.5219 \text{ kpsi for higher shaft section}$$

Safety factor using distortion-energy theory:

$$N = \frac{S_y}{\sigma'} = \frac{230 \text{ kpsi}}{104.5219 \text{ kpsi}} = 2.20 \text{ for higher shaft section}$$

Fatigue analysis of shaft section

The inside diameter was assumed in the FEA model, but resulted in maximum stress well within the allowable range given the material selection of 4340 steel. For further reinforcement and to ensure minimal stress concentration at the critical points, ribs and fillets were added at these corresponding positions. Ideally, calculations would be performed to further validate the FEA fatigue analysis model. But given that these calculations are complicated by the added reinforcements and the overestimated maximum stresses found in both the worst landing and hard landing are well below the maximum stresses found through FEA analysis, it was reasonable to assume that the proper assumptions were made when designing the shaft section.

2.3.4.2 FEA STRESS STUDY

1. Loading and boundary conditions

- Vertical load applied at the base of the strut body. Value for worst case landing is 2711 lbf and 4233lbf for hard landing.
- The horizontal load is also applied at the base of the strut body. It is important to point out that this arrangement is an approximation of the actual set up as the force in reality will be transmitted through the interface between the strut shaft and the strut body.

The reason why this approximation is valid is because there are no stress concentrations in the column part of the strut body so the component will not fail there and because the stresses in the critical points (where the column part intersect with the tube features for the joints) are unaffected by this approximation. Calculating the corresponding lateral forces for hard and worst case landing:

$$\frac{\text{Vertical distance between joint and shaft}}{\text{horizontal loading}} = \frac{\text{Vertical distance between joint and strut base}}{\text{Model horizontal loading}}$$

$$63.5 \text{ in} \cdot 1500 \text{ lbf} = 24 \text{ in} \cdot \text{Hard landing loading at strut body base}$$

$$\text{Hard landing loading at strut body base} = 2215 \text{ lbf}$$

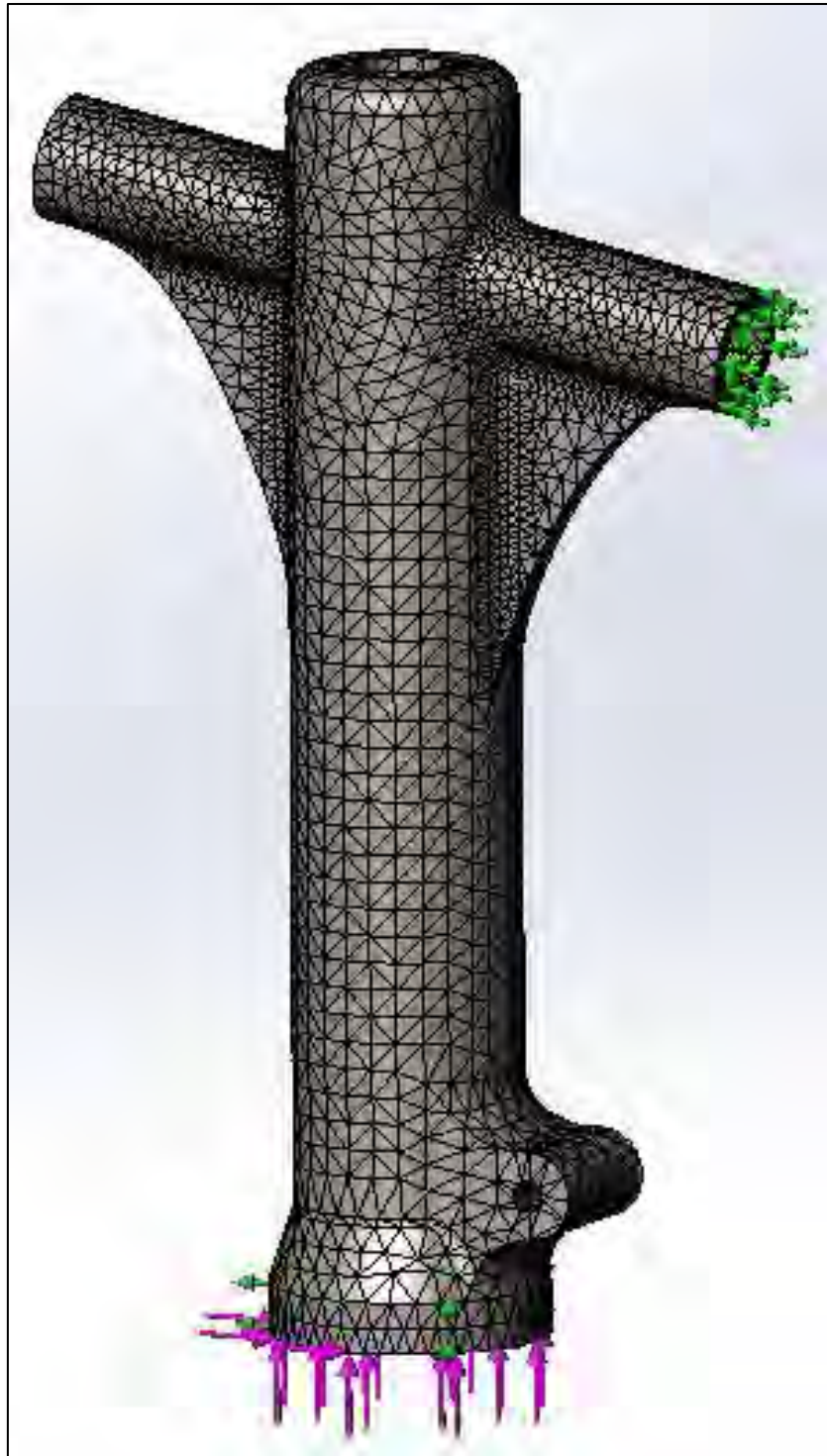
Following the same procedure:

- Pressure inside the strut body due to compression of the working fluids was calculated to be 1500 psi in tutorial.
- The front joint is fixed in a way as to provide a reaction force only in the vertical direction.
- The rear joint is fixed in a way as to provide a reaction force in both the vertical and horizontal direction.

2. Meshing the FEA model

- A simulation with a coarse mesh was performed to determine the stress concentration points so the mesh can be refined accordingly.
- The mesh density was increased around the sections where the stress or the error were high.

FIGURE 30 FINAL ITERATION OF MESH USED FOR THE STRUT BODY STRUCTURAL SIMULATIONS



3. Run FEA models

FIGURE 31 WORST CASE LANDING FEA STRESSES AND ERROR PLOT

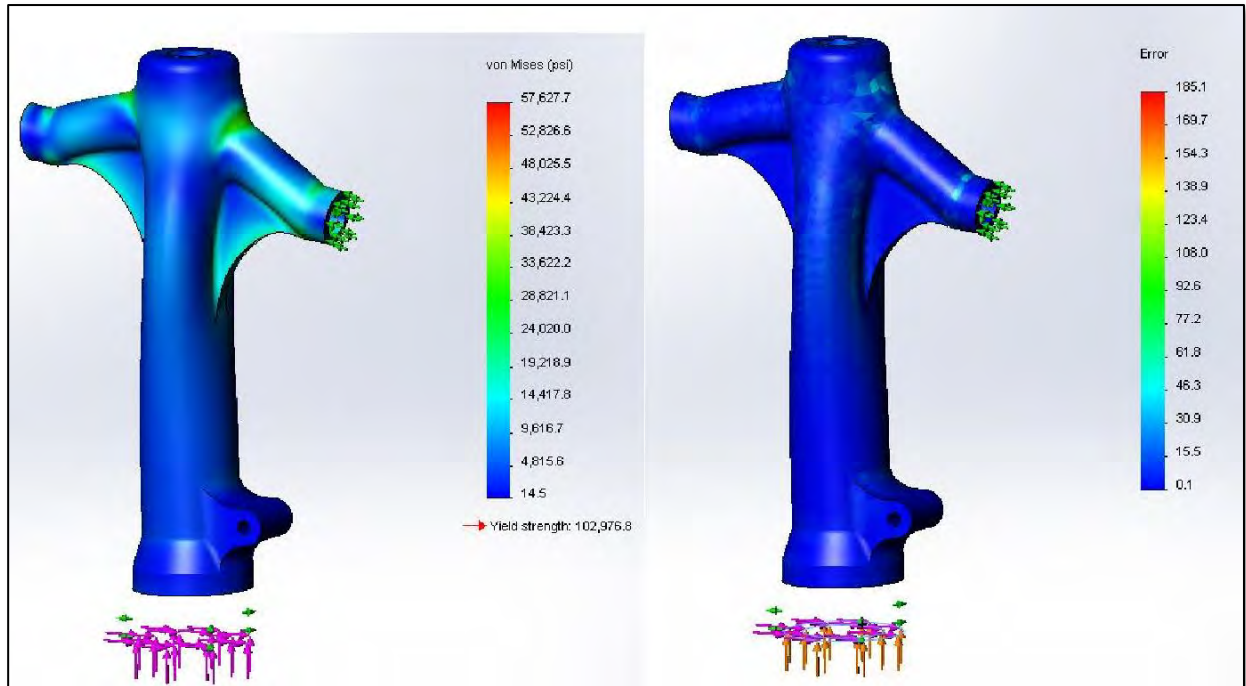
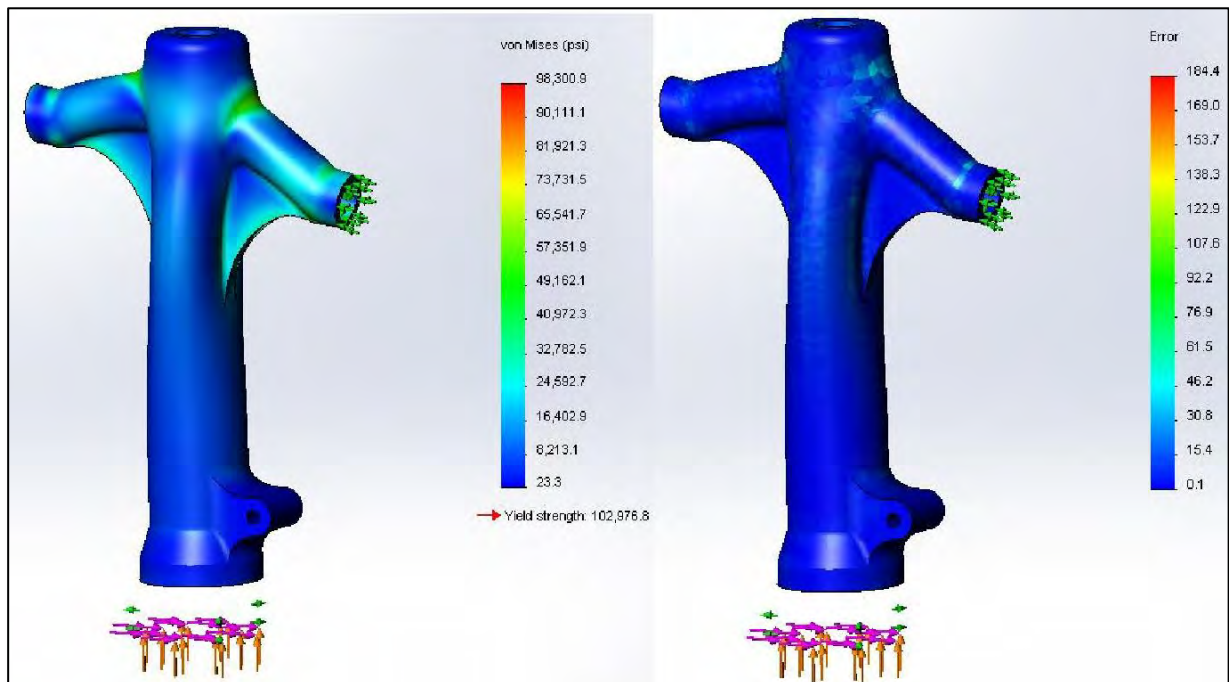


FIGURE 32 HARD LANDING FEA STRESSES AND ERROR PLOT



2.3.4.3 FEA FATIGUE STUDY

FIGURE 33 FE FATIGUE STUDY RESULTS FOR WORST CASE LANDING – EXPECTED LIFE
AND LOAD FACTOR

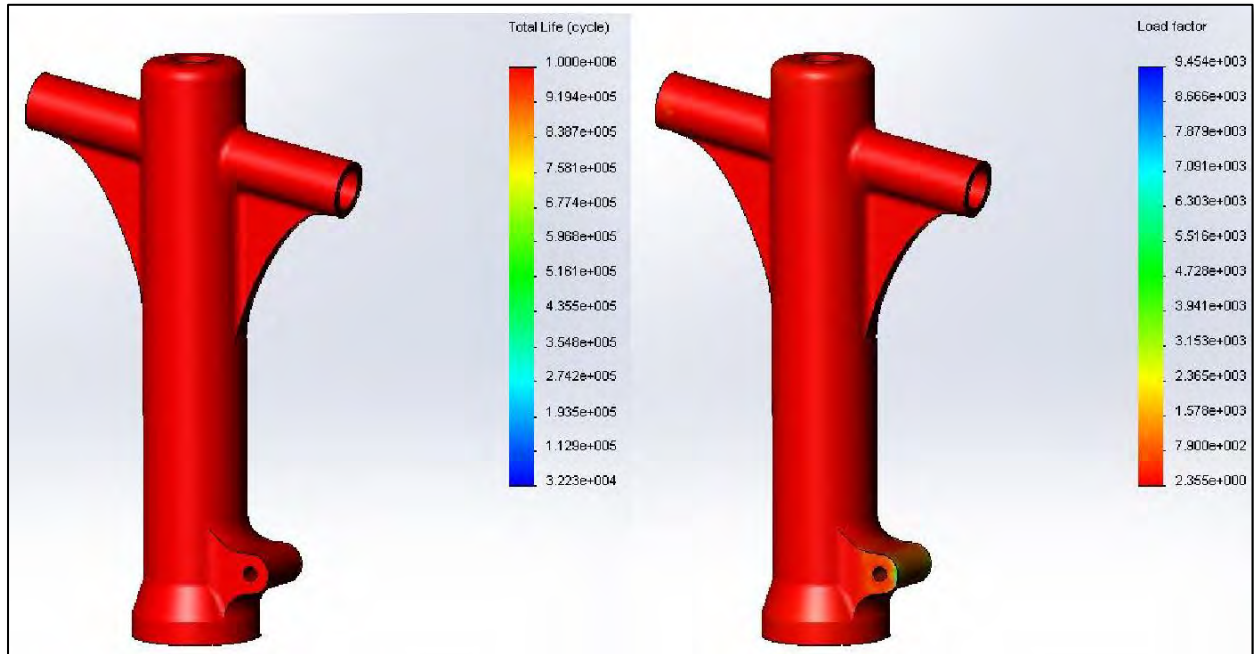
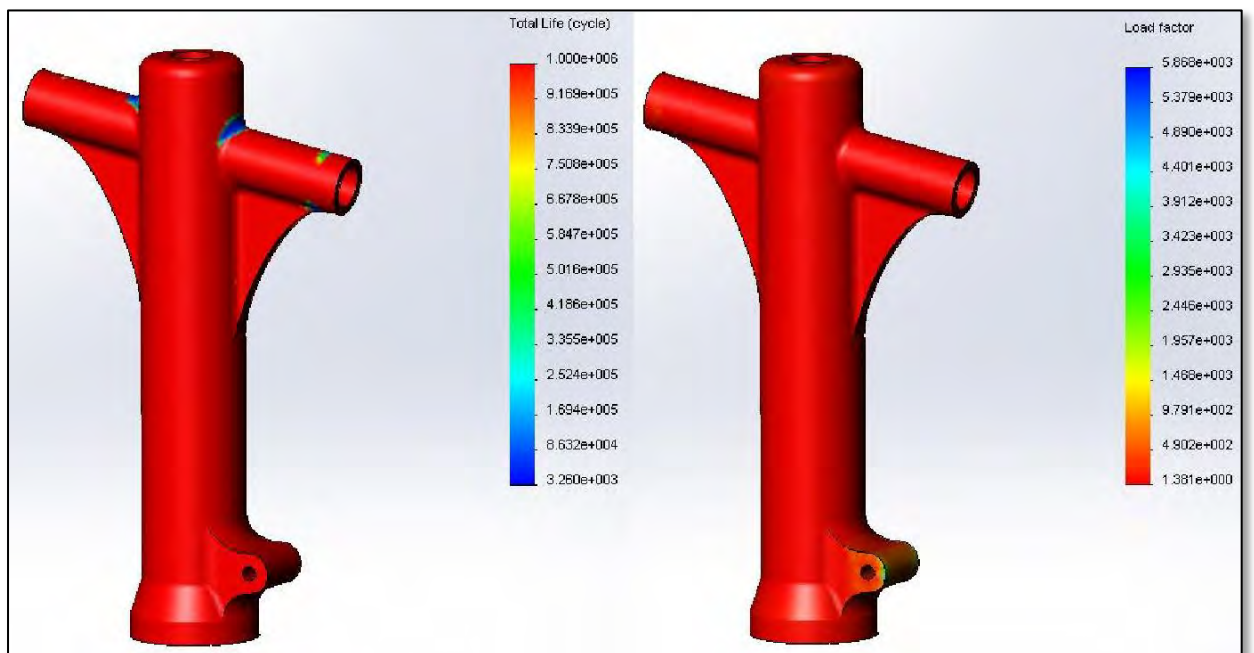


FIGURE 34 FE FATIGUE STUDY RESULT FOR HARD LANDING – EXPECTED LIFE AND LOAD
FACTOR



2.3.4.4 SUMMARY OF STRUT BODY DESIGN

TABLE 11 STRUT BODY DESIGN SUMMARY

Parameter/Dimension	Value	Source
Material	AISI 4340	
Strut stroke (in)	5	
Weight (lbs)	3.72	SolidWorks model
Worst case landing maximum stresses (ksi)	34	FEA model
Worst case landing Safety factor	3.03	
Expected worst case landings before failure (cycles)	$>10^6$	
Worst case landing Load factor	2.36	
Hard landing maximum stresses (ksi)	58	
Hard landing Safety factor	1.78	
Expected hard landings before failure (cycles)	3260	
Hard landing Load factor	1.38	

- Note that due to errors around the assumed boundary conditions the measured maximum stresses are significantly higher than the stresses at the expected stress concentration points. The maximum stress column indicates the maximum stress at the stress concentration points (or the points of interest).
- The load factor is the factor by which the current load must be multiplied to have the component fail in 1000 cycles or less.

2.3.5 Strut motion study

The goal of the motion study is to simulate the response of the strut during a worst case landing and a hard landing. The master assembly of the landing gear was used for this purpose. The oleo-pneumatic strut was modeled as a linear spring-damper system where the spring coefficient was 120 N/mm, the spring relaxed length was 171.121mm and the damping coefficient was 2.5 Ns/mm.

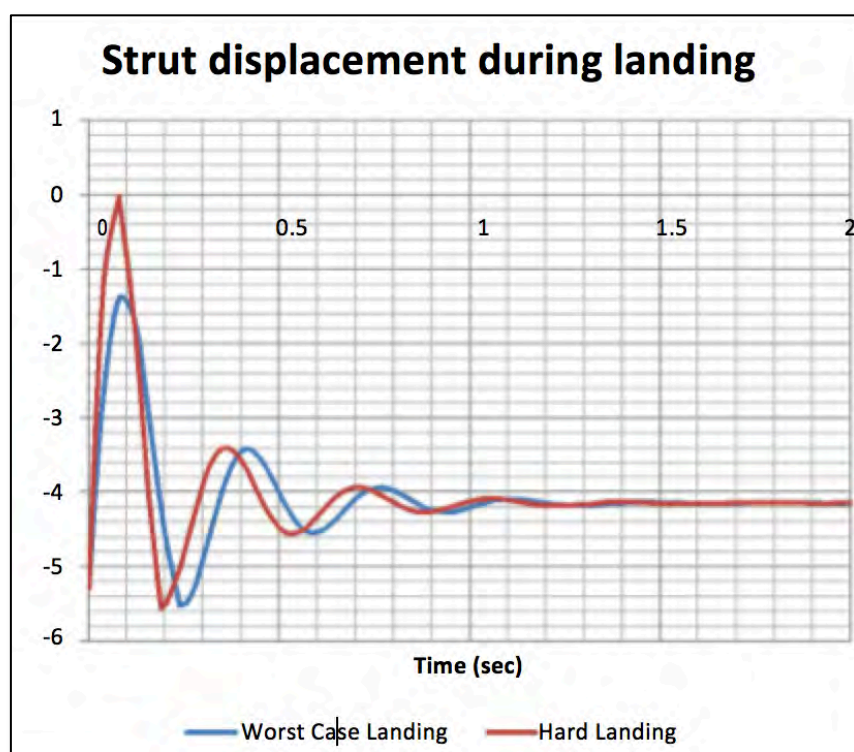
For simplicity, a somewhat reverse set-up was chosen for the actual simulation: the strut body was fixed in space, the shock absorber was fully extended and gravity was assigned to point upwards. Then a mass of 760lbs was attached to the fork and was given an initial velocity upwards of 6.124 ft/s for worst case landing and 10 ft/s for hard landing. Note that 760lbs is the uncorrected (no safety factor applied) static load on one of the main landing gears. The calculations can be found in section 2.1.1 Specific tire requirements.

Further assumptions and special conditions include:

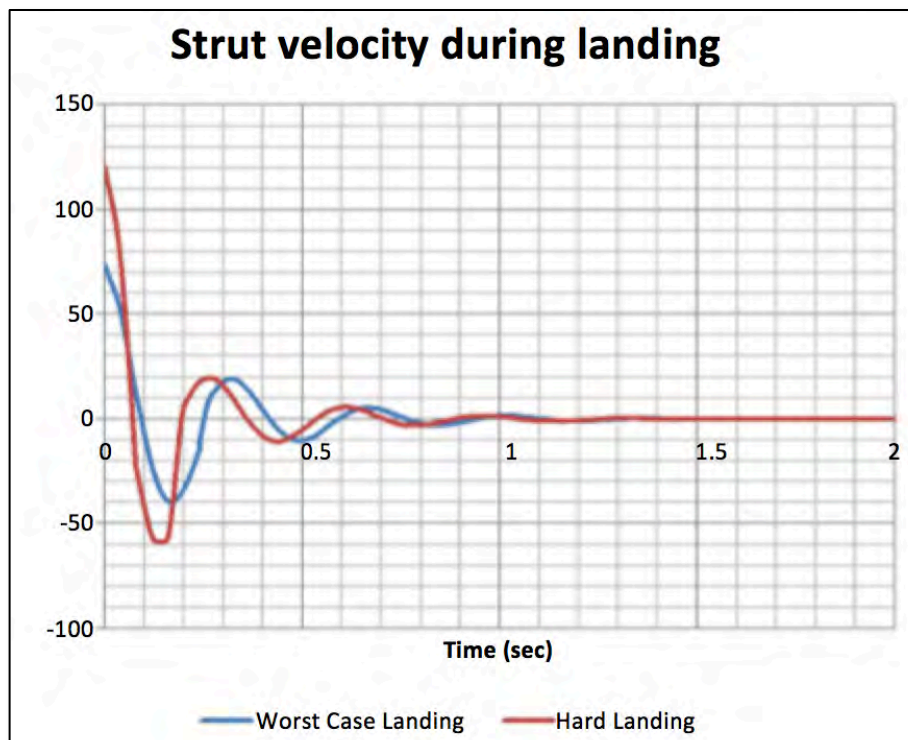
- Ignoring friction between strut body and strut shaft
- Simulating impact between components during worst case landing
- Simulating friction between torque links, strut body and fork

The response can be found in the following graphs:

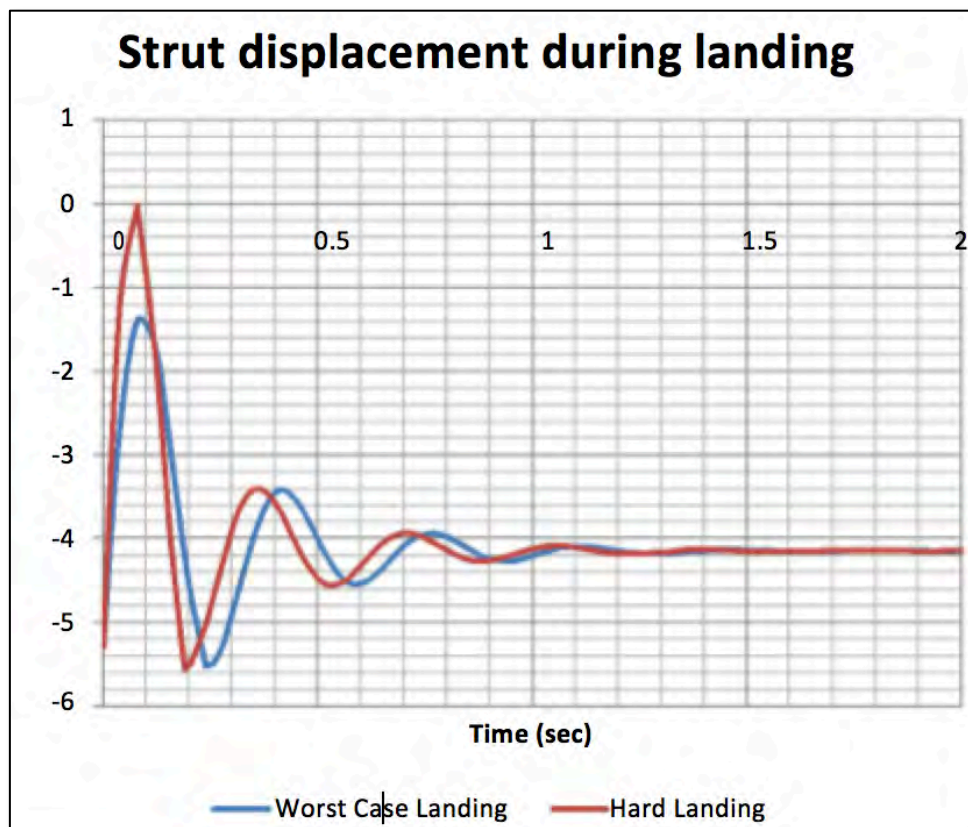
GRAPH 2 MOTION STUDY OF STRUT DISPLACEMENT DURING LANDING



GRAPH 3 MOTION STUDY OF STRUT VELOCITY DURING LANDING



GRAPH 4 MOTION STUDY OF STRUT ACCELERATION DURING LANDING



Note that the peak at ~ 0.2 seconds is something that the simulation does not account for – rebound. What happens at this moment during hard landing is that the plane bounces off the ground because the spring was fully compressed. The acceleration goes to an exceptionally high peak because the strut body is “fixed” and is not allowed to “bounce” off as it would in real life. This indicates that further refinement of the model is required.

Potential paths of refinement of the strut motion study:

- Model the spring coefficient and the damping coefficient in a way to account for their variance as the strut compresses (for example account for variable damping piston diameter).
- Include friction between all moving components.
- Include thermal stresses due to compression of working fluids.
- Include material damping where the components themselves provide the damping
- Include the compression of the tire in the model.
- Account for possibility of plane bouncing off track.

2.4 Torque Link



2.4.1 Specific torque link requirements

The torque link should be able to withstand worst case landing conditions and resist the maximum expected torsional moments about the oleo strut axis.

Because of its role in transmitting torsion between the lower and upper oleo parts, the torque link is a critical mechanism in the landing gear. During landing, heavy fluctuating loads will be applied to the torque link and it is important to ensure that it will not fail prematurely.

1. FAR requirements

- Use factor of safety of 1.5

2. Model-specific requirements

- Due to insufficient data regarding the torque link calculations during the research, I was unable to calculate the required resisting torsional moments correctly. There for, I used an approach based on the information found during the research. Since I designed my torque link to be smaller than the original design, my designed torque Link should be able to resist the max expected torsional moments about the oleo strut axis which corresponds to = 5000 in · lbs

Relevant calculations made on the torque link:

$$T_E = 5000 \text{ lbs} \cdot \text{in}$$

$$9R_2 = T_E \rightarrow R_2 = 555.55 \text{ lbs}$$

$$3.92R_2 = R_3 \rightarrow R_3 = 1405 \text{ lbs}$$

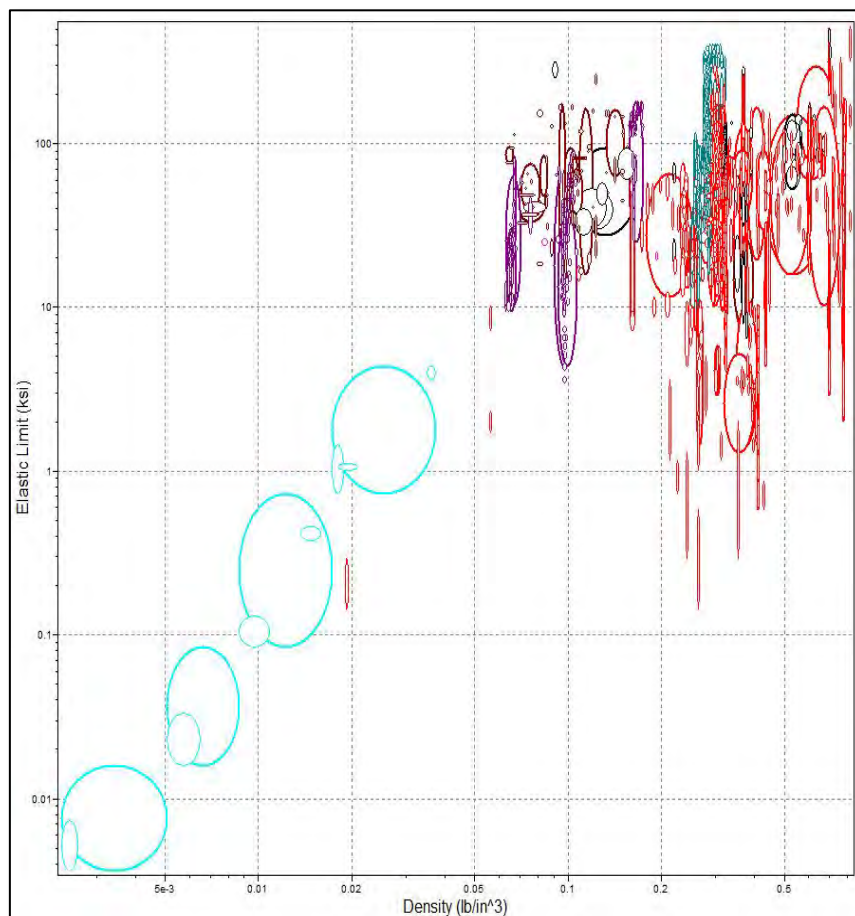
2.4.2 Material selection

The main criteria for the material selection of the mentioned components were the density, the strength and fatigue crack resistance of the alloy. The components will be exposed to water vapor, salt and some other environmental corrosives. Thus, they are normally manufactured from aluminum for its corrosion resistance and lightweight. However, we will apply our research through CES 2005 (material selector software) on all known metals with the following criteria

- Good resistance to fresh water
- Very good resistance to organic solvents.
- Average resistance to sea water.
- Poor good resistance to strong acid.
- Very good resistance to UV.
- Very good resistance to wear.
- Average resistance to weak acid.
- Good resistance to weak alkalis

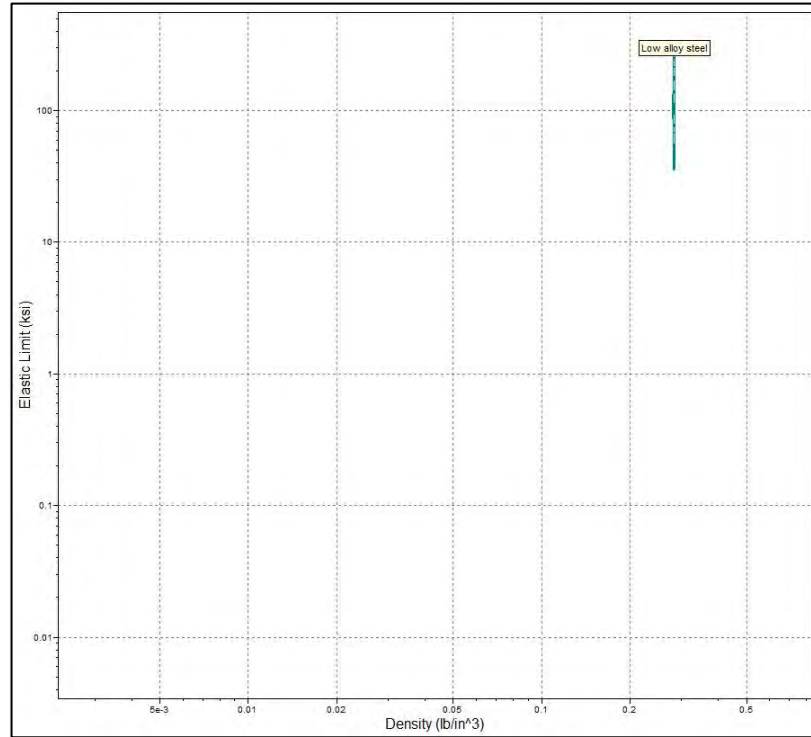
Density versus elastic limit to select the strongest and lightest material among the potential metals:

FIGURE 35 DENSITY VERSUS ELASTIC LIMIT OF ALL POTENTIAL METALS



To limit the remainder types of metals we limited the tensile strength values, the yield strength values and low prices for low alloy steels and the following graph was created:

FIGURE 36 DENSITY VERSUS ELASTIC LIMIT OF POTENTIAL LOW ALLOY STEELS



There for, the most suitable material with the cheapest price is AISI-4340

TABLE 12 SUMMARY OF MATERIAL SELECTION FOR TORQUE LINK

Material	Steel AISI-4340
S_{ut} (ksi)	250
S_y (ksi)	230
S_e (ksi)	48
W hard landing (lbs)	4233
W worst landing (lbs)	2880
Density (lb/in³)	0.2854
Cost (CAD \$/LB)	0.6702
Does the material satisfy the requirements?	YES

2.4.3 Fatigue analysis

Using the Free body diagram of the torque link I determined that the analysis on the torque link should be performed on the left side (critical point) of the link since it will experience the max stresses:

$$T_E = 5000 \text{ lbs} \cdot \text{in} = M$$

There for the resultant force for R_2 & R_1 can be easily found using simple Pythagoras

$$F_{\text{exerted on left side of link}} = 1510 \text{ lbs/link}$$

$$\text{For the 2 torque links} = 755 \text{ lbs/link}$$

It's noticed that the resultant force acting on our critical point is almost double the value for our worst-case landing. This can be attributed to the fact that I designed my torque link to be almost half the length of the torque link in the original design. By doing that the resultant force were doubled as mentioned.

TABLE 13 SUMMARY OF TORQUE LINK REQUIREMENTS

Requirement type	Requirement statement	Requirement target value
FAR	Use of Factor of Safety (FS)	1.5
Model-specific	Support static weight of aircraft	1200 lbs
Model-specific	Support maximum landing velocity	114 mph
Model- Specific	Max force created from resisting torsional moment T_E	1510 lbs

2.4.4 Fatigue analysis calculations

$$S_e' = 0.5S_{ut} = 100 \text{ kpsi}$$

$$C_{load} = 1 \text{ (for bending)}$$

$$C_{temp} = 1 \text{ (Room temp. assumed)}$$

$$C_{reliab.} = 0.753 \text{ (} R = 99.9 \% \text{ reliability assumed)}$$

$$C_{surface} = 2.7S_{ut}^{-0.265} = 0.625 \text{ (machine surface)} \quad S_{ut} = 250 \text{ kpsi}$$

$$C_{size} = 0.869 \text{ deq}^{-0.097} = 0.975686$$

$$A_{95} = 0.05 bh = 0.007036$$

$$\text{deq} = \left(\frac{A_{95}}{0.0766} \right)^{1/2} = 0.303$$

$$S_e = C_{load}C_{temp}C_{reliab.}C_{surface}C_{size}S_e' = 45.92 \text{ kpsi}$$

$$\sigma_a = \frac{\sigma_{max} \pm 0}{2} = 1.4 \text{ kpsi} \quad \text{assuming} \quad \sigma'_a = \sigma_a$$

$$S_m = 0.9S_{ut} = 225 \text{ kpsi}$$

$$\log a = \log S_m - 3b$$

$$a = 223279.6$$

$$\log S_n = \log a + b \cdot \log N$$

$$S_n = 10^{4.7584} = 60.97 \text{ kpsi}$$

$$b = -\frac{1}{z} \log \left(\frac{f \cdot S_{ut}}{S_e} \right) = -\frac{1}{3} \log \left(\frac{0.775 \cdot 250}{125} \right) = -0.0634$$

$$N_f = \frac{S_f S_{ut}}{\sigma_a S_{ut} + \sigma_m S_f} \quad \sigma'_a = \frac{S_f S_{ut}}{N(S_{ut} + S_f)} = 25.8 \text{ kpsi}$$

Using AISI 4340 steel and the safety factor = 1.5 I obtain 25.8 kpsi which is much bigger than the one that was calculated using resisting torque of 5000 lb · in. Therefore our design of the torque link should withstand this force and in the same time satisfy the safety factor of (1.5).

2.4.5 Finite element analysis

To make sure that the stresses and deformations in the torque link component were not severe, I used the final element analysis function in solid works to generate motion studies on the Torque arm. The fatigue analysis was solved to obtain the dimensions of the cross section for a safety factor of 1.5 using excel. According to “Aircraft Landing Gear Design: Principles and Practices”, a retractable landing gear should be able to operate for at least 5000 cycles under normal landing condition and 1000 cycles under emergency conditions. In our analysis, we made sure that the torque link would be able to sustain 3650 cycles under emergency conditions.

For Max force created from resisting torsional moment TE

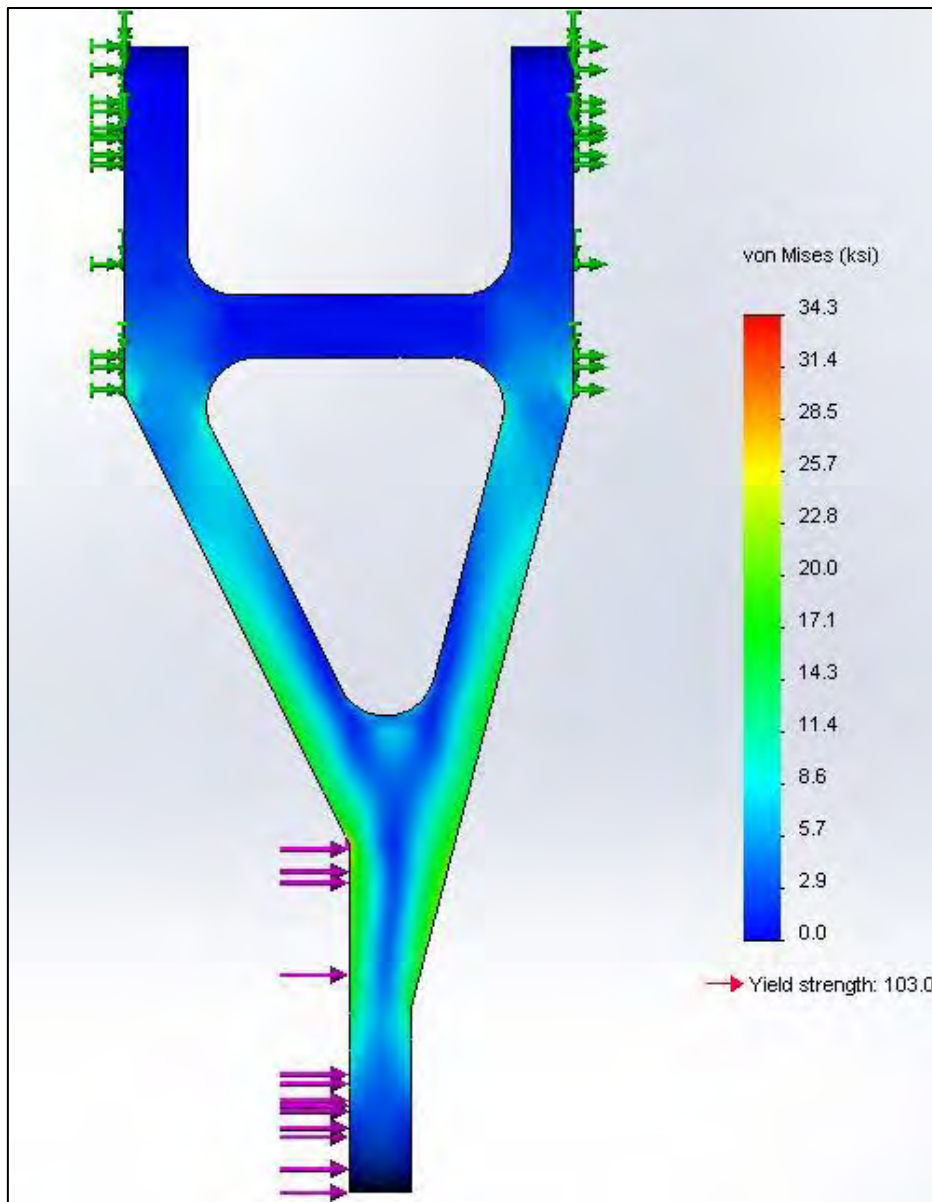
Loading conditions: use force of 700 lbs

Boundary conditions: Torque link is subjected to loading on the both upper and lower face of the eye section of the main body as well as it is required to fix the upper face of Main pin and lower face with another torque link.

Meshing: The complicated component geometry does not allow for a very fine mesh so curvature based meshing was used where the mesh is significantly denser around sharp corners.

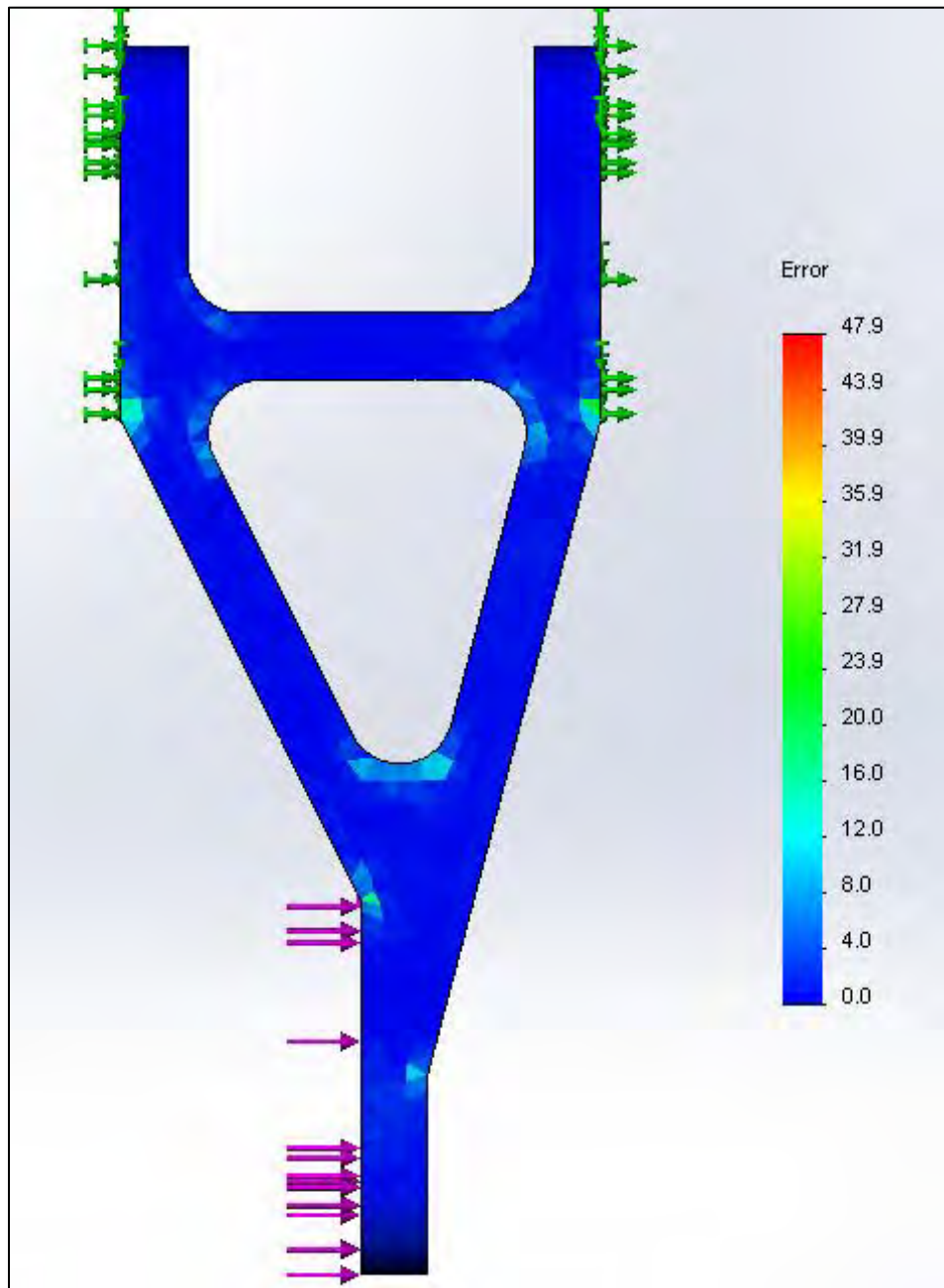
Due to contact of parts, unavoidable stress concentration is formed. In order to refine the simulation, the mesh is increased around sharp edges near the area where the load is applied. Ignoring the stress concentrations, the approximate maximum stress is around 34 kpsi. Comparing these values with the expected max stress of 25.8 kpsi yields an error of 25 %.

FIGURE 37 STATIC ANALYSIS OF FORK



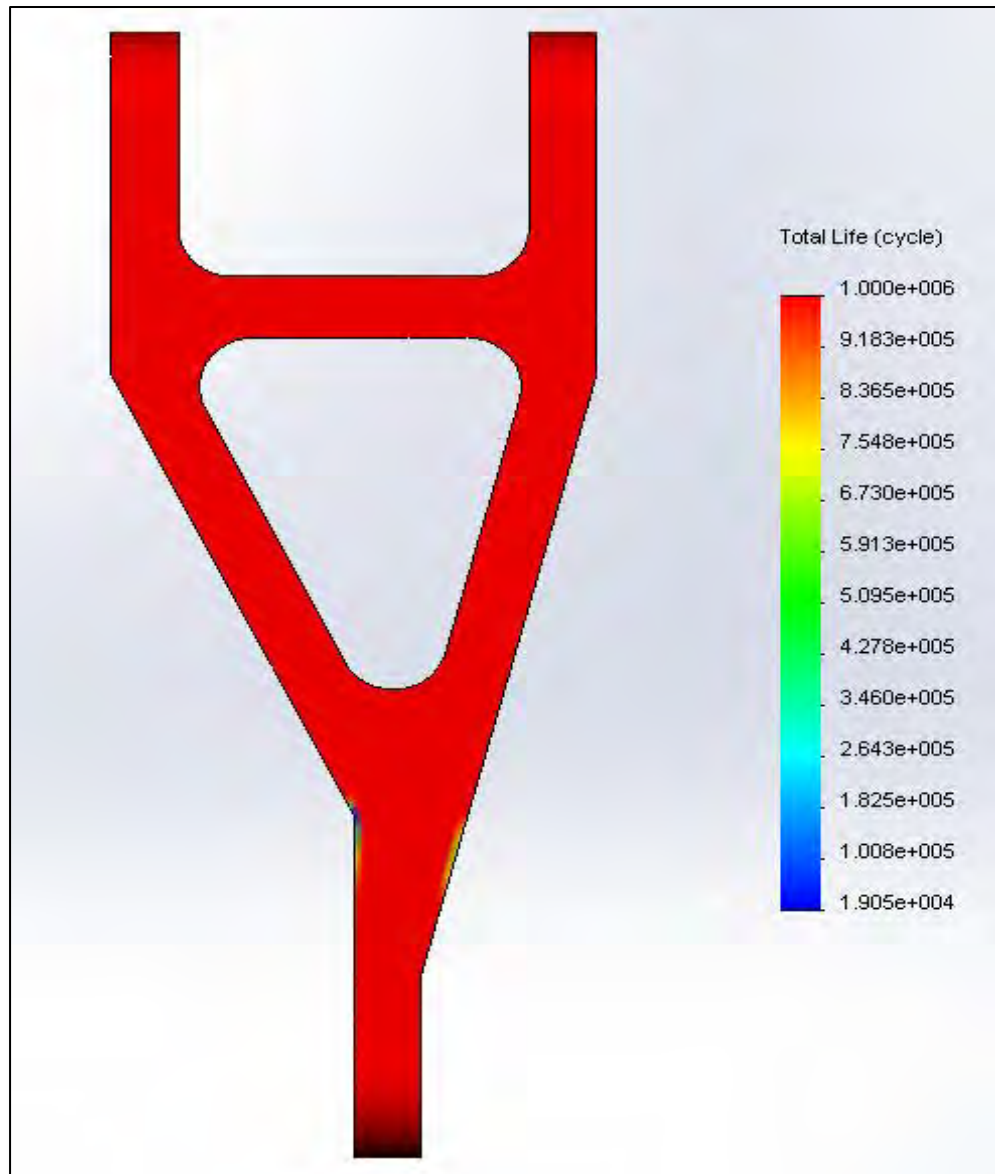
- The values near the fixed surface are very high (30 ksi). This is due to the location of a false stress concentration arising from the way the fixture is defined. This can be observed better in the error plot below:

FIGURE 38 ERROR PLOT OF FEA ANALYSIS FOR FORK



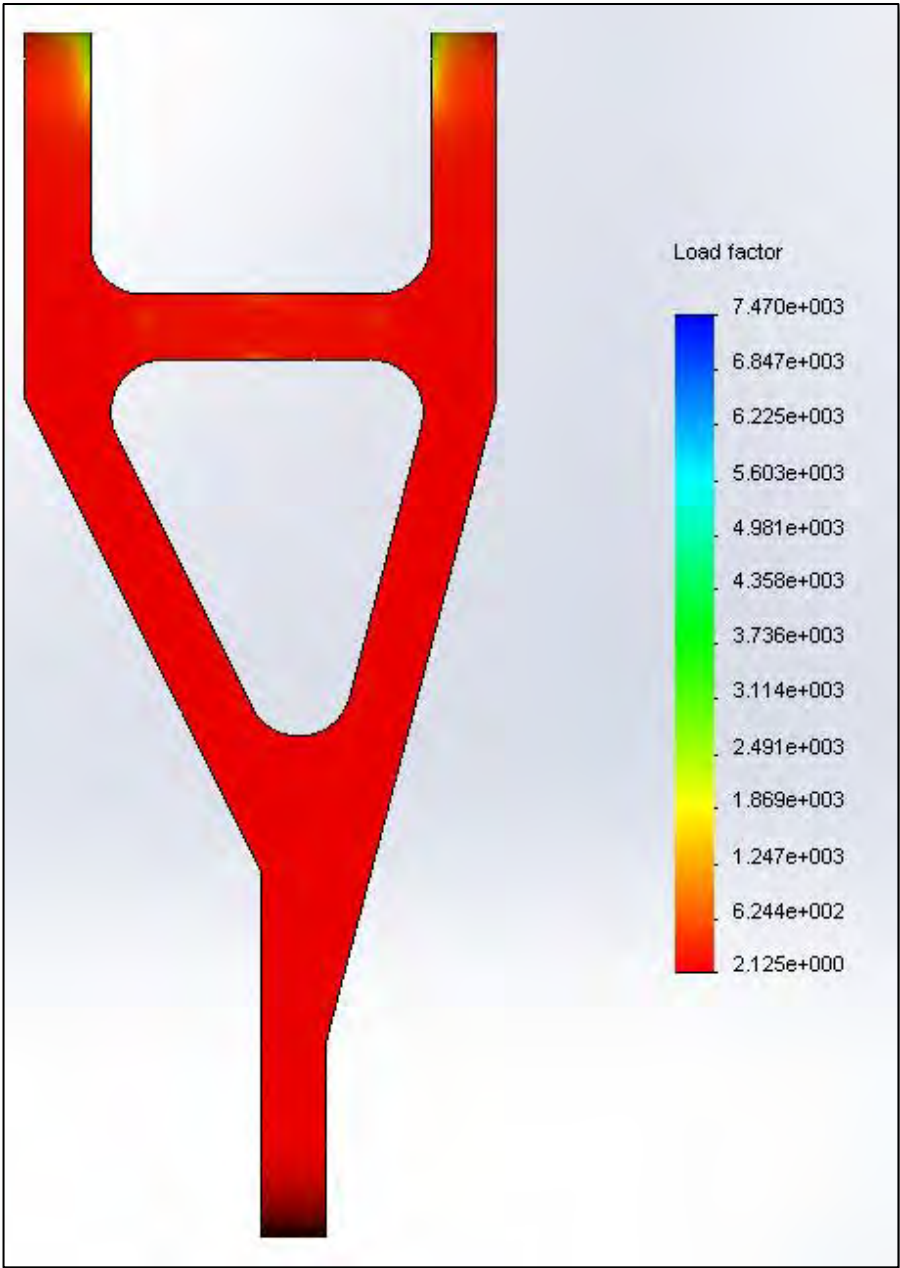
- The error is listed in percents so taking 24% off 30 ksi gives 22.76 ksi. The model can now be used for further FEA analysis.

FIGURE 39 FATIGUE ANALYSIS OF FORK



$$N_f = \frac{S_f S_{ut}}{\sigma'_a (S_{ut} + S_f)} = 1.7 \text{ (using the correct stress concentration of 22.76 kpsi)}$$

FIGURE 40 LOAD FACTOR FOR FORK



Torque arm FEA discussion

Since the testing is performed till the part fails beyond its design ultimate load level, for that case we carry out the analysis process in order to find the ultimate load and yield stress for the torque link. The torque link was designed using finite element analysis and analysis for maximum stress condition. The torque link was fabricated using 4340 STEEL. Static tests demonstrated the load carrying capabilities in undamaged and damaged condition of the torque link.

When performing the FEA simulations I encountered many errors due to the complexity of the part.

My first problem was determining the load that can be applied on the torque link. Throughout the scope of the research and due to its complicity the torque link was never discussed in details. Therefore, I never had a chance to learn how to calculate the reacting moments acting on the component. Consequently, I used an assumption for the expected torque that would be able to resist the max expected torsional moments about the oleo strut axis.

I designed my torque link to be smaller than the original design to reduce the mass and achieve the goal of this project. Furthermore, when I applied the given torque in the tutorials from the original design the part failed. Therefore, I couldn't use the same resultant force given in the tutorials and an applied force of 700 lbs was assumed.

Due to the lack of experience in performing simulations a few assumptions were made when setting up the fixtures on the component. This led to having errors in the simulations and thus having errors in the results.

2.4.6 Summary of torque link design

Final dimensions and properties

FIGURE 41 3D MODEL OF TORQUE LINK

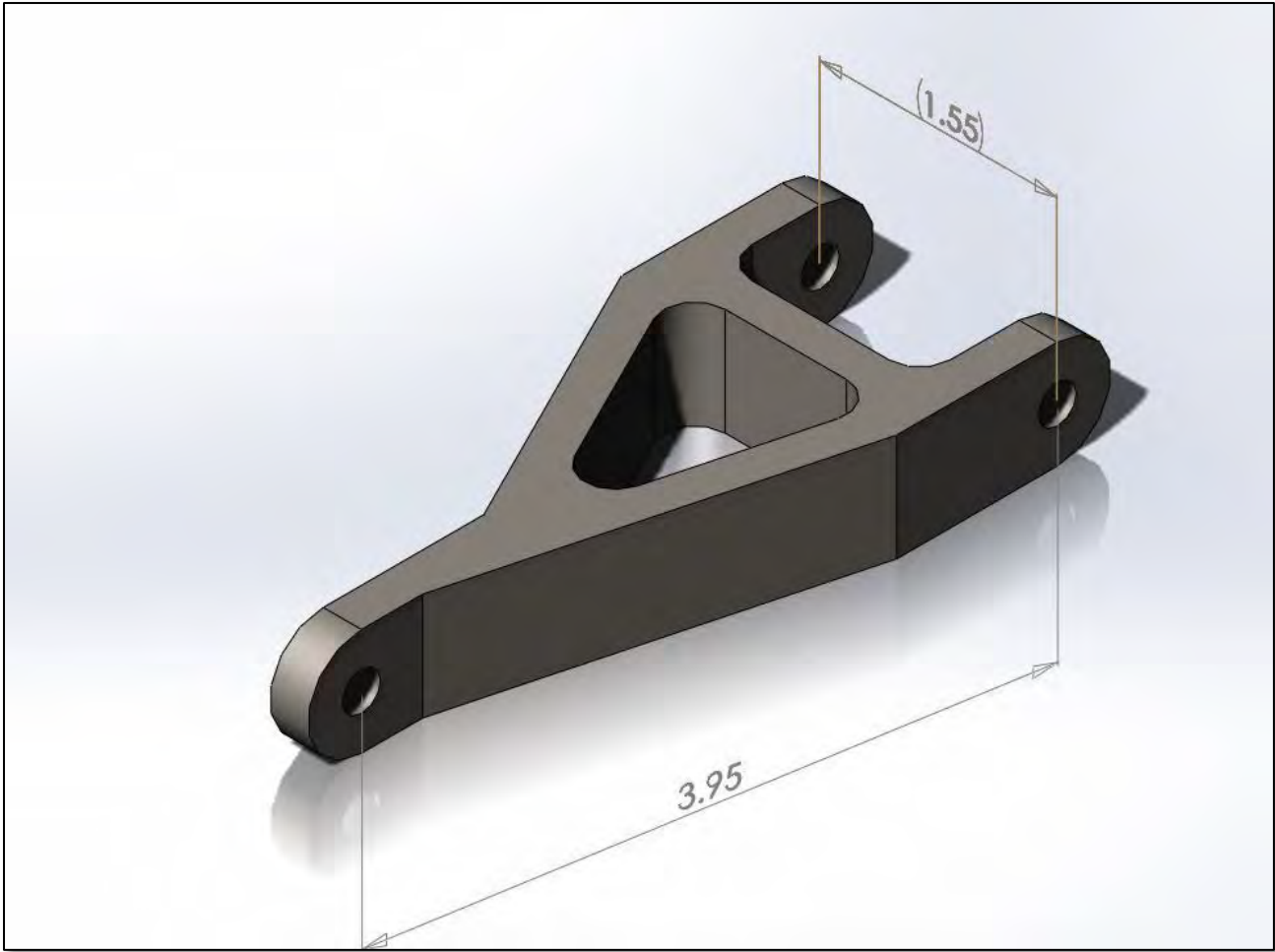


TABLE 14 SUMMARY OF FORK DESIGN

Volume	Mass	Surface
1.68 inch ^3	0.48 lbs	17.12 inch^2

The differences between the materials we selected and the original design's materials are the density (affects mass) and price. While the low alloy steels are stronger and cheaper, the aluminum alloys has less density and higher prices. A coating of the part is required to reduce corrosiveness. Coating parts is always cheaper than creating a type of steel with resistance to corrosion.

Recommendations:

Due to the fact that I am using steel instead of the conventional aluminum the next recommendations to reduce the corrosiveness are introduced. Most components are required to have maximum corrosion protection. Corrosion control is needed for all ferrous and non-ferrous materials of aircraft structures by considering:

- Inspection/monitoring of corrosion
- Use of a corrosion allowance
- Coatings and/ or cathodic protection
- Control of humidity for internal zones (Compartments)

2.5 Fork



2.5.1 Specific fork requirements

The fork clamps the wheel to the strut and shock absorber. The construction of it is done in a way that the curving moments are scaled down to a lowest due to the certainty that the wheel and strut are in the same axis. However, the fork must be able to support amplitude of static loading conditions and be contrived to avoid fatigue failure over number of cycles.

The most important requirements are that the fork must not be heavy and should be on the lighter side. It should be hard, inflexible and solid while keeping all costs at a low price

FAR requirements

According to FAR standards section 25.303, unless otherwise specified, a safety factor of 1.5 must be applied to the prescribed limit load which is considered external loads on the structure. Normally 1.2 safety factor is used for heavy shock loads, but for essentials parts of landing gear which bear maximum loading during the landing, safety factor of 1.5 is considered

Model-specific requirements

The fork must be able to support the corresponding fraction of the weight of the aircraft. The weight of the aircraft is set as 1914 lbs, which is (66% of the original weight of 2950lbs). The goal will be to determine the ideal thickness of the cross section by assuming a safety factor of 1.5 for both static and fatigue failure.

Investigate Static failure using the von Mises effective stress and iterating to obtain the thickness of the component. Moreover, estimation fatigue failure by assuming the aircraft will be landing once per day over the course of 20 years. Therefore, the maximum number of landings is $20 \times 365 = 7300$. Half them are worst landing and half of them are hard landing.

TABLE 15 REQUIREMENTS FOR FORK

Requirement type	Requirement statement	Requirement target value
FAR	Use of Factor of Safety (FS)	1.5
Model-specific	Support static weight of aircraft	1200 lbs
Model-specific	Support maximum landing velocity	114 mph
Model-specific	Worst Case Landing, nose gear clear, max vertical force	2711 lbs
Model-specific	Worst Case Landing, nose gear clear, max horizontal force	838 lbs
Model-specific	Hard case landing	4233 lbs

2.5.2 Material selection

The materials that I will be testing are AISI-4340 Steel and 7050 Aluminum. Those materials are commonly used in the aircraft industry due to their high strength and there superior properties of bearing tensile, bending and shear loads.

Properties of 7050 Aluminum

- Lightweight and High strength
- Resistance to corrosive humid and marine environments.
- Ultimate Tensile Strength: 83 ksi
- Tensile Yield Strength: 73 ksi
- Density: 0.10 lb/in³
- Cost: 0.84 CAD\$/lb
- Elongation at Break: 11 % at 1/2 in. (12.7 mm) Diameter
- Modulus of Elasticity: 71.7 GPa

Properties of AISI-4340 Steel

- Ultra High-Strength alloy Steel
- Can be used for parts stressed under heavy-duty conditions.
- Capable of providing excellent strength and hardness at extremely elevated temperatures.
- Ultimate Tensile Strength: 250 ksi
- Yield Strength: 230 ksi
- Cost: 0.672 CAD\$/lb
- Density: 0.2854 lb/in³
- Elongation at Break, Average value: 19.2 % at 1in (25.4mm) Diameter
- Modulus of Elasticity: 205 GPa

Analytical calculations:**Static loading:**

Material: AISI 4340 steel

$$S_{ut} = 250000 \text{ psi}$$

$$S_y = 230000 \text{ psi}$$

$$F_a = 2880 \text{ lbs}$$

Dimensions:

$$r_i = 3.5 \text{ in (length of the fork)}$$

$$r_o = 5 \text{ in (difference between the two)}$$

$$D = r_c = 4.25 \text{ in (distance from center of the wheel to fork)}$$

$$\text{Thickness} = r_o - r_i = 5 \text{ in} - 3.4 \text{ in} = 1.6 \text{ in}$$

$$\text{Area} = 1.6 \text{ in} \cdot 1.5 \text{ in} = 2.4 \text{ in}^2$$

$$\sigma = 68500 \text{ psi (yield strength of alloy steel 4340)}$$

$$e = r_c - \frac{(r_o - r_i)}{\log \frac{r_o}{r_i}} = 0.04 \text{ in}$$

$$c = r_c - r_i = 4.25 - 3.5 = 0.75 \text{ in}$$

$$F_a = 1.5F = 1.5(2880) = 4320 \text{ lb}$$

$$M = F \cdot D = F \cdot r_c = 4320 \cdot 4.25 = 18360 \text{ lb} \cdot \text{in}$$

Therefore,

$$\sigma = \frac{M}{eA} \cdot \frac{C_i}{r_i} + \frac{F}{A} = 41804.86 \text{ psi}$$

$$N = \frac{S_y}{\sigma} = \frac{230000 \text{ psi}}{41804.86 \text{ psi}} = 5.5$$

The safety factor against static loading is given as is used as in iteration to find the ideal thickness to obtain a factor of 1.5.

Fatigue failure for high cycle loading

As explain previously I will assume 7300 cycles for the fatigue analysis and a safety factor of 1.5.

$$F_a = F_m = \frac{F}{2} = \frac{4320}{2} = 2160 \text{ lbs}$$

$$M = F_a \cdot r_i = 2160 \cdot 3.5 = 7560 \text{ lbs}$$

$$\sigma_a = \sigma_m = \frac{Mh}{2I} = \frac{7560 \cdot 1.5/2}{1.5^3 t/12}$$

$$\sigma'_a = \sigma'_m = \sigma_a = \sigma_m = \frac{26880}{b}$$

$$N_f = \frac{S_f S_{ut}}{\sigma_a S_{ut} + \sigma_m S_f}$$

Calculating the endurance limit for steel:

$$S_e = C_{load} C_{temp} C_{reliab.} C_{surface} C_{size} S_e'$$

$$S_e' = 100 \text{ ksi (for } S_{ut} > 200 \text{ ksi)}$$

$$C_{load} = 1 \text{ (for bending)}$$

$$C_{temp} = 1 \text{ (Room temp. assumed)}$$

$$C_{reliab.} = 0.753 \text{ (} R = 99.9 \% \text{ reliability assumed)}$$

$$C_{surface} = 2.7 S_{ut}^{-0.265} = 0.625 \text{ (machine surface) } S_{ut} = 250 \text{ kpsi}$$

$$C_{size} = 0.869 \text{ deq}^{-0.097} = 0.887 [(\cdot bh)^{1/2}]^{-0.097} \text{ (for } 0.3 \text{ in} < d < 10 \text{ in)}$$

$$A_{95} = 0.05 bh$$

$$\text{deq} = \left(\frac{A_{95}}{0.0766} \right)^{1/2} = (0.652 \cdot bh)^{1/2}$$

$$S_e = C_{load} C_{temp} C_{reliab.} C_{surface} C_{size} S_e' = 41.744 (bh)^{-0.0485}$$

$$N_f = \frac{250 \cdot 41.744(bh)^{-0.0485}}{\frac{26880}{b}(41.744(bh)^{-0.0485} + 250)}$$

A first thickness of 1.5 is assumed and then repeated until the wanted safety Factor that is 1.5 obtained.

Approximating the S-N curve:

$$S_f(N) = aN^b$$

$$\log S(N) = \log a + b \cdot \log N$$

$$\log a = \log S_m - 3b$$

$$b = -\frac{1}{z} \log \left(\frac{S_m}{S_e} \right)$$

$$z = \log N_1 - \log N_2 = -0.69897$$

$$S_m = 0.9S_{ut} \text{ (bending)}$$

Computing the effective stress using von Mises

Finally we obtain the safety factor using: $N_f = \frac{S_f S_{ut}}{\sigma_a S_{ut} + \sigma_m S_f}$

The thickness is modified until a safety factor of 1.5 is achieved.

- Final Dimensions of the fork is 1.6 in x 1.5 in = 2.4 in²

For 20 years life cycle:

$$F = 2711 \text{ lb}$$

$$F = 4233 \text{ lb}$$

$$\text{Total} = 7300 \text{ landings}$$

$$n/N = 7300/10^6 = 0.0073$$

$$b = 1.6 \text{ in}$$

With the given values, if the fork has a cross section of 2.4 in², it is expected to fail after 4430 worst-case landings and 2870 hard landings.

2.5.3 FEA fork analysis

AISI STEEL 4340 was used instead of 7050 Aluminum alloy because its ultra-high strength in heavy load conditions and even its sustainability in extremely high temperatures. Loading conditions are as follow for the finite element model of the fork.

- Vertical load for worst case landing is 2711 lbf
- Vertical load for hard case landing is 4233 lbf
- Torque calculated assuming the point of application of load at a distance of 2.5in from the axis for worst case landing is 6777.5 lbft and for hard case landing is 10582.5 lb · ft

FIGURE 42 FORK MESHING

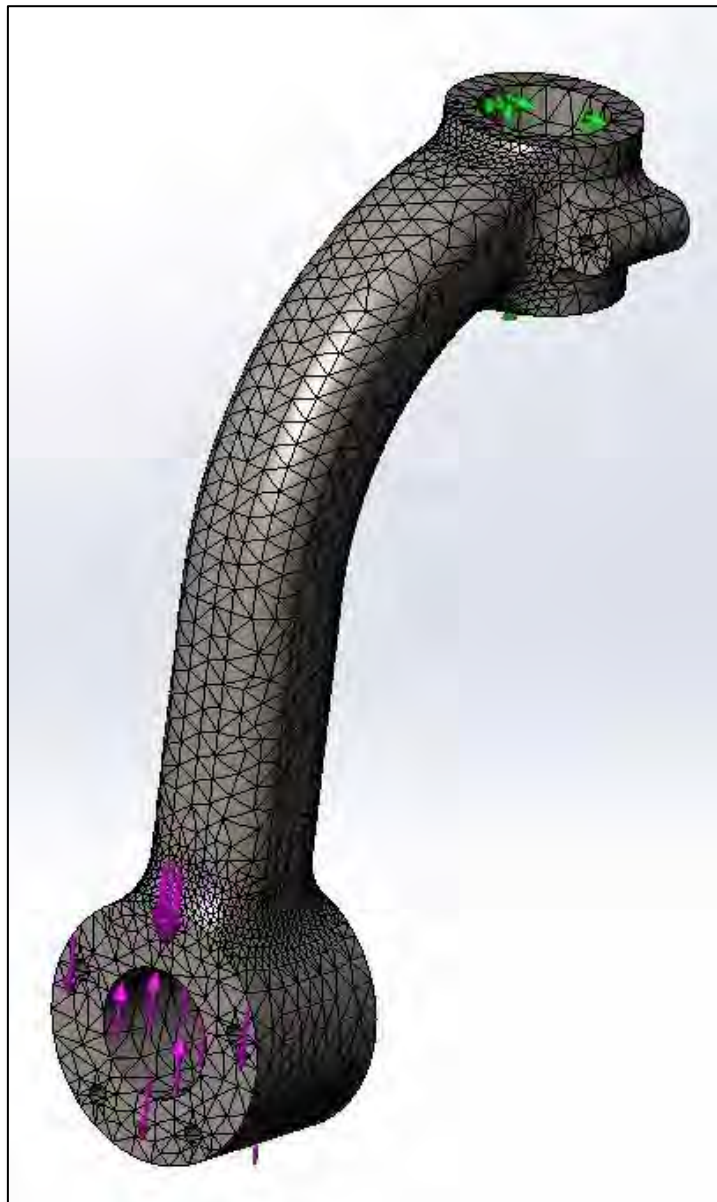


FIGURE 43 FORK STRESSES DURING WORST CASE LANDING

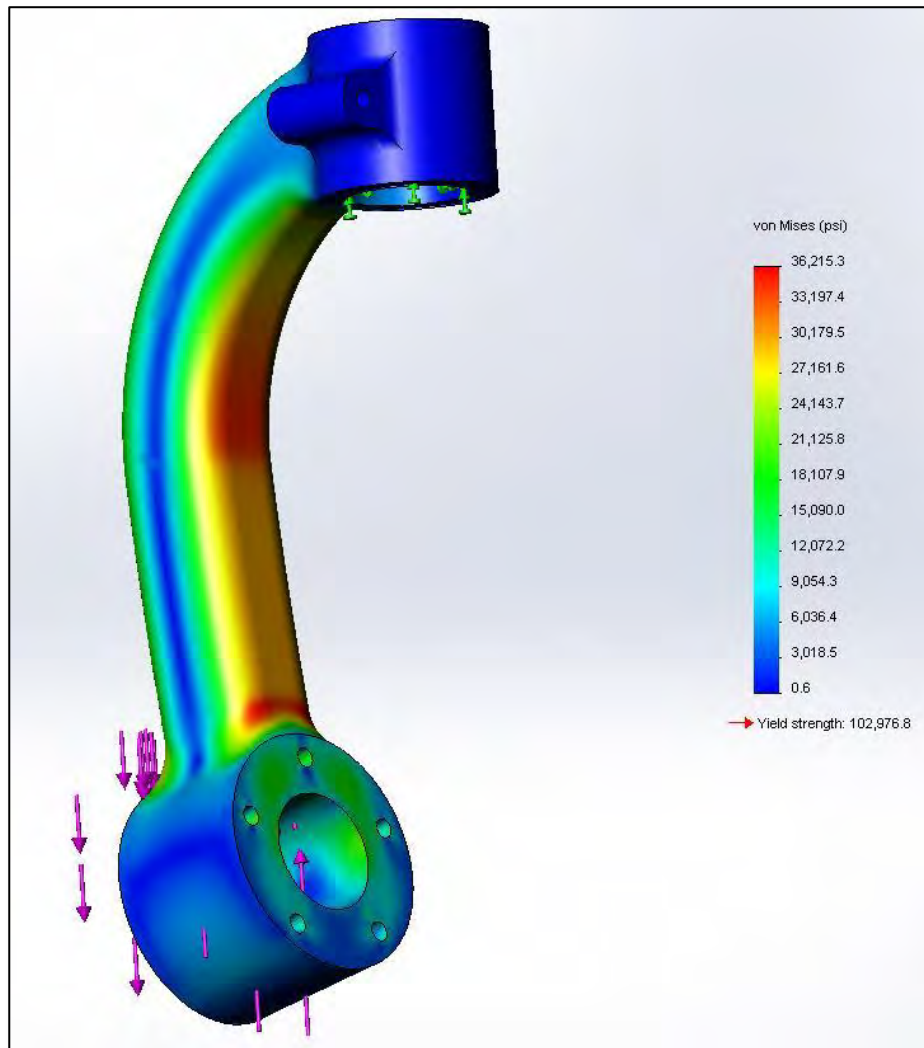
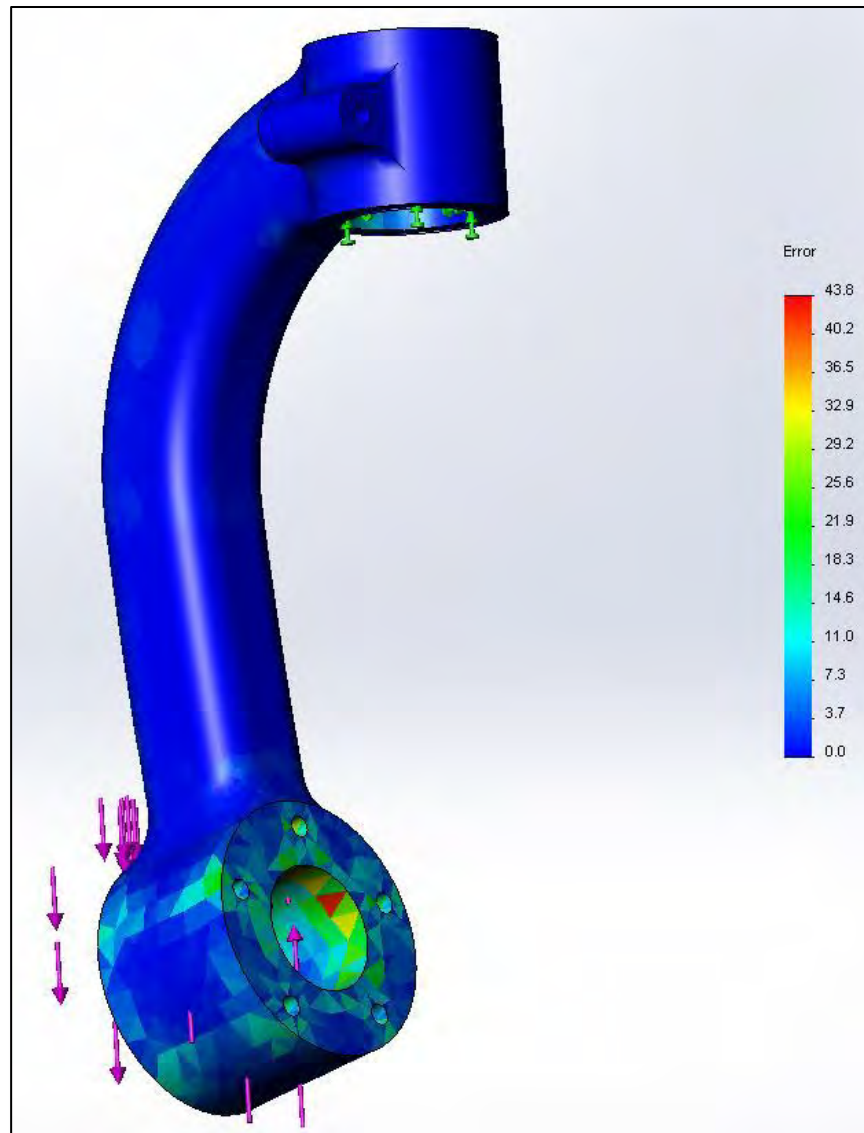


FIGURE 44 ERROR PLOT OF FORK STRESSES DURING WORST CASE LANDING



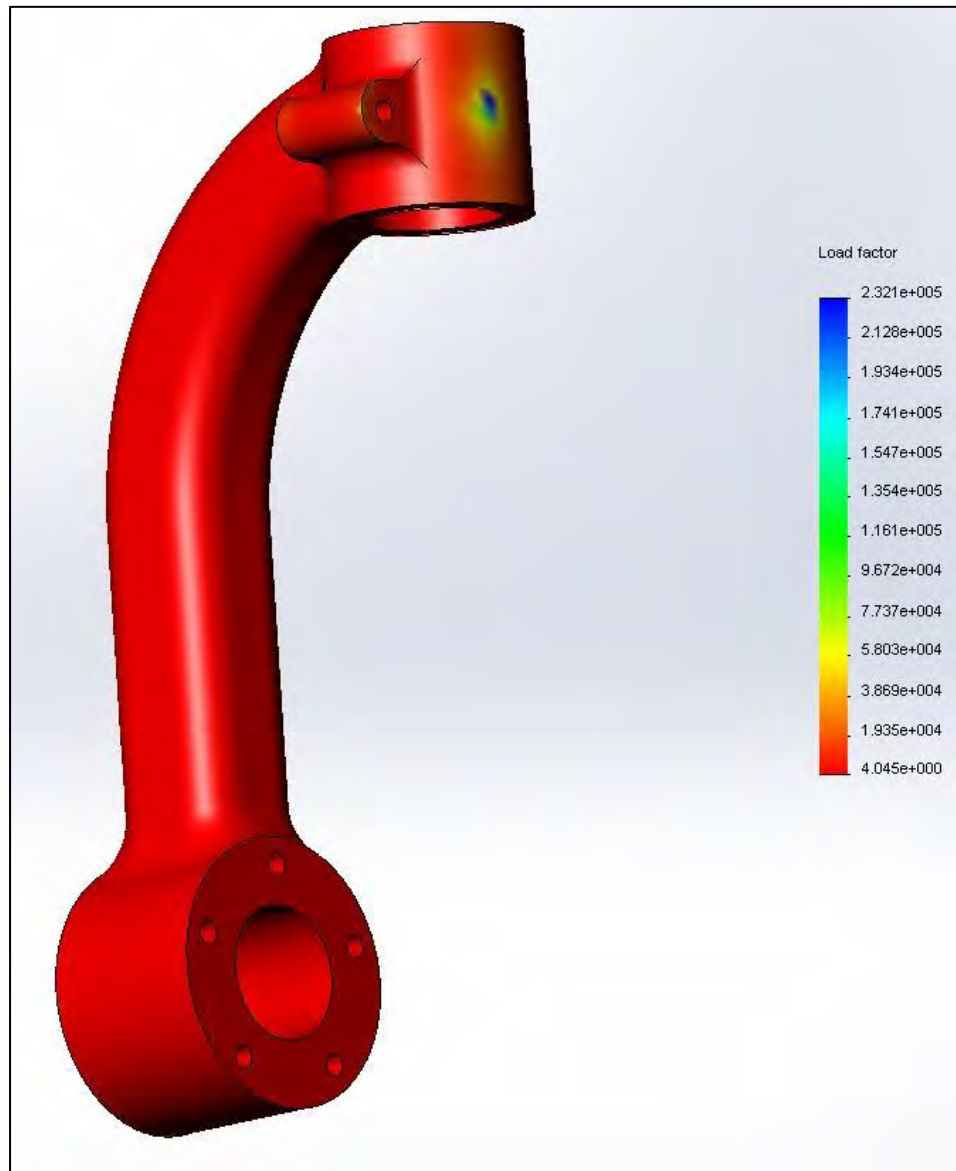
As it can be seen from the error plot that the deviation for the fork at highly stressed regions is at max of 43% and however for the low stress areas like fork bend and upper part of the fork the deviation lies around 1 to 8%. After running the simulation for the fork loaded at 2711 lbf vertical force we came around 36.2 ksi von Mises stress, which is mainly concentrated on inner and outer surface of the bend of the fork. The Yield strength of AISI 4340 Steel is around 230 ksi, so for the fork loaded at 2711 lbf of vertical force, the factor of safety will be around 3. Thus the design is safe until now.

Calculating torque for these loading condition

By approximate assumption the torque is acting at a distance of 2.5in from the center axis of the fork, thus the total torque experienced by the fork will be:

$$2.5 \times 2711 \text{ lbft} = 6777.5 \text{ lb} \cdot \text{ft}.$$

FIGURE 45 LOAD FACTOR FEA ANALYSIS OF FORK



After running the simulation on the model we can see from the figure provided above that the load factor is 4.04, thus if we increase the current load by the factor of 4.04, the fork will fail after 10^6 number of cycles.

But as explained previously the maximum number of cycle that we want this fork to have is 7300, thus the design until now is a safe design.

The vertical load for the hard landing used is 4233 lbf. Simulation plots of this scenario are given below.

FIGURE 46 FORK STRESSES DURING HARD LANDING

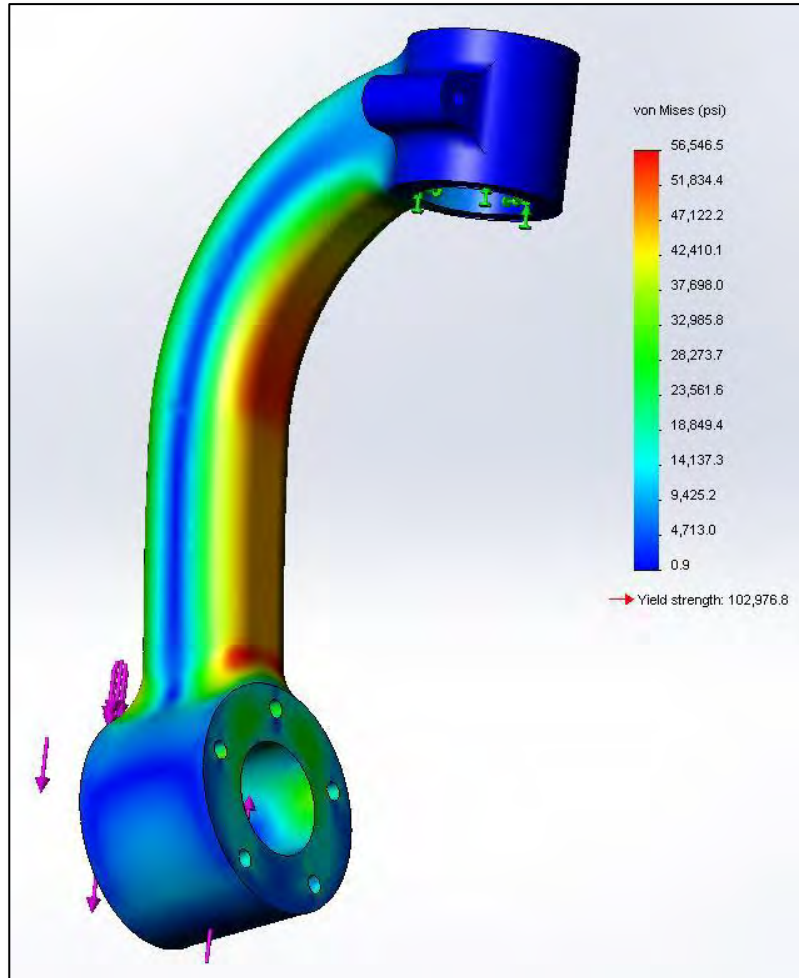
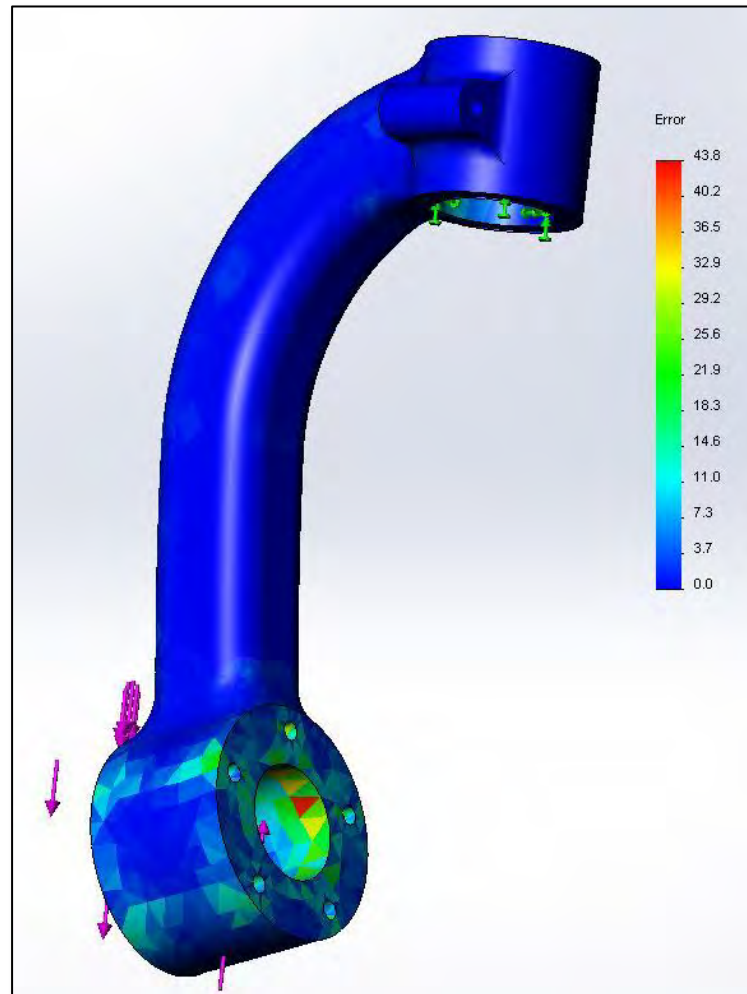


FIGURE 47 ERROR PLOT OF FORK STRESSES DURING HARD LANDING



As we can see from the error plot given above for the Hard case landing conditions that we applied on the fork, the maximum deviation is 43 to 44% was seen in the bottom cylindrical part, same as it was in the worst case landing conditions. But the deformation scale for the worst case landing was 17.097 while that for the hard case landing is 10.9499 thus making it more venerable and reducing its strength. The deviation for the rest of parts of the fork is 0 to 3.7% which is different from worst case landing. From the plot of the von Mises stresses given above of the error plot, we can see that Maximum stress of 56.5 ksi is concentrated at the inner surface of the bend of the fork and at the inner part of the neck connecting fork bend and the lower part of the fork. Rest of the parts of the fork are having less stress concentration than that. The Yield strength of the AISI 4340 Steel is 230 ksi thus giving us the safety factor of 2, which is more than the given factor of safety. Thus our design is a safe design for hard case landings.

Calculating Torque for this loading condition

As the torque is acting at a distance of 2.5in from the center axis of the fork, thus the total torque experienced by the fork will be $2.5 \times 4233 \text{ lb} \cdot \text{ft} = 10582.5 \text{ lb} \cdot \text{ft}$.

FIGURE 48 LOAD FACTOR PLOT FOR THE HARD CASE LANDING (4233LBF) OF THE FORK

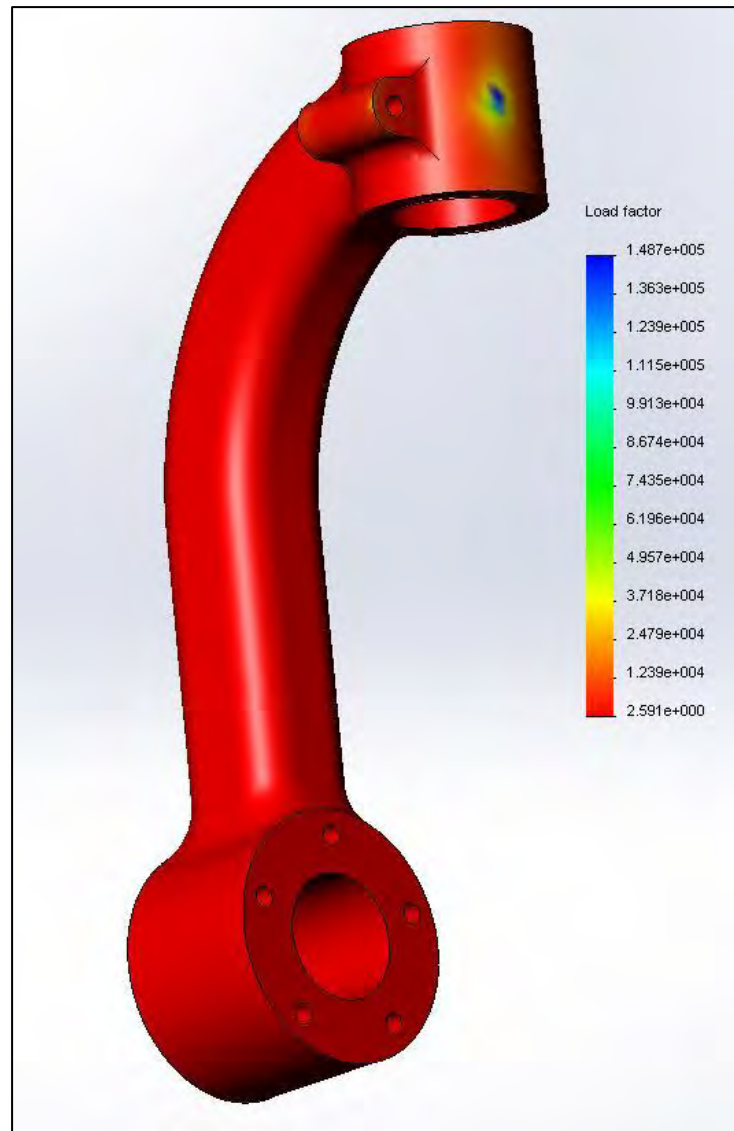
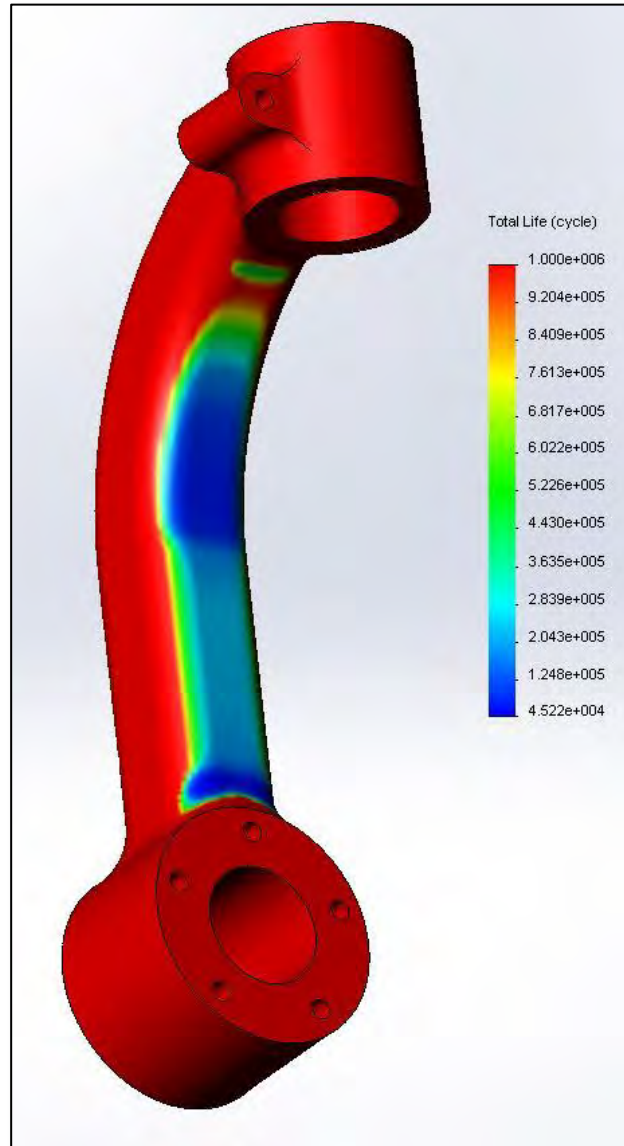
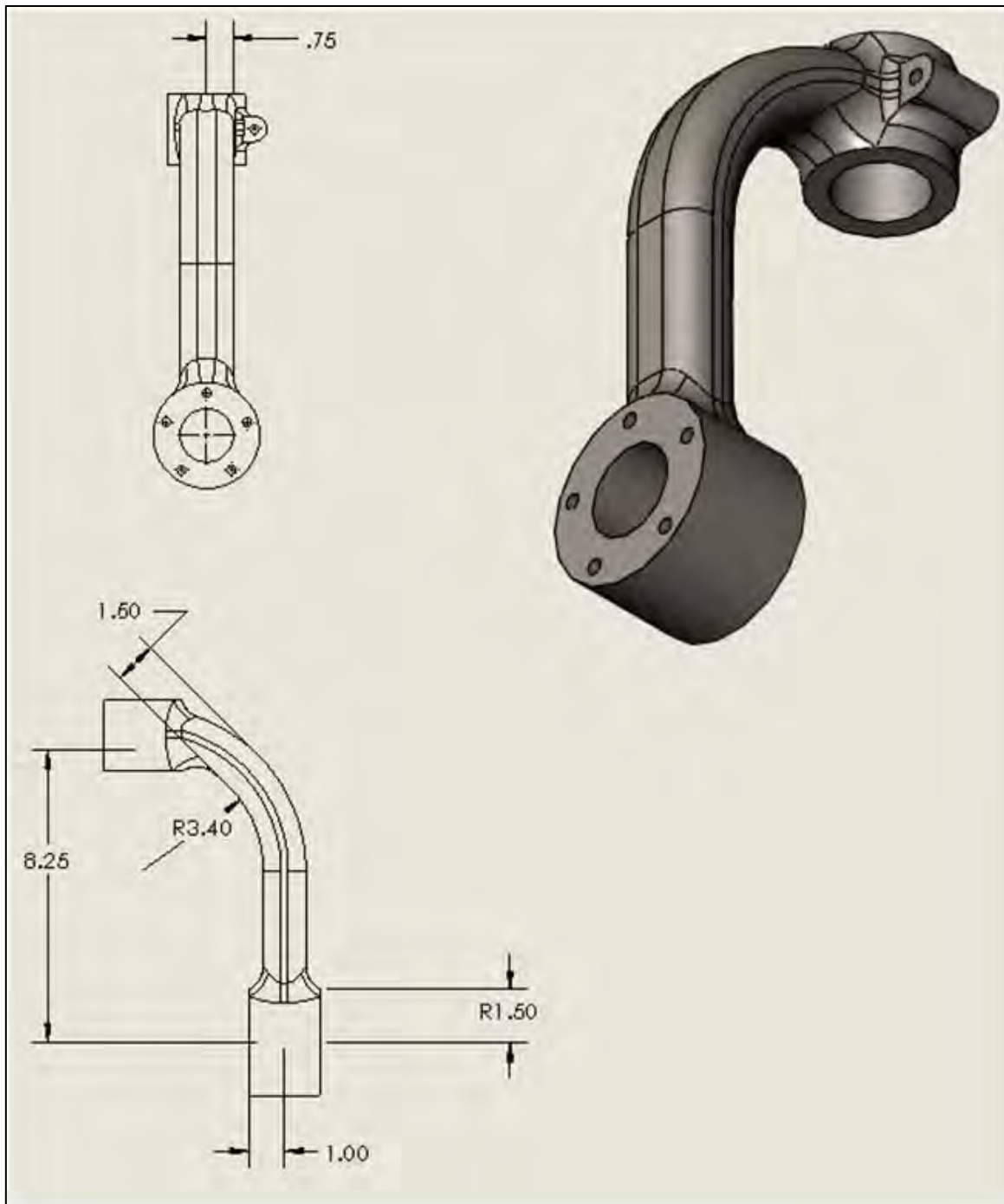


FIGURE 49 TOTAL LIFETIME ESTIMATION PLOT FOR THE HARD CASE LANDING (4233 LBF)
OF THE FORK



As seen from the Load factor plot, the value of the load factor came out to be 2.59, thus we can conclude that increasing the current load of 4233 lbf by the factor of 2.59, the model of the fork will fail after 45220 numbers of cycles. Which are way more than 7300 numbers of cycles, which is the requirement for a sound design. Thus the Simulation shows that the current thickness of 1.6 will be an Ideal thickness for the fork.

FIGURE 50 FORK TECHNICAL DRAWING



2.5.4 Summary of fork design

TABLE 16 SUMMARY OF FORK DESIGN

Parameter/Dimension	Value	Source
Material	AISI 4340	Design choice
Thickness	1.6	
Weight (lbs)		Solid Works model
Worst case landing maximum stresses (ksi)	36.2	FEA model
Worst case landing Safety factor	3	
Expected worst case landings before failure (cycles)	$>10^6$	
Worst case landing Load factor	2.36	
Hard landing maximum stresses (ksi)	56.5	
Hard landing Safety factor	2	
Expected hard landings before failure (cycles)	45220	
Hard landing Load factor	2.59	

Section 3: Landing gear assembly and integration

3. Landing gear assembly and integration



- Derive torque link requirements
- Design and modeling and material selection of torque link
- Fatigue analysis
- Fatigue analysis calculations

3.1 *Final landing gear design*

FIGURE 51 FINAL LANDING GEAR ASSEMBLY



3.2 Landing gear exploded view and Bill of materials

FIGURE 52 LANDING GEAR EXPLODED VIEW



Bill of materials for one main landing gear:

TABLE 17 BILL OF MATERIALS FOR ONE MAIN LANDING GEAR

Sub-Assembly	Component name	Number	Weight (lbs)
Wheel	5.00-5 Ply Rating 6 Tire	1	4.6
	Rim	1	3.55
	Wheel shaft	1	1.36
	5709K27 (Bearing)	2	1.2
	91847A041 (18-8 Stainless Steel Thin Hex Nut 1-1/2"-6 Thread Size, 2-1/4" Width, 27/32" Height)	1	0.3
Brake	Brake disk	1	2.38
	92245A539 (Mil Spec SS Hex Head Cap Screw 1/4"-20 Thread, 5/8" L – brake fasteners)	12	0.01
	Brake bracket	1	0.06
	Brake base	1	0.48
	Brake pad (pair)	1	0.5
Shock absorber	Fork	1	9.75
	Strut shaft	1	1.82
	Strut piston	1	1.91
	Strut body	1	3.72
	90101A050 (18-8 SS Nylon-insert thin hex locknut 3/4"-10 Thread Size, 1-1/16" Width, 13/32" Height)	1	0.07
Torque link	Torque link	2	0.56
	93890A132 (headless Clevis Pin Grooved, 18-8 SS 1/4" Dia, 2-3/8"L)	2	0.03
	93890A116 (headless Clevis Pin Grooved, 18-8 SS 1/4" Dia, 7/8"L)	1	0.01
Total Weight			34.18

- Note that the attachment brackets that fix the LG to the plane are not included in the bill of materials. The expected weight of these brackets is approximately 2.2lbs each.
- The deployment mechanism is also not included in the bill of materials. The expected weight is approximately 5 lbs.
- The approximate total weight of the landing gear becomes approximately 45 lbs.

Section 4: Conclusion

4. Conclusion

4.1 Goal and requirements re-evaluation.

The goal of this project was to design several components of a main landing gear for a plane that is 66% lighter than the Piper Arrow IV so that its dry weight would be optimized to be as light as possible. The modified weight of the plane and subsequent weight reduction of the landing gear was established as the primary requirement. The main components to be redesigned based on this requirement were: the tire-rim-shaft assembly, brake, strut, torque link and fork. The weight addition of these components along with the fasteners would comprise of the total dry weight of the main landing gear.

In order to reach the design goal, the “Nine steps of design” were applied:

First, the need was recognized as a design project required of a fourth-year mechanical engineering student in order to finish and complete her degree.

Second, the problem was defined as the design of components of a main landing gear for a theoretical plane that is lighter than one in existence. At this point, the design tasks were vaguely formulated and the constraints were unclear.

Third, the planning of the project involved identifying the appropriate requirements and constraints that would have to be respected. Several requirements include: static/dynamic load requirements, manufacturability and aircraft structural integrity.

In-depth planning was only possible once information was gathered, which is the fourth step. Therefore, tutorials, lectures and posted documentation were essential in the planning of the project. These resources helped provide an estimate into the scope of this open-ended project.

At this point, the main components were known and identified. Tasks were identified and distributed throughout the period of time available to develop my project. In order to efficiently organize these tasks and deadlines, a tutor was chosen. I wrote emails to my tutor in Spain after every weekly meeting to reiterate what was discussed and prepared with my tutor in Canada.

The appropriate FAR standards were researched and consulted prior to making every design decision. Material selection would have to be optimized for strength and weight from a list of reasonably priced materials, given that strong, light-weight expensive materials like titanium were restricted.

Steps 5, 6 and 7 involve conceptualizing, evaluating and selecting the best alternative. The procedure started with solving the problems in the tutorials accounting for the weight reduction. If applicable, several iterations of analytical calculations were performed. When information was not readily available, educated assumptions were made based on the existing design and/or on engineering common sense.

Next, a preliminary set of materials was chosen based on the calculated loading requirements. Components similar to those in the landing gear model found in the tutorial locale were modeled in Solidworks.

Finite element analysis of static and fatigue stress was performed on each applicable component, based on previously acquired failure theory. A designed component of certain material was considered acceptable if it was not expected to fail for a predetermined number of cycles at a certain factor of safety and met all applicable requirements. Material was removed at low stress concentrations points in order to reduce weight and finite element analysis was performed until the most optimized design was reached.

The last two steps in the design process are communicating and implementing the preferred design. This report along with the presentation is the communication of the preferred design.

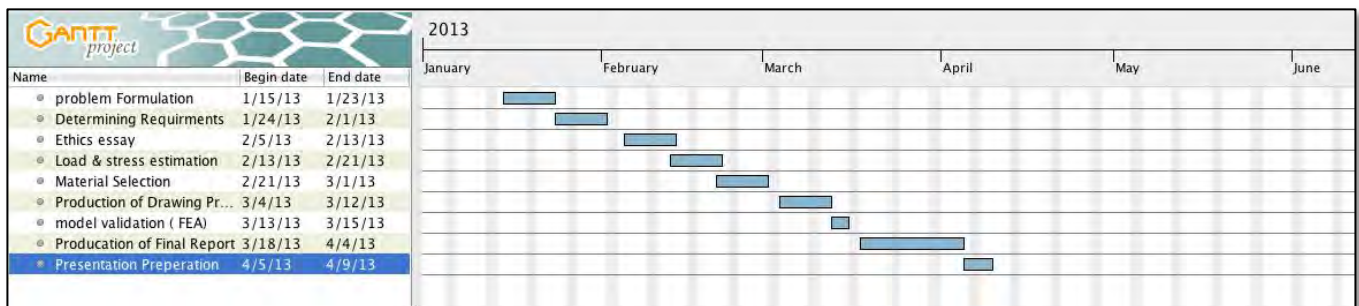
In order to ascertain if the goal of this project has been reached, the goal must be quantifiable. The primary goal defined at the onset of the project was to optimize the design in order to have the lightest landing gear that satisfies all pertinent requirements. A percentage weight reduction could only be calculated if an initial weight of the landing gear was known. Regarding weight, the only certain parameter was that the mass of the whole airplane was reduced by a given percentage. Therefore, an assumption was made that the ratio of airplane mass to its landing gear mass could be used to approximate the initial redesigned landing gear—without the optimization. This rudimentary calculation yielded an initial modified landing gear weight of about 42 lbs. The addition of the total weight of the landing gear can be found in the Bill of Materials in Table 17. It accounts for the fasteners, wheel assembly, brake assembly, shock absorber assembly and torque

link. This total weight of 34.18lbs is considered the dry weight, since no working fluids were ever considered. This would mean a reduction in weight of about 19%--based on the components that were redesigned in this project. A few other components are missing from the weight addition and their weights were estimated based on engineering sense. The two attachment brackets that fix the landing gear to the plane were assumed to weigh a total of 2.2lbs each and the deployment mechanism

is estimated to be about lbs. The total weight that accounts for every component of the landing gear would then be approximately 45lbs. This results in a weight increase of 7%. Therefore, the quantifiable goal of this project was not met.

However, the less quantifiable and arguably more important goal of the project—applying the principles of design—was met. These principles included learning to satisfy specific design requirements, criteria, constraints, standards and regulations while optimizing the desired technical performance. Knowledge from several engineering disciplines was applied. Important skills were developed such as time management, software skills and critical thinking. The skills learned and/or developed through the realization of this project serve as valuable experience in my career as mechanical engineers.

FIGURE 53 GANTT CHART



Section 5:

5. REFERENCES

- [1] S. Chai and M. W.H., "Landing Gear Integration in Aircraft Conceptual Design," 1996. [Online]. Available: http://www.dept.aoe.vt.edu/~mason/Mason_f/M96SC.html. [Accessed 24 March 2013].

- [2] A. Abbasi, A. Raouf, B. Kamal, P. Docter, B. Polderman, A. Schichetanz, E. Stee and D. Van Zuilden, "Airbus A320 Landing Gear Project Report," 2007. [Online]. Available: http://erwinsteen.info/attachments/File/Project_5_LandingGear.pdf. [Accessed 6 April 2013].

- [3] N. S. Currey, "Landing Gear Design Principles and Practices," 1988. [Online]. Available: <http://www.scribd.com/doc/15917156/Aircraft-Landing-Gear-Design>. [Accessed 7 April 2013].

- [4] Piper Aircraft Corporation, "Piper Arrow IV Parts Catalog," August 1983. [Online]. Available: www.bomar.biz. [Accessed 7 April 2013].

- [5] B. Chartier, B. Tuohy, J. Retallack and S. Tennant, "Landing Gear Shock Absorber," [Online]. Available: ftp://ftp.uni-duisburg.de/FlightGear/Docs/Landing_Gear_Shock_Absorber.pdf. [Accessed 7 April 2013].

- [6] F. P. Beer, Mechanics of Materials, McGraw Hill, 2006.

- [7] U. G. P. Office, "Electronic Code of Federal Regulations," 4 April 2013. [Online]. Available: http://www.ecfr.gov/cgi-bin/text-idx?SID=8e5fac7d752601506937121b4c61c38b&c=ecfr&tpl=/ecfrbrowse/Title14/14cfrv1_02.tpl. [Accessed 6 April 2013].

